# UNIVERSITY OF SOUTHAMPTON

FACULTY OF ENGINEERING, SCIENCE AND MATHEMATICS

School of Civil Engineering and the Environment


## Field and physical model investigation of seawall toe scour and associated wave flow processes

by


**Andrew Morris Charles Pearce**


**Thesis for the degree of Doctor of Philosophy**

**June 2008**

**UNIVERSITY OF SOUTHAMPTON**
**ABSTRACT**
**FACULTY OF ENGINEERING, SCIENCE AND MATHEMATICS**
**SCHOOL OF CIVIL ENGINEERING AND THE ENVIRONMENT**
**Doctor of Philosophy**

# FIELD AND PHYSICAL MODEL INVESTIGATION OF SEAWALL TOE SCOUR AND ASSOCIATED WAVE FLOW PROCESSES

**By Andrew Morris Charles Pearce**

In the UK one third of seawall failures are attributed to scour, placing the communities living behind these structures at risk of flooding or erosion. Despite this, field evidence of scour remains anecdotal. Our current understanding is adapted from deepwater breakwater studies and small scale seawall model tests which do not adequately represent shallow water sediment processes. Two medium scale model tests have been conducted, providing guidance for only a limited range of conditions. However a link between the key hydraulic processes and the resulting sediment transport has yet to be developed.

As part of a larger research project, beach level data was collected from the toe of a vertical seawall in Blackpool over a 3 year period, and over a 1 month period at a 1:2 sloping seawall in Southbourne. These results were combined with model experiments conducted at medium scale using irregular waves on a sand beach. To clarify the toe scour processes and the interaction of breaking waves with vertical seawalls, a hydraulic flow study was conducted at small scale.

The research demonstrated a causal relationship between wave breaking and the risk of toe scour at seawalls. Waves impacting at the wall generated high velocity downrush flows, peaking at 0.6 $m.s^{-1}$ in a 1:40 scale model and producing an intense toe vortex. By combining knowledge of the near wall wave breaker type, flow pattern and sediment response, improved methods to predict and mitigate scour were demonstrated.

The deepest scour occurred when the wave conditions and toe water depth were optimal for waves to impact onto the seawall ($d_t / L_m \approx 0.018$) and generate high flow velocities. Flows velocities were reduced under spilling and pulsating wave conditions. The duration of exposure to the most critical condition determined the scour risk, though the depth of maximum scour always remained less than incident wave height. Further model tests and field experiment are required to extend this research to a wider range of beach and wave conditions.

## LIST OF CONTENTS

## LIST OF FIGURES

### Chapter 2



### Chapter 3



### Chapter 4

**Chapter 5**



**Chapter 6**

**Chapter 7**

## LIST OF TABLES

**Chapter 2**



**Chapter 4**



**Chapter 5**



**Chapter 6**



**Chapter 7**

# ACKNOWLEDGEMENTS

I would like to thank the following who played important parts in my doctorate over the past three years:

Annabella, whose continued support enabled me to get through the tough times and her understanding and trust in my decision to leave employment and return to University; to my family and friends for asking questions, answering questions and providing support throughout; to Dr Gerald Müller for supervising my thesis, the numerous discussions over coffee and his support in producing this final document; Dr James Sutherland for his open mind and willingness to listen, and particularly his support with developing the scour predictor and the direction of my work; Dr David Rycroft for putting together this PhD and getting me started; and finally to Sally, Luke, Ivan, Mark and Dan for answering my frequent questions, providing programming tips, topical discussions and presentation advice.

# NOTATIONS AND ABBREVIATIONS

| | | |
|---|---|---|
| $cot\ \alpha$ | - | Beach gradient |
| $d$ | - | Water depth offshore (m) |
| $d_b$ | - | Depth at point of wave breaking (m) |
| $d_t$ | - | Depth at wall Toe (m) |
| fps | - | Frames per second |
| $g$ | - | Acceleration of Gravity = 9.81 $ms^{-2}$ |
| $h$ | - | Water depth (m). |
| $k$ | - | Wave number (=2.π / $L_o$) |
| $k_b$ | - | $H_{99\%} / H_s$ |
| $k_r$ | - | Coefficient of reflection |
| mODN | - | Metres Ordnance Datum Newlyn |
| $w_s$ | - | Sediment fall velocity ($m.s^{-1}$) |
| | | |
| $C$ | - | Constant: 0.4 for fine sand suspension (Xie, 1981) |
| $C^*$ | - | Wave reflection factor |
| CD | - | Chart datum |
| CEE | - | '*School of*' Civil & Environmental Engineering |
| Defra | - | Department of the Environment, Food and Rural Affairs |
| $D$ | - | Sediment grain size (mm) |
| $D_{50}$ | - | Mean sediment diameter (mm) |
| $D_{ws}$ | - | Dean fall speed parameter |
| EPSRC | - | Engineering and Physical Sciences Research Council |
| $H$ | - | Wave height- regular waves (m) |
| $H_b$ | - | Shallow water breaking wave height (m) |
| $H_o$ | - | Offshore significant wave height- irregular waves (m) |
| $H_s$ | - | Significant wave height- irregular waves (m) |
| HRW | - | HR Wallingford |
| $L_m$ | - | Mean wavelength (m) |
| $L_p$ | - | Peak wavelength (m) |
| $L_o$ | - | Offshore wavelength (m) |
| MHWN | - | Mean high water neap (tide) (m) |
| MHWS | - | Mean high water spring (tide) (m) |
| $N_g$ | - | Model, prototype gravity scale, assumed to equal 1. |
| $N_L$ | - | Model, prototype length scale |
| $N_T$ | - | Model, prototype time scale |
| $N_V$ | - | Model, prototype velocity scale |
| PIV | - | Particle Image Velocimetry |
| RMSE | - | Root Mean Square Error (Total) |
| $RMSE_S$ | - | Systematic Root Mean Square Error |
| $RMSE_U$ | - | Unsystematic Root Mean Square Error |

| | | |
|---|---|---|
| $R^2$ | - | Coefficient of determination |
| $S_m$ | - | Maximum scour on beach profile (m) |
| $S_t$ | - | Scour at seawall toe (m) |
| SWL | - | Still Water Level (m) |
| $T$ | - | Period- regular waves (s) |
| $T_p$ | - | Peak wave period- irregular waves (s) |
| $T_m$ | - | Mean wave period (s) |
| $U_{cr}$ | - | Sediment motion threshold, depth averaged velocity ($m.s^{-1}$) |
| $U_w$ | - | Maximum orbital velocity at bed ($m.s^{-1}$) |
| $V$ | - | Velocity ($m.s^{-1}$) |
| $x$ | - | Position offset of maximum scour relative to seawall toe (m) |
| $X$ | - | Observed value |
| $Y$ | - | Predicted value |
| | | |
| $\xi$ | - | Inshore Iribarren number |
| $\upsilon$ | - | Kinematic coefficient of viscosity ($m^2.s^{-1}$) |
| $\hat{Y}$ | - | Trend line prediction, based on least squares fit |

# 1. Introduction and overview

## 1.1. The development of coastal communities

The 19th century marked an important shift in the use of the British coastline from a place of commerce and fortification, to a source of leisure and a place to live. To support this growth, rigid shoreline defences were constructed. These typically consisted of promenades and vertical seawalls (French, 2001), due to their straightforward design and efficient use of valuable shoreline space. These provided improved public access to the seaside and enabling coastal communities to develop, without fear of erosion or flooding.

Over the past century, seawalls have enabled the development of commercial and residential property right up to the defence line. Though in recent years the use of 'softer' beach nourishment schemes have gained in popularity, vertical seawalls continue to be constructed to protect key infrastructure and assets, when the balance between social, environmental and economic criteria can be justified.

As we continue into the 21st century, these structures come under increasing pressure from sea level rise and anthropogenic interruptions to sediment supply, which can cause beach lowering and erosion, leading to wall failure. Before this point, the risk must be managed or suitable replacements constructed for the next 100 years, alternatively the defence line must be retreated and coastal developments migrated inland.

### 1.1.1. Seawall erosion and scour

When a seawall is exposed to sea level rise or an anthropogenic change in sediment supply, the beach level in front of the wall will fall through a shift in the beach profile position (Bruun, 1962) or loss of sediment down drift (McInnes, 2003). This exposes the structure to wave activity, with the potential for localised erosion to occur at the wall toe, a process termed toe scour. Toe scour has the potential to expose and damage the wall foundations, enabling further undermining and possible failure of the defence line.

Defence failure can lead to erosion and flooding of property, damage to local infrastructure, and in some locations could encourage more widespread geotechnical failures in cliffs and steep ground. In sensitive locations e.g. nuclear power stations,

which are often sited on the coast to access ocean cooling water, scour failure of a seawall could lead to severe human and environmental impact.

### 1.1.2. Investigating the problem

Observing toe scour remains difficult due to the rapidly changing water levels and resulting coastal process that occur in front of the wall. In a twelve hour period a typical location could switch from a dry beach and wide surf zone at low water, to highly reflective wave conditions at high tide and back again. When this is combined with the significant energy released from breaking waves, the corrosive salt water and abrasive sediment, direct measurements of scour during storms has thus far proven difficult.

To understand these processes, coastal scientists often rely on scaled physical models, to provide a simplified situation in which to observe and measure transport processes and wave dynamics. However relatively few toe scour experiments have been conducted at a suitable scale to accurately model the key sediment transport processes. Early flume studies were often conducted at small scale, with regular period waves, which tended to exaggerate scour depths. Current scour guidance and prediction methods are largely based on anecdotal observations and simple equations fitted to laboratory datasets. These issues are compounded by the lack of field measurements to validate model results.

For practicing engineers and scientist, the current empirical equations available to predict scour are limited to either unbroken (reflective) or breaking waves. However in reality both conditions may exist over a tidal cycle. Furthermore, these equations only represent the final scour depth. A causal relationship between the key hydraulic processes and resulting sediment transport has yet to be established, enabling informed judgement. To take the current state of knowledge forwards, a hypothesis was derived and tested.

## 1.2. Hypothesis

**Seawall scour is driven by both wave breaking and wave reflection processes. The position, magnitude and occurrence of the deepest toe scour can be determined more accurately by studying the interaction of these waves at the seawall structure and measuring the resulting sediment transport. By considering these processes, improved predictions of scour depth and risk guidance can be developed.**

## 1.3. The research need

Existing field evidence of toe scour is largely based on anecdotal field evidence and visual observations, to date no direct measurements have been conducted to verify scour depth under storm events. Our current understanding of scour and scour prediction equations is largely based on model tests, which at small scale are prone to scale effects. Of the relatively few medium scale scour tests experiments conducted, each tends to adopt a different methodology and most are biased towards deep water breakwater structures, limiting comparison and integration.

There is a clear need to collect field validation data and to conduct physical model tests at a medium scale in order to observe the key sediment transport processes. This will enable the existing datasets to be unified to produce a fundamental understanding of the key scour processes and their effect on the scour depth risk. In turn this can be utilised to provide improved guidance and design.

## 1.4. Research aims

The aim of the research was to conduct a scientific study of seawall scour to:

- Improve understanding of the key mechanisms of toe scour;
- Collect field observations to validate physical model results;
- Combine field and flume measurements to understand the effect of wave breaking flows on scour depth;
- Produce maximum scour depth estimates, using simple equations with few fitted coefficients;
- To understand how, why and when scour will occur and applying this knowledge to provide coastal engineers and risk managers with improved guidance.

## 1.5. Research objectives

This research will:

- Review existing literature and datasets to develop the current state of knowledge;
- Collect field evidence of scour from both vertical and sloping seawall structures;
- Validate the results of a recent medium scale sediment transport physical model study and interpret these to observe scour depth variation;

- Examine the interaction of waves and structures, and the consequences for sediment transport tests using hydraulic flow measurements;
- Unify the field, sediment transport and hydraulic results to develop an understanding of the scour process, leading to improved scour risk, depth and mitigation guidance.

Through the combination of the various research methods, the guidance provided will be robust and applicable to range of prototype situations, providing a benchmark for future scour research.

## 1.6. Research limitations

- The research will primarily focus on vertical seawalls, as these are more common than sloping walls and are at a higher risk of failure due to their configuration;
- Only beaches with sandy sediment will be considered, very limited scour research has been conducted into coarse sediment and collection of field and flume data is significantly more difficult;
- The flume studies will only consider normal wave directions, and only limited wave angles will be sampled in the field research. These are assumed to represent the worst case situation for wave driven sediment transport at a seawall;
- The effect of longshore flows or other 3D nearshore processes (e.g. rip currents) will not be assessed.

## 1.7. Contributions

In a recent scoping study, Sutherland *et al.* (2003) identified the need for new research to provide improved understanding of the risk of beach lowering and toe scour causing seawall failure. As a result of this study, a research project jointly funded by the UK Department of Environment, Food and Rural Affair's (Defra- FD1927) and the Engineering and Physical Sciences Research Council (EPSRC) was proposed, and awarded to a research partnership between HR Wallingford and the University of Southampton.

The Defra project included the collection of field data and physical model tests to investigate seawall toe scour, to improve scour prediction and to develop risk based management tools. The author was involved in planning and implementing the field experiments, collecting and interpreting the physical model data and developing a scour

predictor. The author also presented the field results at the International Coastal Engineering Conference in 2006 (Pearce *et al.* 2006- Appendix A).This thesis presents the author's key inputs into the project, and takes forward that work with more detailed experiments recently conducted by the author at the University of Southampton.

## 1.8. Thesis structure

The thesis is organised into 8 Chapters, these are as follows:

1. Introduction – An introduction to the research issue, hypothesis and study aims, objectives and limitations;
2. Background- A review of seawall design, coastal processes and physical modelling issues related to scour research;
3. Literature review- A review of literature related to beach storm interaction, physically modelling toe scour and recent numerical modelling;
4. Field study – The aims, method, results and conclusion of the field data collection project;
5. Sediment transport study – An overview of the recent medium scale sediment transport study results and development of an empirical scour predictor;
6. Hydraulic study - An in depth investigation of the key sediment transport tests using a hydraulic flow study to interpret wave flow processes;
7. Combined analysis & discussion- Combined discussion of the three preceding studies to develop an improved understanding of toe scour and new guidance;
8. Conclusions- overall conclusions and future work;
9. References.

# 2. Background

## 2.1. Beaches and seawalls

On receding coastlines seawalls are typically constructed to prevent further erosion of the coastline and to provide a tidal flood defence. To provide an efficient design and reduce the exposure of the structure, a fronting beach is often included. This reduces energy dissipation at the wall though the formation of a wide surf zone. However in the longer term, if the defence scheme prevents updrift erosion or longshore sediment supply, e.g. through construction of a terminal groyne, the beach level will fall, increasing the exposure of the seawall. Though beaches can be artificially maintained by nourishment, this is not always feasible due to the high cost and the timescales involved in planning and implementing these types of scheme. During period of low beach level, structures are prone to toe scour.

Under storm wave conditions, the fronting beach will be quickly reworked by the incident waves to form a cross shore profile in equilibrium with the active processes (Dean, 1977). In general this process moves sediment offshore, to extend the profile and form additional bars, increasing energy dissipation (Lee *et al.* 1998). However when beach levels are low, the profile adjustment may exceed the volume of available sediment, leading to wave breaking at the seawall. Under these conditions the maximum height at the structure becomes dependent on the toe water depth, generating a feedback mechanism for increased transport. While a small percentage of wave energy will be dissipated through wave reflection offshore, the potential for further scour and structural damage due to wave impacts increases.

For the purpose of this study, low beaches were defined as a section of coast where waves come into contact with the seawall at least once per year. An example is shown in Figure 2-1, which illustrates significant cross shore profile change on a sand beach in Southbourne, Dorset, fronted by a sloping seawall. Figure 2-1a (January 2005) was taken at mid tide after a period of moderate wave activity which reduced the beach level to around mean sea level and caused a scour trough at the toe of the wall. Figure 2-1b (April 2005) indicates the typical beach level during calmer conditions. The lowest handrail post is indicated in each photo, to indicate the significant changes in beach crest level that can occur, once the seawall is exposed to breaking waves.

**Figure 2-1: Southbourne: a) 11 Jan 05 (0.1mODN) b) 28 April 05 (1.6mODN)**

### 2.1.1. Wave breaking on beaches

When waves approach the shoreline the water depth deceases and they become affected by the seabed, causing wave shoaling and refraction. This reduces the wave celerity and leads to refraction towards a direction normal to the beach slope. Incident waves can be broadly split into two categories depending on their period. Where waves have a short period (<8 s), commonly generated by local wind stress, they will be relatively steep. As these waves shoal in the surf zone, they slow down, shortening their wavelength, leading to an increase in steepness. These waves quickly reach a point where they become overly steep and break.

Longer period waves are generated by ocean low pressure storm systems. These blow over the ocean for a longer duration and over a wider area (i.e. fetch length) leading to a longer period (>10 s) and larger wave heights. This decreases the wave steepness, therefore these waves must undergo shoaling for a longer duration before they become overly steep and break. As a result longer period waves break in shallower water compared to the short period waves, and are more intense, as they contain a larger mass of water.

The type of wave breaking is dependent on the water depth, with waves generally breaking in a water depth slightly greater than their height (Komar, 1998). Therefore when large storm waves approach the shoreline, the wave height at the shoreline is often significantly smaller due to the wave becoming depth limited when $H_0 / d \approx 0.78$.

When waves break at the beach, the form of the breaker can be broadly categorised into three key types according to the beach slope and the incident wave steepness as described by the Iribarren number ($\xi$) (Figure 2-2). Spilling waves occur when short period waves become overly steep, they also occur on gentle sloping beaches, where the critical breaking depth is reached gradually or when strong onshore winds push over the top of the wave. Plunging breakers tend to occur when moderately steep (longer period waves) move into shallower water or when the water depth decreases rapidly (e.g. at a longshore bar). This produces an intense breaking wave as the water mass is thrown forwards. The final type, surging, occur on very steep beaches (e.g. shingle), where the offshore water depth is significant, preventing shoaling and wave breaking causing the unbroken wave to flow up the beach.

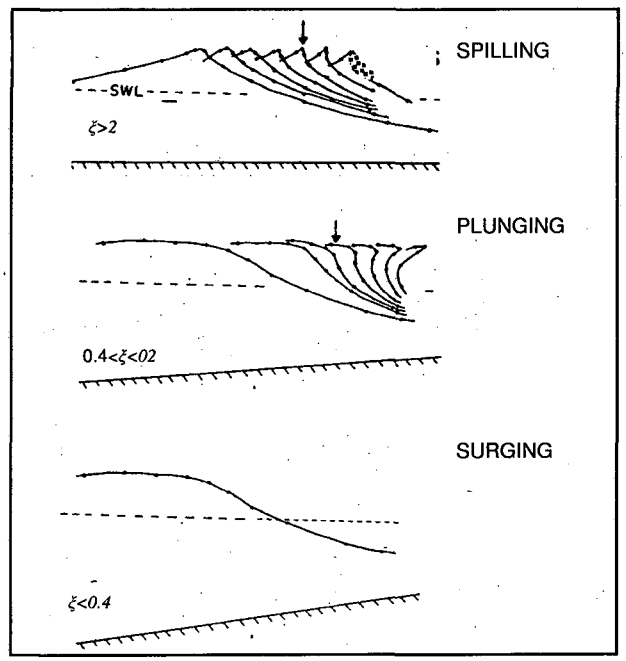


**Figure 2-2: Wave breaking types and shapes (adapted from Komar, 1998)**

### 2.1.2. Wave breaking at coastal structures

When a coastal structure obstructs the wave and prevents further shoaling, the wave energy is either dissipated by breaking at the structure, reflected or elements of both. In physical model test of vertical breakwaters, Oumeraci *et al.* (1993) classified four types of wave breaking at structures: Turbulent bore; well developed plunging; plunging; upward deflected. These are summarised in Figure 2-3 below.

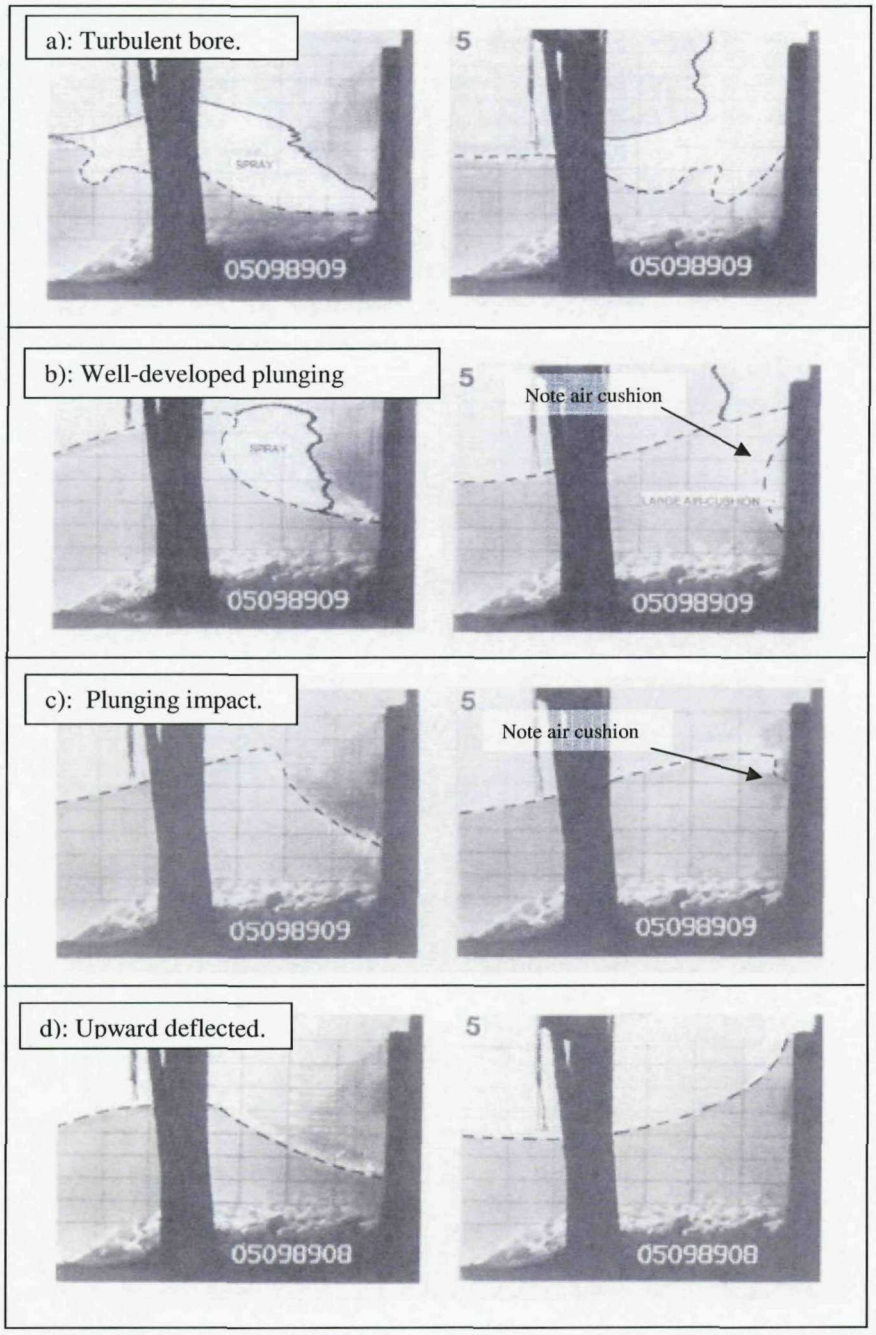


**Figure 2-3:Classification of breaking waves at vertical structures prior to impact (left) on impact (right) (from Oumeraci *et al.* 1993): a): Turbulent bore; b): Well-developed plunging; c): Plunging; d): Upward deflected.**

The breaker types were classified by the ratio of the water depth below the wave as breaking commenced ($d_b$) to the still water depth at the wall face just prior to impact ($d_t$), and the ratio of the horizontal breaking wave velocity ($v_H$) and vertical velocity ($v_v$) of the water level at the wall during impact. The key structures and features of each breaker are described below, based on observations reported and interpretation of the more extensive series of images in Oumeraci *et al.* (1993):

The turbulent bore breaker forms when the water depth below the breaking was significantly greater then the toe water depth. ($d_b / d_t << 1$) causing the wave to become overly steep and begin spilling offshore of the wall. On impact the velocity of the wave is significantly greater then the rise in still water level at the wall ($v_H / v_v >> 1$). The impact of the bore at the seawall is less violent due to the dampening effect of the turbulent foam bore. In the case of the well-developed plunging breaker breaking occurs just before the wall ($d_b / d_t < 1$). This causes the still water level at the wall to rise at an increased velocity compared to the turbulent bore ($v_H / v_v > 1$). During wave impact a large air cushion is trapped next to the wall, becoming highly compressed and producing a vertical jet of water and significant spray.

In the case of the plunging breaker, wave breaking water depth is less then the water depth at the wall face and wave breaking occurs closer to the wall ($d_b / d_t > 1$). The increased water depth at the wall, is a result a rapid increase in the vertical velocity of the water level in front of the wall and is close to the velocity of the incident breaking wave ($v_H / v_v \geq 1$). This reduces the air cushion trapped at the wall compared to the well-developed plunging breaker. In the last case (Upward deflected) wave breaking commences very close to the wall, this causes the water velocity at the wall face to increase very rapidly, causing the water level to exceed the expected point of wave crest impact at the wall ($d_b / d_t > 1$, $v_H / v_v >> 1$). As a result, a wave horizontal impact does not occur, instead the wave is directed upwards, marking the threshold between reflective and impacting wave / wall interactions.

The criteria above can be applied to describe wave breaking at seawalls. Though four keys types were identified by Oumeraci *et al.* (1993) it is important to emphasise that on a natural beach, variations in beach slope and an irregular wave spectrum will produce a range of breaking wave types ranging from turbulent bore to unbroken reflective waves, though one type may be more prevalent.

## 2.2. Seawall structures and failure

### 2.2.1. Structure types and construction

The primary aim of a vertical seawall structures is to hold the coastline position and to reduce the risk of coastal flooding. The vertical orientation produces a smaller footprint than other defence types (e.g. rock revetments) and by their nature, walls are a structure people are familiar with. Modern seawalls are typically cast insitu with reinforced concrete or using precast interlocking concrete units. Older seawalls were constructed using regular shape blockwork or mass concrete with a masonry facing. The wall cross sections in Figure 2-4 represent typical configurations of seawalls found around the UK coast. Sloping seawall structures are also common and typically vary from a slope of 1:1 to 1:4. Though performing a similar function to vertical walls, they occupy a larger plan area, which requires additional space behind the defence line or construction of the structure out onto the foreshore which may not be viable.

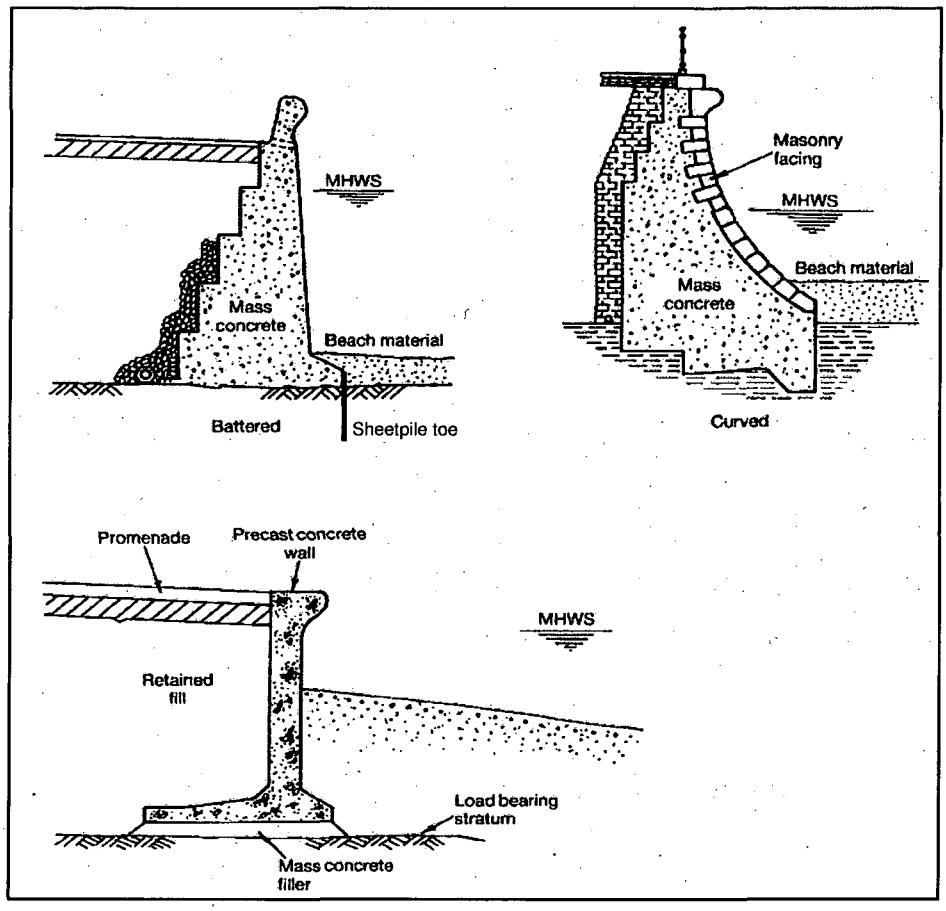


**Figure 2-4: Typical seawall cross sections (from Thomas & Hall, 1992).**

To prevent undermining, seawalls are generally founded on hard bed rock. Where this is not possible or the wall foundations are already susceptible to scour, sheetpiles can be used to extend the seawall toe. However this solution is expensive, and often only represents a short term solution, as the increased water depth in front of the structure permits larger waves, which increase the risk of further scour and erosion (Cooker & Peregrine, 1990).

### 2.2.2. Seawall failure modes

With a low beach level and waves breaking onto the wall face, sediment can become mobilised, leading to scour and exposing the wall foundations to wave action. In turn, the bearing material supporting the wall can be eroded, causing total failure through sliding or overturning (Figure 2-5a). If the scour extends beneath the wall, this can lead to the supporting backfill being washed out, causing damage to the promenade and services located behind the wall.

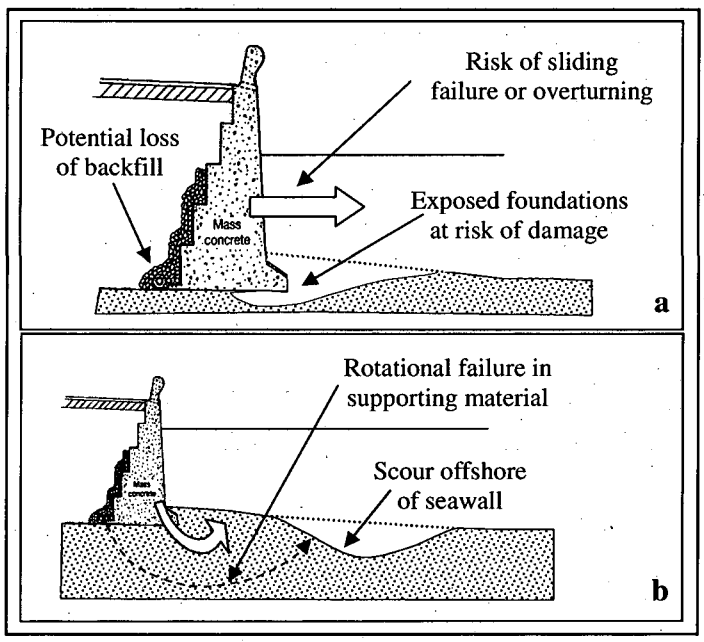


**Figure 2-5: Seawall scour failure modes**

When scour occurs further offshore (Figure 2-5b), and combines with significant overtopping or rainfall, saturating the ground behind the wall, rotational failure can occur in the bearing soil, leading to a sudden seaward movement of the slope and seawall. Reducing the risk of this type of failure is more complex and would require detailed geotechnical investigations to determine the failure plane and possible remedial options. Sloping seawalls are also at risk of this type of failure, but are less prone to

overturning and sliding due to their wide cross section profile; though the potential for undermining and foundation damage remains.

### 2.2.3. Evidence of failure due to scour

A survey of local authorities in the UK revealed that toe erosion was responsible for 33% of all seawall failures and indirectly responsible for a further 5%, including failure through breaching and loss of backfill (CIRIA, 1986).This is expected to be amplified by sea level rise and any increase in storm activity associated with climate change.

The collection of field and visual scour measurements remains difficult due to the high energy environment in front of the wall. Furthermore, it is likely that infilling occurs during the falling tide or receding storm conditions, hiding any damage that could be visible at low tide (Powell & Lowe, 1994). Occasionally photographs have captured what appear to be scour troughs or runnels along the toe of the wall, however the size and extent of these features at the peak of the storm remains unknown (Figure 2-6).


**Figure 2-6: Southbourne, Dorset UK. A trough at the toe of a sloping seawall**

**Case study – Seaford, East Sussex**

A well known example of beach erosion and potential for seawall failure occurred at Seaford, East Sussex during the early 1980s. Following construction of a harbour wall, the longshore supply of sediment was reduced, leading to erosion of the shingle beach, allowing waves to break onto the seawall. During storm events, scour close to the wall toe led to further removal of material exposing the foundations and causing partial collapse of the promenade (Figure 2-7). Total failure would have caused severe erosion and flooding of the town located behind the wall. The ability to accurately predict the scour depth would have enabled these risks to be assessed and mitigation measures

implemented if required. In 1987 a coastal protection scheme was implemented to repair the seawall and to re-nourish the beach, preventing further scour.

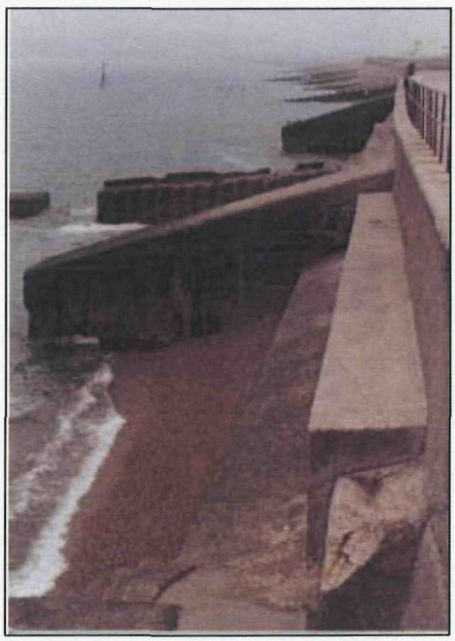

**Figure 2-7: Seaford- East Sussex, vertical seawall with exposed toe c.1983. From Sutherland *et al.* (2003)**

### 2.2.4. Future shoreline change and toe scour risk

Looking to the longer term (50-150 years), climate change research acknowledges that sea levels are rising. Though precise predictions remain subject to speculation, current Defra guidelines suggest the greatest sea level rises will occur in Southeast England due to a combination of rising sea level and falling land level. The guidance suggests an allowance of 4 mm per year should be made up to 2025. Beyond 2025 the rate of sea level rise is forecast to accelerate leading to a rate of 15mm per year from 2085 onwards (Defra, 2006). In this scenario, beaches where the defence line is held or which suffer from an interrupted sediment supply will gradually diminish in width, as predicted by Brunn (1962). Without human intervention, the long term beach levels will drop, exposing structures to increased wave activity, and initiating a feedback cycle where higher wave energy can reach the structure, causing further erosion.

Without an understanding of the occurrence and likely scour depth, the risk of failure cannot be anticipated in the design of new coastal structure, nor the risk managed adequately in existing structures. When a seawall fails, the damage due to flooding and erosion can be severe and in some locations could lead to loss of life and significant economic damage. Furthermore repairing a damaged structure following scour, is both

costly and difficult to implement as beach levels have often fallen below the mid-tide level.

## 2.3. Modelling seawall scour

The coastal zone involves complex interactions between physical structures, geological sediments and hydraulic processes which vary over a variety of different temporal and spatial scales. The key scour variables and notations used to describe wave and scour elements in front of seawall structures are denoted in Figure 2-8.

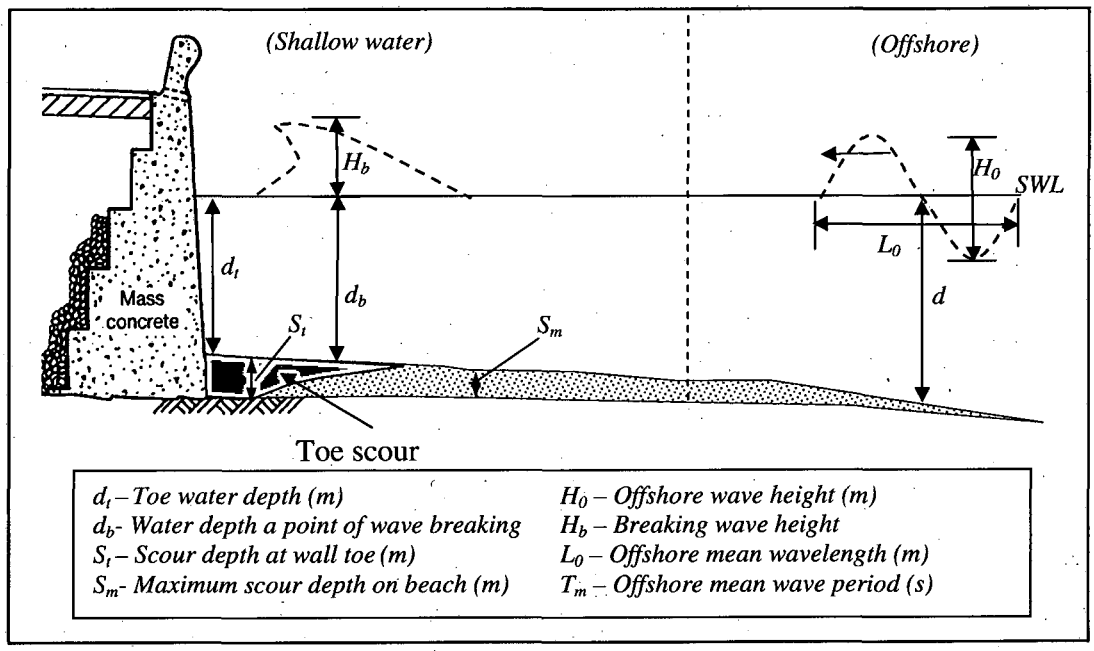


**Figure 2-8: Seawall scour risks and key parameters**

The wave parameters can be considered as either offshore where the water depth ($d$) is significantly greater then the significant wave height ($H_0$), intermediate waves, or shallow water waves where the water depth ($d_b$) is approximately equal to the wave height and wave breaking occurs ($H_b$). In all cases the parameters refer to the significant wave height. Where regular waves are referred to, the parameter $H$ is used and the water depth specified.

Scour can occur both at the seawall toe ($S_t$) and also on the beach profile ($S_m$) further offshore. Observing scour in the field environment is difficult, as the profile changes occur at the seabed and are the net result of various hydraulic and sediment transport processes. In an attempt to control these variables, and to observe and measure scour depth, experiments can be conducted within scaled physical models to provide a

simplified, repeatable simulation of the coastal environment, which can also be used to test prototype designs (Hughes, 1993).

Physical model experiments investigating cross shore transport are typically constructed in long, narrow flume channels (Figure 2-9). The size of the flume, i.e. the model scale, limits the maximum wave height that can be generated, which in turn dictates the scale of the hydrodynamic and sediment transport processes. Therefore establishing the correct model scale is critical in planning and executing a research study.

**Figure 2-9: 40 m 2D wave flume, HR Wallingford UK.**

### 2.3.1. Model scale

The model scale refers to the ratio between elements in the model and the prototype situation (Equation 2.1). This is typically the length scale, hence the scale ratio would be termed $N_L$, other ratios include $N_T$ (Time) and $N_g$ (Gravity). When a model is scaled by its length and remains true in both *x* and *y* directions, the model is said to be geometrically undistorted.

$$Scale\ Ratio = N_{(.)} = \frac{Variable_{(Prototype)}}{Variable_{(Model)}} \qquad (2.1)$$

Table 2-1 categorises a range of model scales, with their respective scale ratios, flume dimensions and wave heights, and was used as a point of reference when considering existing physical model tests and literature.

**Table 2-1: Model scale categories**

| Criteria | Scale factor | Typical | | |
|---|---|---|---|---|
| | | Wave height | Flume length | Flume depth |
| Large scale | 1:1 to 1:5 | > 0.5 m | 100 m | 5 m |
| Medium scale | 1:5 to 1:20 | 0.15 m to 0.5 m | 50 m | 2 m |
| Small scale | 1:30 to 1:100 | < 0.15 m | <30 m | < 1 m |

Therefore in an undistorted large scale model of length scale 1:2, the beach length, structure and wave height would be 50% smaller than those occurring in the prototype, clearly this would require a very large flume, which would be both costly to construct and commission. When the scale factor is increased, a smaller flume can be used. These are simpler to setup and cheaper to run, however maintaining the similitude of the fluid flow (kinematic similitude) and wave forces (dynamic similitude) becomes increasingly difficult. Where similitude cannot be maintained, unwanted effects occur, and have the potential to compromise the reliability of the model results.

**Scale and laboratory effects**

Model effects can be categorised as either laboratory effects or scale effects. Laboratory effects are elements present in the natural environment which are not included in the model e.g. wind stress, saline water. Though it is possible to incorporate these items into a model, in most cases the benefit of including them is outweighed by the practical difficulties of recreating them accurately in the laboratory (e.g. scaling both hydrodynamic and aerodynamic processes together). Furthermore, the use of saline water is highly corrosive to the sensitive equipment used in the laboratory.

Scale effects refer to the difficulties of working at a reduced scale compared to the prototype. This principally affects the fluid density and viscosity due to the use of the same fluid (water) in both the model in prototype. These effects become particularly important when attempting to model physical processes such as sediment transport and air entrainment at small scale.

To analyse the deviation of a model from prototype, scale laws can be applied. The Froude and Reynolds number are considered to be the most useful when physically modelling hydraulic processes (Hughes, 1993). The Froude number (Equation 2.2) represents the balance between the force of inertia and gravity. The Reynolds number

(Equation 2.3) represents the balance between inertia and viscous forces and can be used to distinguish between laminar and turbulent flow.

$$\text{Froude Number} = Fr = \frac{V}{\sqrt{gd}} \qquad (2.2)$$

$$\text{Reynolds Number} = \text{Re} = \frac{VL}{\nu} \qquad (2.3)$$

Where $g$ = Acceleration of gravity (9.81 $ms^{-2}$) and $\nu$ = Kinematic coefficient of viscosity ($1.36x10^{-6}$ $m^2s^{-1}$, fresh water, 10°C). The remaining variables are taken to equal representative quantities within the model. For example, $V$ =Velocity scale ($ms^{-1}$) could equal the sediment fall velocity, wave celerity or a current speed. Similarly, $d$ (m) the depth could also represent the length scale.

Scale ratios can be calculated for both equation (2.2 & 2.3), in a similar form to the length scale presented in Equation 2.1. By modifying the model length and velocity parameters, is it possible to achieve similitude between model and prototype (i.e. $Fr_{\text{prototype}} = Fr_{\text{model}}$). However, it is not possible to maintain similitude of both Froude and Reynolds numbers at the same time, in the same model. Therefore in the coastal zone, when modelling surface waves, where gravity forces can be assumed to dominate over viscous forces, the Froude scaling is usually applied and the Reynolds scaling compromised (Hughes, 1993).

Equation 2.2 can be used to determine the Froude length scale ratio and to calculate the model size required to maintain similitude. However when determining the velocity scale factor ($N_v$), the time and length scale must both be scaled using Equation 2.4 to remain dimensionless. Within the equation, $N_g$ the gravity scale ratio, is assumed to equal one and is typically omitted from the calculation.

$$\text{Velocity scale ratio} = N_V = \sqrt{N_g . N_L} \qquad (2.4)$$

Table 2-2 below demonstrates the effect of maintaining Froude similitude on the wave characteristics for a range of model sizes, using a prototype wave condition $H$ = 2 m, $T$ = 8 s, $L$ = 100 m.

**Table 2-2: Effect of model scale on wave parameter using Froude scaling**

| Scale | Scale ratio | $H$ (m) | $L$ (m) | $T$ (s) |
|---|---|---|---|---|
| Full scale | 1:1 | 2.0 | 100 | 8 |
| Medium scale | 1:10 | 0.2 | 10 | 2.5 |
| Small scale | 1:40 | 0.05 | 2.5 | 1.3 |

## Scaling sediment transport

Though the correct wave geometry can be obtained through Froude similitude, when modelling sediment transport, the size of sediment must also be scaled correctly. The key forces acting on a submerged suspended particle are the viscous drag and gravity. By applying the Reynolds scale ratio, the deviation of these factors from model similitude can be measured and the potential for sediment transport scale effects estimated. Table 2-3 compares the Froude and Reynolds scale ratios of the examples in Table 2-2, using the sediment fall velocity as the numerator in Equations 2.2 & 2.3 for model and prototype. Sediment fall speeds were derived from Soulsby (1997).

**Table 2-3: Comparison of Reynolds scale ratios and Reynolds number for a range of experiment scales and particle sizes**

| Scale | $H_o$ (m) | Proposed model sediment | | Model scale ratio | | |
|---|---|---|---|---|---|---|
| | | Indicative grain size(mm) | Fall velocity (m/s) | Length | Froude | Reynolds |
| Full scale | 2.0 | 0.30 | 0.0500 | 1:1 | 1 | 1 |
| Medium scale | 0.2 | 0.10 | 0.0080 | 1:10 | 1 | 33 |
| Small scale | 0.05 | 0.04 | 0.0014 | 1:40 | 1 | 152 |

In the table, the Reynolds scale is distorted in small and medium scale experiments, as a result of using water in both the model and prototype, which causes the viscosity to be too high in the model. This scale effect increases the particle drag and the boundary layer at the water sediment interface, consequently the threshold for sediment movement is increased and it is more difficult for particles to be lifted in suspension. Suspended sediment transport is a key process in the movement of particles on a sand beach, and therefore critical to toe scour, where turbulent wave breaking and high velocity flows occur in front of the wall.

In the medium scale example, where the wave height was large compared to the sediment diameter, the wave generated velocities (hence energy) would be sufficiently to dominate over the effect of the increased viscosity. However in the small scale tests, the Reynolds scale ratio were even greater, suggesting that viscous forces would be dominant and act to impede suspended sediment transport. Even if the Reynolds scale was relaxed and Froude similitude enforced, the small scale test would require a $D <$ 0.06 mm. This would contain a significant proportion of silt material which would be washed out changing the material grading; furthermore when $D < 0.06$ mm, the bed shear stress threshold increases due to the development of viscous inter-particular forces, which change the character of the material from granular to cohesive. The smallest diameter sand available has a typical mean diameter ($D_{50}$) of around 0.1 mm, despite this would continue to be transported as bedload in a small scale flume.

Researchers have attempted to overcome these issues using lightweight sediments with a distorted fall velocity. The fall velocity represents the balance between gravity pulling the sediment particle mass towards the bed and the drag on the particle, which is dependent on the water viscosity and particle diameter. By maintaining a sediment particle size in the grain size range, flocculation is prevented and the drag is increased. To offset the increased mass, the particle density is reduced using plastic materials e.g. Bakelite (Bettess, 1990). This produces a material with a slow fall velocity which is easily suspended. However these particles are often angular in shape and have tendency to stick to the water surface due to surface tension, therefore they are not widely used in coastal scour research.

Alternative methods for achieving suspended sediment transport include Dean (1985), who supported by Hughes & Fowler (1991), suggested the Dean fall speed parameter should be used to maintain Froude kinematic similitude between the prototype and model sediments (Equation 2.5).

$$D_{ws} = \left[ \frac{H_0}{w_s T_p} \right] \tag{2.5}$$

Where $H_0$ (m) is the significant wave height, $w_s$ (ms$^{-1}$) is the fall speed of the mean sediment diameter and $T_p$ (s) is the peak wave period. The equation represents a balance between wave forces lifting the sediment and the gravity driven settling velocity of the

particles towards the bed. When investigating toe scour, Xie (1981) proposed a similar mobility number for maintaining similitude and suggested that if the threshold in Equation 2.6 was exceeded, suspended sediment transport would occur in the model.

$$\frac{U_w - U_{cr}}{w_s} \geq 16.5 \qquad (2.6)$$

Where $U_w$ (ms$^{-1}$) is the maximum value of orbital velocity at the bed and $U_{cr}$ (ms$^{-1}$) is the critical velocity for incipient sediment transport. The equation represents the balance between the wave generated peak bed velocity, which causes sediment suspension and velocity of the sediment falling back to the bed ($w_s$). Taking forward Table 2-2, but using the smallest diameter sand possible in the small and medium scale experiments, Table 2-4 demonstrates the Dean fall speed parameter (Equation 2.5) and Xie mobility number (Equation 2.6) for a range of tests conditions.

**Table 2-4: Model scale based on Dean fall speed parameter and Xie mobility number**

| Scale | Scale ratio | $H$ (m) | Grain size (mm) | Dean fall speed parameter | Xie mobility number |
|---|---|---|---|---|---|
| Full scale | 1:1 | 2 | 0.3 | 5.8 | 47 |
| Medium scale | 1:10 | 0.2 | 0.1 | 5.8 | 40 |
| Small scale | 1:40 | 0.05 | 0.1 | 2.9 | 18 |

While similitude can be maintained between the fall speed parameters in the full and medium scale tests, the limited sand diameter available for the small scale test prevents this model reaching similitude. The Xie mobility number indicates that in the both the full and medium scale conditions, suspended sediment transport would occur, however the small scale test is close to the threshold, indicating that a degree of bedload transport would also occur, and highlights the risk of conducting small scale sediment transport studies to investigate seawall scour.

### Summary of model scale criteria

Achieving similitude for both Froude and Reynolds numbers is not possible; therefore a compromise solution must be sought. In the case of modelling coastal scour, Froude scaling is the most appropriate with the Reynolds similitude relaxed. The investigation of the Reynolds number and sediment mobility numbers for a range of model scales, demonstrated that the smallest sand available ($D_{50} \approx 0.1$ mm) should be used at

minimum of medium scale, with a wave height of 0.2 m or greater to achieve sediment suspension and avoid the effects of cohesion. Small scale experiments, which are relatively inexpensive to conduct and quick to setup remain useful when conducting hydraulic studies into wave impacts and flow processes at the seawall structure, but do not accurately recreate suspended sediment transport.

## 2.4. Summary

This chapter examined the different type of seawall structures and the wave and sediment transport processes occurring in front of them. Interruptions in the sediment supply and the effect of sea level rise were shown to cause the beaches fronting these structures to lower and as a result allow wave action to reach the wall. Waves breaking onto the seawall were found to either break before, onto, or remain unbroken and be reflected offshore. Wave breaking induces turbulent and causes erosion at the toe of the wall. This can lead to structural damage, undermining and eventual failure, resulting in coastal erosion and flooding.

Field evidence of toe scour is largely based upon anecdotal evidence and visual observations due to the harsh energetic environment, forcing researchers to build scaled physical models. Model tests require careful planning due to the choice of model fluid and sediment being limited. Reliable results can be achieved by applying appropriate scaling rules. However it remains difficult to achieve suspended sediment transport in small scale tests. These observations suggest a need for collection of new physical model data at medium scale and field data to validate these experiments.

# 3. Literature review

This review is split into five sections. The first section provides an overview of key literature reviews already conducted in this field; the second investigates existing field research into the broad scale interaction of storm events and the beaches, and anecdotal field evidence of scour. The third and fourth sections review the results of 2D & 3D physical model studies and of reported numerical modelling. The final section sets out the current design guidance for the prediction of toe scour, before establishing the future research requirements.

## 3.1. Existing literature review conclusions

The review entitled "*The effect of seawalls on the beach*", by Kraus (1988) included a comprehensive analysis of laboratory model studies, field experiments and conceptual arguments. He proposed in the short term, that beaches with seawalls undergo similar changes to adjacent natural beaches. In the longer term seawalls impound sediment and prevent erosion, leading to a slow reduction in beach levels. However this was not the case at the seawall toe and at the end of the structure, where significant short term processes could cause highly localised erosion.

Based on small scale physical seawall model tests and supported by additional breakwater studies with flat beach profiles and non-breaking reflective waves (i.e. out of the surf zone), the review recommended that the maximum scour depth would approximately equal the deepwater incident wave height, though it was noted that the scour process was highly complex. The review highlighted the importance of reflected waves in the scour processes and the need for more frequent coastal monitoring.

In their updated review paper (Kraus & McDougal, 1996), an array of field and laboratory experiments were added to the earlier review to explore beach and seawall interaction. Specific to toe scour these included two medium scale physical model tests and additional field monitoring studies of beach profiles. However, no direct measurements of field scour were available. The authors retracted their previous conclusion, that wave reflections were critical to toe scour, which was found to be biased by the dominance of breakwater studies in their existing review. The review presented a wealth of information to show seawalls have no short term adverse impact on beach level erosion and recovery compared to unwalled beaches. The maximum

scour was suggested to occur at the highest water level, as this would allow the largest waves to reach the wall and cause sediment suspension, which would be transported by currents. The hydraulic processes occurring at the wall face, and the possibility that wave impacts and vertical flows could affect scour were not discussed. The authors appear to place significant confidence in their own work in Kraus & Smith (1994), which supports these conclusions, though they only conducted three medium scale tests ($H_0$ = 0.7 to 0.8 m) using a seawall.

The review recommended that additional flume experiments be conducted at both medium and full scale to overcome scale effects present in the small scale tests reviewed in the previous study. They reinforced the need for field measurements from the perspective of developing long term beach profile trends; this recommendation seems to overlook the need to measure short term toe scour events too.

Sutherland *et al.* (2003)'s review followed and produced a comprehensive scoping study report for Defra. The study investigated beach lowering in front of coastal structures and was the first to consider both the medium term morphological effect of seawalls on the beach and the short term localised scour effects. The review included discussion of both reflected and breaking wave flows and the effect of the tide which would limit the water depth, hence the risk of scour at the structure.

The review criticised the use of small scale sediment transport physical models, due to their severe scale effects and emphasised the need to collect field data. It was suggested that scour may be a relatively short lived phenomena, perhaps peaking at the height of the storm, when it is not possible to make beach profile measurements, then infilling before evidence can be collected. This hypothesis was supported by the work of Powell & Lowe (1994), who conducted shingle scour modelling at the same institution as Sutherland. Sutherland *et al.* (2003) recommendations led to the funding for the Defra beach lowering study project, and formed part of the author's own research.

Based on these comprehensive reviews, my review focused on literature pertinent to localised scour at the toe of seawall structures with sandy sediments. The review did not include scour at shingle beaches, as only two studies (Powell & Lowe, 1994., Loveless & Grant, 1995) had been conducted.

## 3.2. Field studies- interaction of storms and beaches

To put the seawall scour literature into perspective, the larger scale processes that occur when beaches are exposed to storm conditions were briefly considered.

Field research by Wright & Short (1984) put forward the concept of reflective and dissipating beach profiles, where sandy beaches tended to form bars and dissipate energy over a wide surf zone and coarse shingle beaches form a steep profile, reflecting wave energy offshore. Using this generic categorisation other researches have extended this work by collecting beach profile measurements during storm conditions.

Lee *et al.* (1998) collected beach profile measurements through the surf zone at Duck, a sandy beach in North Carolina USA, using a towed carriage, before, during and after a moderate storm ($H_m > 4$ m). The results confirmed that beach material was transported from the upper beach face and deposited offshore to form a bar, in response to increasing wave height. As the storm diminished the new material, being uncompacted, was rapidly transported back onshore. This study highlights the mobility of beach profiles and the cautious use of post storm beach profiles to detect small scale, short duration processes, such as toe scour.

Dean (1986) reasoned that beach profile changes were also likely to occur at beaches fronting coastal structures, suggesting the depth of scour would equal the area of sand that would have been transported offshore if beach profile was not impounded by the wall. The physical model studies of Barnett & Wang (1998), Kamphuis *et al.* (1992), McDougal *et al.* (1996) support this concept. However the balance of scour and accretion was found to be out of equilibrium. It also seemed unlikely that this transfer could continue *ad infinitum*, as the increased water depth would eventually reduce sediment transport at the bed. Until cross shore beach profile field measurements are conducted on a beach with a seawall, this theory remains unproven and does not explain why a localised trough would form at the wall toe, as witnessed in physical model experiments.

Though beaches are often studied in 2D, the possible effect of 3D and longer period motions (> 60 s) was briefly considered. Russell (1993) measured a range of nearshore processes including undertow currents and infragravity wave processes in the surf zone on a sand beach. The experiment demonstrated that although wave breaking and

shoaling may appear relatively consistent, the longshore, cross shore and internal flow processes occur over a range of temporal and spatial scales. In particular cross shore flows can become entrained at seawalls to become longshore flows. Though forming part of the overall sediment transport process, these flows were considered less important then the dominant cross shore effect of wave breaking and wave reflection.

### 3.2.1. Field evidence of toe scour

Physical evidence of toe scour in the field remains elusive. Despite seven years of routine beach profile monitoring in Monterey Bay, California, Griggs *et al.* (1994) found no evidence of scour trenches in front of any of the seawalls surveyed. It was not clear how soon after a storm the profiles were collected, and is therefore possible falling tide or receding storm conditions rapidly reworked the beach. Without continuous measurements it is not possible to conclude either assumption, therefore routine beach profile measurements were excluded as a source for toe scour data.

A body of anecdotal evidence does however remain. In a meeting of leading coastal engineers (ICE, 1985) toe scour was proposed as the most common cause of seawall failure and was followed by a survey of UK local authorities (CIRIA, 1986) to determine the most likely form of damage to seawalls. Of all the reported seawall failures, toe scour was identified to be the most common cause (34%) and was a contributing factor in a further 5% of cases, through removal of backfill and breaching. To the author's knowledge a similar survey has not been reported. However, news articles and continued interest at conference events, suggests that scour is a continuing concern for coastal engineers and managers.

Occasionally professionals have provided photographic evidence of toe scour features (Figure 2-1a, 3-1, 3-2). These often show troughs or runnels along the toe of a seawall, however the size and extent of these features at the peak of the storm remains unknown.

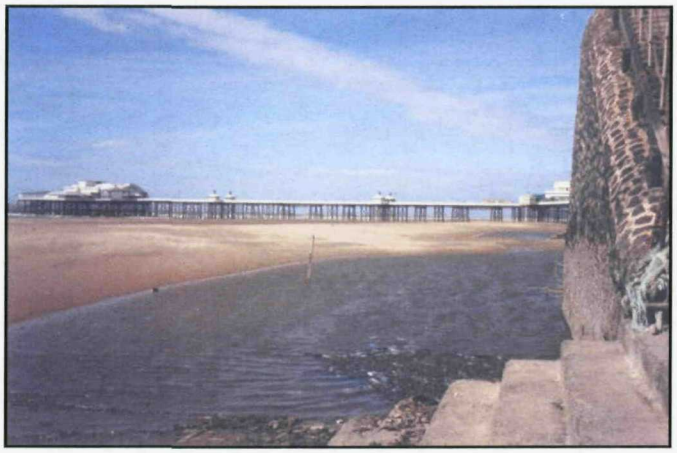

**Figure 3-1: Blackpool, UK - A trough at the toe of a vertical seawall (from HR Wallingford, 2005)**


**Figure 3-2- Summerplace, Florida,USA. Trough below vertical sheet piles (from Clark, 2004).**

It is suggested these features did not completely infill due to the storm wave height decreasing rapidly or tide levels falling before the beach could establish a new equilibrium profile. In the case of Figure 3-2, the photo was taken on the Florida coast following hurricanes Francis and Jeanne, where it would be expected that significant offshore sediment transport would have occurred under these exceptional conditions.

Several authors have collected post storm scour data from breakwater structures (e.g. Silvester & Hsu, 1997; Sato *et al.* 1968). These established that toe scour is often equal to the offshore significant wave height, and that agitation by reflected waves followed by transport by currents appeared important. However transferring these results inshore to seawalls is difficult, due to the effect of tidal range on the water depth.

Though not directly concerned with toe scour, Miles *et al.* (2001) collected simultaneous sediment transport data from a walled and non-walled beach at Teignmouth, UK. The short dataset included suspended sediment concentrations, the current velocity and the incident wave conditions. Under relatively mild, 'dissipative' conditions, ($H_0$ 0.2 to 0.3 m), slight accretion was noted on the beach, whereas no accretion occurred at the seawall. No toe scour troughs were observed during the experiments.

The suspended sediment concentrations were found to be up to three times higher in front of the wall, due to incident and reflected waves moving sand into suspension. Longshore currents were also found to be higher at the seawall, indicating the potential for longshore transport. Under similar conditions cross shore transport was greatly reduced at the seawall and the net transport was lower due to the phase of the wave reflections (Miles *et al.* 2001). Unfortunately these observations were only collected under in mild conditions, but highlight the need to achieve sediment suspension in physical model experiments.

There have only been three attempts to collect real time beach level data from the toe of a seawall. Two of these studies, at Blackpool and Southbourne using HR Wallingford *Tell-Tail* sensors, are presented in Section 4. A further study conducted at Teignmouth using the same instruments, as part of COAST3D (HR Wallingford, 2001), did not reveal clear evidence of toe scour due to a highly mobile shingle layer. These experiments were severely limited to just two point measurements, with low resolution due to the highly robust design necessary to withstand the intense forces and flows occurring in front of coastal structures. A detailed field monitoring campaign to observe both beach profile and toe scour in unison has yet to be conducted.

The lack of field research literature supports Sutherland *et al.* (2003) who emphasised the need for further monitoring experiments and improved sensor designs to enable collection of data for validation of model results. At present the combined effect of wave breaking and turbulence on sediment transport and the resulting toe scour can only be observed in detail within physical models.

## 3.3. Coastal physical models

Coastal physical models typically consist of either large shallow basins to generate 3D coastal processes for an entire section of coast, or narrow tanks with deeper water to represent a 2D cross section of the shore profile. Most seawall physical model studies have been conducted using 2D flumes as these enable larger wave heights and simpler interpretation. However, the waves are limited to a shore normal direction. A range of 2D model studies were reviewed based on their scale, followed by a review of two 3D experiments relevant to seawall sediment transport.

### 3.3.1. 2D Physical modelling of seawall toe scour

**Past studies**

The earliest research into scour at vertical seawalls was published by Russell & Inglis (1953) who used fine sand and small scale regular waves ($H$ = 0.07 m) to simulate the effects of tide on a beach before and after installation of a seawall. In the tests, a vertical structure was inserted into an equilibrium beach profile. This caused an immediate drop in nearshore beach level at the wall, though the beach profile further offshore remained relatively unchanged. These changes were attributed to turbulence and the effect of reflected waves, with maximum scour equal to the incident wave height and localised at the top of the beach profile. The results suggested erosion would cease when the water depth at low tide equalled the wave height, i.e. the waves would break. The authors proposed that scour depth would remain less than the incident wave height, a 'rule-of-thumb' still used by coastal engineers today.

Ichikawa (1967) conducted a range of breakwater tests at small scale using sand $D_{50}$ = 0.23 mm. Though modelling breakwaters, the tests utilised broken, breaking and reflected waves by varying the water depth. The key finding was that maximum scour occurred at the wall toe, increased with wave height and was greatest when curling breakers fell onto the face of the breakwater. Figure 3-3 shows the scour depths for tests which produced plunging breakers. The relative scour depths appear greater then those reported by Russell & Inglis (1953), and would appear to be a result of the steep beach slopes used in the tests (1:5 & 1:10), which would be expected to flatten to a more natural slope exaggerating the toe scour depth. In the majority of cases the maximum scour depth did not significantly exceed the incident wave height.

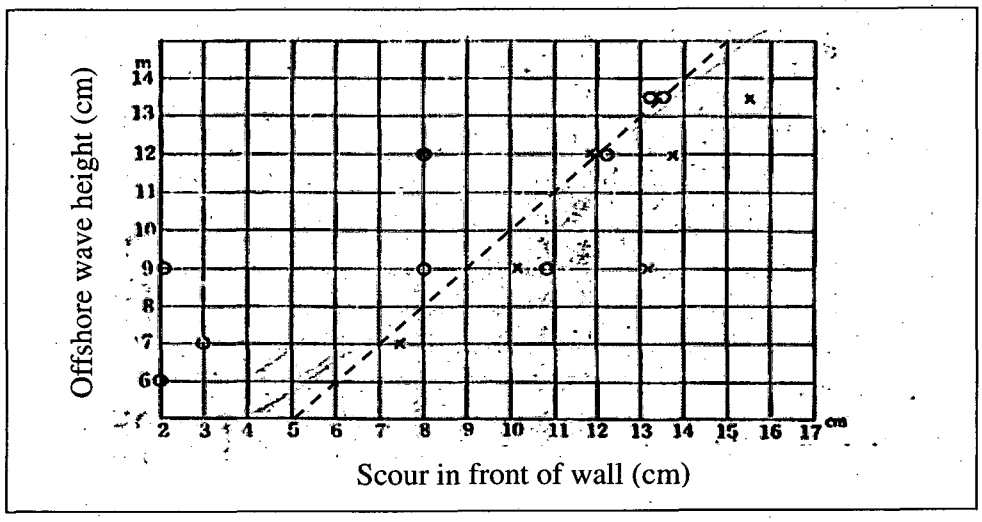


**Figure 3-3: The effect of wave height on the toe scour, for plunging breakers. X= 1:5 slope, O=1:10 slope (from Ichikawa, 1967)**

Despite conducting several similar tests, it is not clear why Ichikawa (1967) did not observe the reflected wave sediment transport patterns reported by Herbich & Ko (1968) who conducted tests at a similar scale, using only non-breaking waves. This paper was the first to show that the scour and accretion regions on the beach profile follow the orbital flows associated with the non-breaking reflected waves. This pattern of scour is clearly different to the processes observed by the previous authors under breaking wave action, highlighting the importance of water depth in the scour process.

Sato *et al.* (1968) conducted both small and medium scale 2D tests into the effect of reflection dominated sediment transport on breakwater structures. The tests used a sand bed ($D_{50}$ = 0.2-0.7mm), regular period waves and radioactive tracers to observe the sediment transport direction; however no comparison was made between the different model scale results. Scour was observed to occur by two different processes depending on the position of the wall in the surf zone. When placed in the offshore zone, sediment erosion and accretion coincided with the standing wave pattern generated by reflected waves. At the wall, flow velocities were reduced, causing sediment accretion, which had the potential to infill any earlier toe scour.

When the wall was placed further inshore, rapid scouring occurred due to breaking waves jetting down into the bed and suspending sediment. The eroded material accreted further offshore, however the volume of accretion was found to exceed the scour volume, suggesting some of this material was transported from further offshore. Low

steepness waves, i.e. long period, were found to cause the deepest scour, which was exacerbated when the wall was placed near the wave plunge point. A series of four scour types were proposed. The maximum scour was suggested to not exceed the offshore wave height.

These tests were comprehensive and included a range of regular period wave breaking conditions and structures. However, the lack of experimental detail limits the useful data that can be extracted. In particular it was not clear at which scale certain results and conclusions were drawn from. Despite this, this paper was the first to publish evidence of both reflection driven scour and wave breaking scour processes together.

Adopting a similar method, Song & Schiller (1977) conducted small scale scour experiments on a seawall at different positions across the surf zone, using fine sand ($D_{50}$ =0.17 mm) and regular waves ($H$= 0.04 to 0.07 m). The deepest scour occurred when the seawall was placed mid way between the wave break point and original shoreline position. When the scour depths obtained by Sato *et al.* (1968) and Song & Schiller (1977) are compared, the small scale tests compare well and both show scour decreasing with increasing wave steepness. However the magnitude of scour in the medium scale tests conducted by Sato *et al.* (1968) was greater then that predicted by Song & Schiller (1997), highlighting the scale problems associated with modelling sediment transport at small scale.

In modelling a permeable breakwater, small scale experiments by Hotta & Marui (1976) were the first to suggest that beach profile change and scour can occur together, as seen in Ichikawa (1967), and to highlight the need to define a common baseline to distinguish between these two processes. This is also of importance when collecting post-storm beach level measurements, which are meaningless without knowing the level and shape of the pre-storm beach profile.

With the exception of the two medium scale tests conducted by Sato *et al.* (1968), all the preceding research was conducted at small scale using regular waves and would therefore have included significant scale effects. The use of regular period waves would also tend to promote reflective wave patterns. Though the qualitative results from these tests are useful, the quantitative scour depths and prediction formulas may have been

compromised, as they are likely to be dominated by bedload transport processes. They were not considered further.

**The seawall versus the beach debate**

Between 1973 and the late 1980s, coastal scour research appeared dominated by studies investigating reflective wave processes at deepwater breakwaters. This was perhaps driven by their increasing popularity for harbour protection around this period and some notable failures prior to this date (French, 2001). Further inshore, research into seawall problems concentrated on the overall effect of these structures on the beach, fuelled by an extensive discussion on the positive and negative aspects of hard engineering structures on the coastline. The argument and debate stimulated by this issue is depicted well in a series of papers in Kraus & Pilkey (1988) special issue of the Journal of Coastal Research-"*The effects of seawalls on the beach*".

**Recent studies**

Xie (1981) undertook a comprehensive study of sediment transport patterns and particle velocities in front of a vertical breakwater. The study was the first to utilise both regular and irregular period waves, different sediment diameters and enabled a comparison between tests conducted at small and medium scale. Using both the 38 m & 46 m flumes at Delft University, non-breaking irregular period reflective wave conditions (0.05 to 0.10 m) were generated over a flat sand seabed.

Using irregular period waves, a nodal scour pattern was formed, which decreased in amplitude with distance from the wall, and was unlike the linear nodal profile in the regular wave period tests (Figure 3-4). The pattern was a result of vertical wall forcing the irregular incident and reflected waves to occur in phase. However, with increasing distance, the two wave trains became increasingly out of phase, reducing the standing wave height. These results suggested earlier regular wave flume studies had overestimated reflective wave scour depths due to regular period encouraging waves to remain in phase over a longer distance from the wall.

Xie's study also noted that the sediment diameter, hence type of transport (suspended or bedload), dictated if accretion or scour would occur at the wall or ¼ wavelengths from the wall (Figure 3-5). The direction of transport was found to be dependent on streaming within the sediment boundary layer. Larger sediment tended to be transported

at bedload, hence were primarily driven by the boundary layer flow towards the node. Smaller sediments achieved suspension, and were transported by the standing wave field, this was directed from the node towards the antinodes.

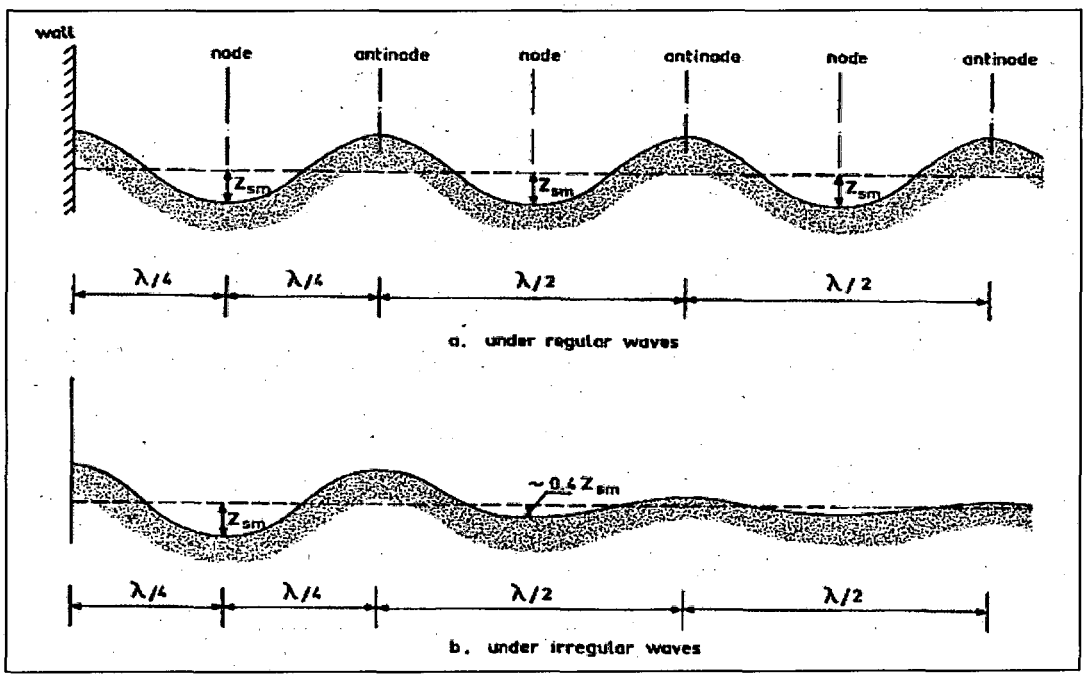


**Figure 3-4: Regular and irregular wave bed scour profile (from Xie 1981)**

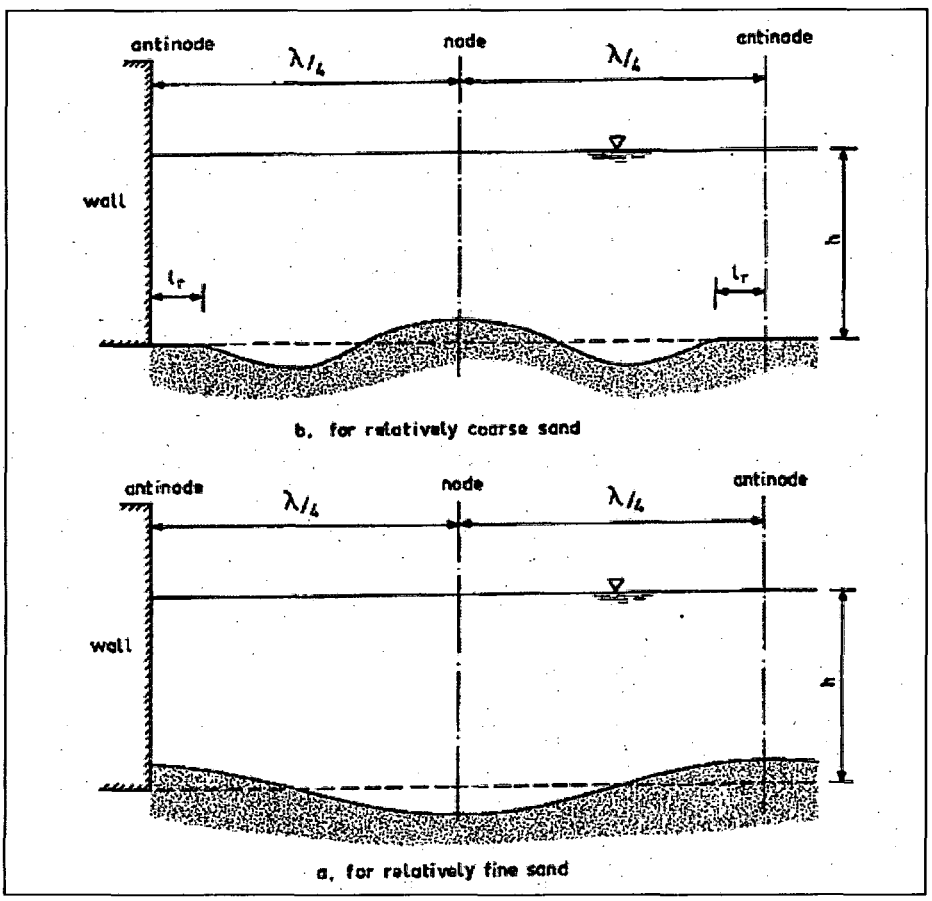


**Figure 3-5: Scour and accretion position relative to sediment size (from Xie, 1981)**

Xie's thesis proposed a scour prediction equation, which was based on the wavelength and toe water depth for regular period non-breaking waves (investigated in detail in Section 5.1.1). In using only the results from the regular wave study, it is probable that the scour predictor overestimates the depth of scour.

Xie (1981)'s results were repeated and extended by Irie & Nadoaoka (1984) using a combination of small scale 2D tests ($H_0$ = 0.65 m) to observe the wave velocity field; medium scale 2D tests to evaluate sediment transport; and a series of 3D tests to observe beach morphology (these are discussed in Section 3.3.2). The terms N-type or L- type transport were applied to describe sediment transport towards the node or to the anti-node respectively, an identical process to that described by Xie (1981). The study found that suspended sediment transport typically occurred when the wave orbital velocity exceeded the sediment fall velocity by a factor of ten. On reflection, these velocities would not have been achieved in the small scale studies preceding this research, confirming previous suspicions regarding the dominance of bed load transport.

Barnett & Wang (1998) re-analysed Dean's (1986) proposition that seawall scour volume would be equal to the volume of beach material impounded by the seawall and hence unable to move offshore to produce an equilibrium profile. Small scale tests were run where a vertical seawall was placed at various points on an equilibrium beach profile. The beach profiles in the walled and unwalled tests remained similar. Though toe scour was generated, it remained less then half the volume of sand material impounded by the seawall. The water depth remained the key variable in controlling the scour depth, with the highest water levels causing the deepest scour. Wave reflections were considered less important. In reviewing the experimental setup, in each test the wave height to water depth ratio was around unity or greater, therefore wave breaking would have been dominant, as opposed to wave reflection as seen the in preceding experiments.

**Investigating the effect of flow on sediment transport**

To understand the scour process, it is important to first explore the fundamental mechanics of sediment transport. In still water, granular sediments remain in place due to the force of gravity and the interlock between adjacent particles (friction). When a flow is introduced, lift is generated above the particles. In addition exposure to the flow induces lateral drag. Sediment transport occurs when the lift and drag forces are sufficient to overcome friction and gravity. By considering the water and sediment as two separate layers moving over one another, these processes can be equated to a shearing stress.

With reference to scour, sediment particles will be transported in regions where the bed shear stress exceeds the critical value for incipient sediment motion. Scour will cease when either the velocity is reduced e.g. the scour increases the water depth, or the sediment becomes reconfigured into a more efficient shape which are less prone to shear (e.g. ripple bedforms).

Hughes & Fowler (1991) conducted a small scale hydraulic wave flow study at the US Army Experimental station in Vicksburg using a fixed seabed and non-breaking reflected irregular period waves ($H_0$= 0.09 m) at a vertical breakwater. By collecting measurements of near bed flow velocity, they identified regions of high shear stress and applied these to the design of breakwater toe armour. These tests then were repeated using a movable sand bed and irregular waves, which confirmed Xie (1981) type patterns of sediment erosion and accretion corresponding to the flow regime. The authors assumed the deepest scour would occur at the position of maximum near bed velocity / shear stress, suggesting scour would cease when the bed profile shape reached equilibrium with the wave flow velocity.

Based on this assumption, the paper proposed a modification to the Xie (1981) scour prediction equation for irregular waves, which led to an overall *55%* reduction in predicted maximum scour depth compared to the original regular wave period equation (Hughes & Fowler 1991, p1897).

O'Donoghue & Goldsworthy (1995) took forward Hughes & Fowler (1991) through a series of small scale hydraulic model experiments using a vertical seawall, with breaking and reflective waves. The results indicated that linear wave theory provided an

acceptable method for the prediction of near-bed velocities at vertical walls. However when the water depth was shallow and waves large ($H_0 / d_t \approx 0.63$), the reflected waves caused the incident waves to break in front of the wall. As a result, linear theory under predicted the near bed velocities. It appears the authors were the first to measure the increase in flow velocities at seawalls due to breaking waves, as witnessed Sato *et al.* (1968), Song & Schiller (1977), and Fowler (1992), who suggested this would cause increased sediment suspension and toe scour.

Research into non-breaking waves continued at the same institution in Seaman & O'Donogue (1996), who used a bed load transport model to study the growth of nodal accretions under reflective irregular waves. The study demonstrated how the asymmetry of the near bed flows caused sediment ripples to migrate, producing accretion at the nodal points, and scour at the antinodes. By using a hydraulic flow model with nodal bedforms moulded from cement and a Particle Image Velocimetry (PIV) system, the lee vortex formation led to the growth and eventual equilibrium at the nodes. These experiments were the first to observe the hydraulic structure of sediment transport under reflected waves; however this did not include an investigation of flows at the wall toe.

To draw together the various scour mechanisms, Loveless (1994) attempted to provide a description of the various scour processes that could occur in front of a seawall over a range of toe water depths. Though the vertical scale of the scour shape is misleading and significantly exaggerated, Figure 3-6 provides a useful summary of the key process thought to dominate scour. This paper provided a good rationale for researchers to expand their limited perspective of the scour process beyond that dominated by either wave reflection or breaking wave impacts. However the article is rarely cited in subsequent studies. This was perhaps a result of its publication at a less well known conference (2$^{nd}$ Conference on Hydraulic Modelling, London) or the lack of experimental data to support these assumptions.

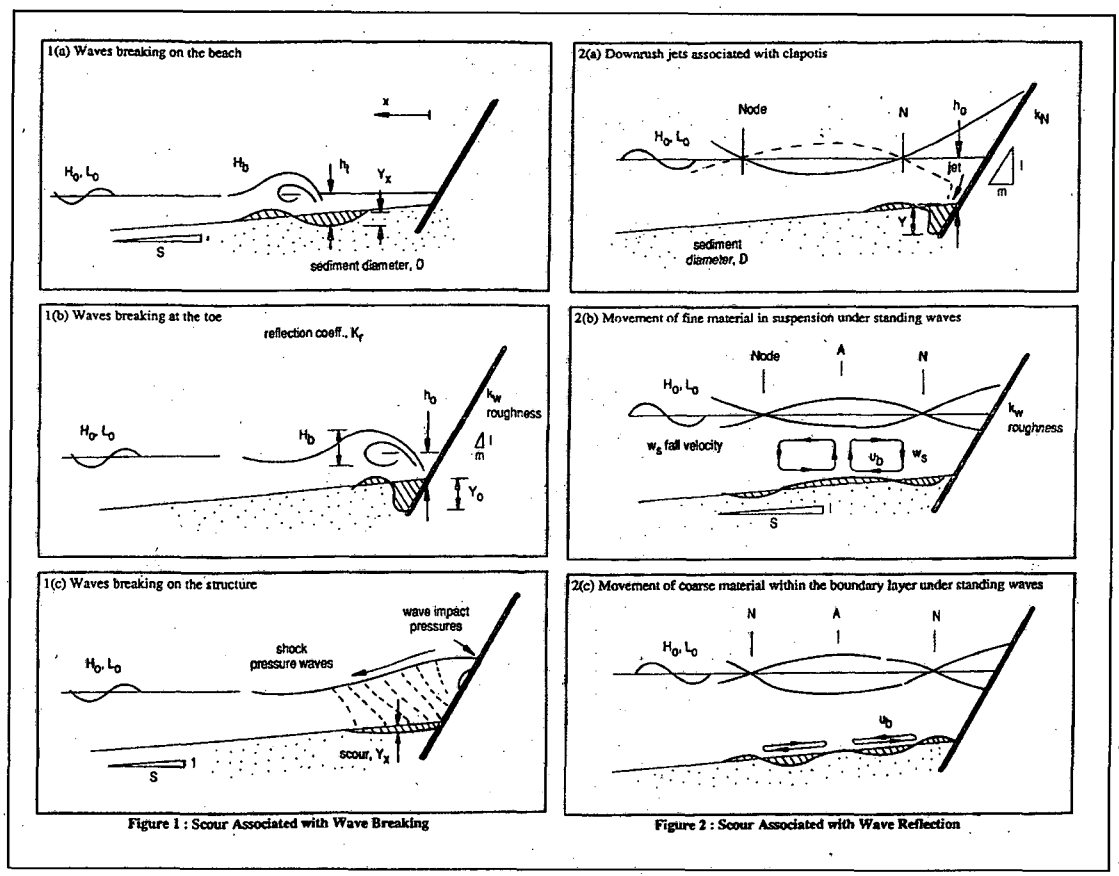


**Figure 3-6: Various toe scour situations leading to scour in front of a seawall (from Loveless, 1994)**

Unfortunately these concepts were not developed further; instead Loveless conducted new research into scaling issues associated with shingle toe scour and sediment liquefaction (Loveless & Grant, 1995. and Loveless *et al.* 1996).

Continuing the theme of wave flows at vertical walls, Gao & Inouchi (1998) used a small scale sediment transport study ($H$ = 0.05 - 0.12 m) to investigate the effect of broken clapotis wave flows on vertical breakwater scour. In the study, regular period waves which had already broken before reaching the seawall, were found to produce deeper scour than either unbroken standing waves or waves breaking at the wall. Four types of scour pattern shape were identified, which were dependent on the balance between wave reflections transporting sediment onshore, and waves rushing down the wall face producing turbulence and offshore flows at the wall toe. Scour was found to increase with wave height, but was also dependent on the sediment diameter; larger sediments tended to be transported as bedload and accreted at the toe of the wall.

The authors also collected video images of the flow pattern and single point velocity measurements in front of the wall. These confirmed the position of the node / antinode wave profile, and the high velocity flows (0.4 to 0.6 $m.s^{-1}$) associated with wave downrush (Figure 3-7). Though collected near the wall, these measurements were less detailed then the measurement collected using PIV by Seaman & O'Donogue (1996), but provide a useful insight into the contribution of breaking wave flows to scour.

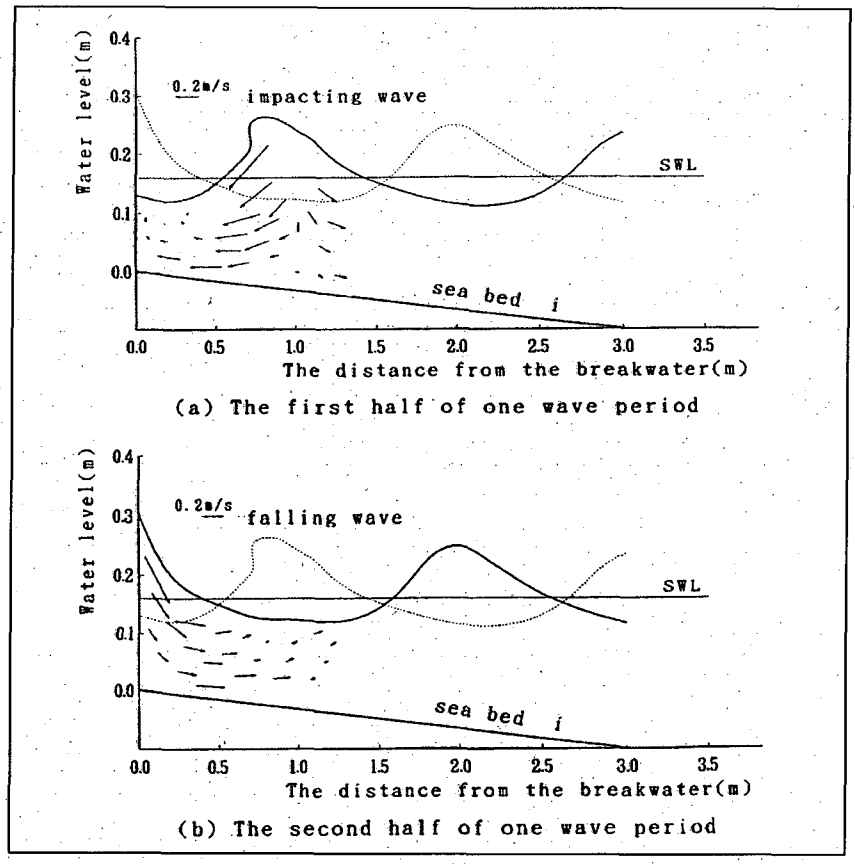


**Figure 3-7: Flow visualisation of broken clapotis wave following reflection from a vertical wall (from Gao & Inouchi, 1998)**

Tsai *et al.* (1998) conducted series of 2D flow visualisation experiments using sloping seawalls and determined the downrush component of the flow at these structures. The flow tended to peak when waves broke at the toe of the wall causing a strong down rush, a rotational toe vortex and turbulence. It was suggested these flows could exacerbate reflection driven scour. Unfortunately the effect of downrush on sediment transport was not measured, however the potential for these flows to contribute to scour under breaking waves was demonstrated. These flows were already known to exist at vertical walls (Gao & Inouchi, 1998), though their effect and magnitude at shallow and intermediate toe water depths ($H_0 / d_t < 2$) has yet to be determined.

**Recent seawall sediment transport studies**

Using a 110 m flume at the US Army Experiment station in Vicksburg USA, Fowler (1992) conducted a series of medium scale sediment transport tests to investigate scour at vertical seawalls. The experiments were the first to combine medium scale irregular waves and suspended sediment transport, with a clear methodology and are considered a key reference in physical model scour research.

Using mostly breaking irregular waves ($H_0$ = 0.2 - 0.3) and four regular wave tests, Fowler measured scour over a flat sand bed with a 1:15 slope and a vertical seawall. The use of fine sediment ($D_{50}$ = 0.13mm), irregular waves and an 8 m beach profile enabled a comprehensive set of results to be collected for breaking wave conditions, which achieved suspended sediment transport. The test commenced from a flat beach profile to allow comparable scour depth measurements to be collected.

The experiments determined toe scour to be primarily dependent on the incident wavelength and water depth ratio, in agreement with the tests conducted by Xie (1981) and Hughes & Fowler (1991). Furthermore the maximum scour depth never exceeded the incident wave height.

A tentative prediction equation was produced for maximum scour by combining the data with regular wave period tests from Song & Schiller (1977) and Barnett(1987). This enabled Fowler (1992) extended his prediction equation into deeper water, despite collecting evidence which showed that regular period waves tend to overestimate scour depth compared to their irregular period equivalents. The prediction equation is discussed further and tested in Section 5.1.1.

Through considering shingle beaches, Powell & Lowe (1994) drew emphasis on the importance of water depth on the scour process. Their peak scour depth ratio ($S_t / H_0$) occurred for a relative water depth between $1.5 < H_0 / d_t < 2.0$. In this range waves would be expected to be breaking in front of or onto the seawall, confirming the importance of wave breaking to the scour process on coarse sediment beaches.

Kraus & Smith (1994), as part of the SUPERTANK test programme, conducted a large scale study (104 m long flume, $H_0$ = 0.4 to 1.0 m) to investigate the interaction of seawalls with beaches. As part of the large test programme, three 2D vertical seawall

model tests were conducted using a medium sand beach ($D_{50}$ = 0.22 mm) with an equilibrium beach profile from the previous model run. In each test only a small trough occurred at the toe of the wall and the beach profile underwent only minor changes using constructive and then destructive waves (McDougal *et al.* 1996).

It appeared that the equilibrium beach profile caused waves to break offshore, and was compounded by the severely depth limited waves at the wall, a result of the shallow toe water depth ($H_0 / d_t < 1$). The tests also used only short bursts of wave activity before changing either the wave height or water depth, limiting the time for scour to develop. A scour prediction equation was developed which included the sediment grain size, and is discussed in more detail in Section 5.1.1.

Of the experiments conducted, Test ST_CO was the only one to generate a small scour trough, and included a shallow toe water depth, with significant wave breaking offshore. When the test was repeated with slightly deeper toe water depth ($H_0 / d_t = 0.9$) scour did not occur, though this test was only run for 570 waves, which was perhaps insufficient time for the beach profile to reach a new equilibrium.

In comparing these results to the larger scour depths found by Fowler (1992), McDougal *et al.* (1996) suggested that these were a result of profile adjustment from the initial planar beach profile in addition to scour. Though an equilibrium beach profile would occur in the prototype situation if sufficient sediment is available, until the mechanics of the scour process are better understood, it is suggested initial beach profile remain planar to allow comparison between model runs and existing research.

### 3.3.2. 3D physical modelling of seawall toe scour

Three dimensional physical modelling utilises large basins, typically between 100 to 500m$^2$ depending on the scale, and enables the assembly of a whole section of coastline. This type of study allows oblique wave directions to be modelled, which generate both longshore and cross shore processes. However wave heights are limited to around 0.1 m, therefore sediment transport is dominated by bedload processes, providing only an indication of the sediment transport pathways. There are only limited examples of 3D experiments directly applicable to seawall scour; most studies were developed to investigate scour at breakwater structures in deep water (see Irie & Nadaoka, 1984., Silvester, 1986., Hsu & Silvester, 1989. and Sumer & Fredsøe 2000).

These experiments found that oblique reflective waves cause a short-crested wave system to become established in front of the wall, leading to toe erosion along the length of the breakwater structure, in addition to wave parallel nodal scour and accretion zones occur further offshore. Scour was particularly severe at the end of the breakwaters, where wave driven flows tended to increase sediment transport. At a seawall, the shallower water depth would cause waves to shoal and refract as they approach the shoreline, limiting the angle of obliquity and hence reducing the magnitude of these processes. Though many 3D seawall studies have been conducted, most are commissioned privately to support scheme design. Of the published studies, three examples specific to seawall scour are considered below.

A 3D scour study was conducted by Toue & Wang (1990), who observed the effect of a seawall structure adjacent to an unwalled section. The tests produced toe scour at the seawall, however the volume of sediment eroded was considerably smaller than the erosion generated by the down-drift effects of the wall. The study determined that the overall volume of erosion in front of the seawall section was less then the unwalled beach section, perhaps suggesting wave energy was reflected back offshore.

Kamphuis *et al.* (1992) conducted a 3D test of a sloping sand beach with seawall under oblique irregular period waves. An initial beach profile (1:10) was allowed to adjust to an equilibrium profile and then the water level was increased to simulate a storm surge. This caused the profile to flatten and a plateau formed between the seawall and the breaker location. A toe scour trough then developed and was observed in all the tests. The percentage of scour attributable to local scour processes or as a result of the steep beach profile re-adjusting was not made clear.

The experiment included measurements of longshore, suspended and bed load transport, which decreased in front of the wall as the beach returned to equilibrium, only remaining active at the breaker point. The tests indicated that wave-induced bedload transport would move sediment offshore, generally flattening the beach profile to maintain the equilibrium beach profile shape, as proposed by Dean (1986). The author did not suggest a mechanism for the formation of localised scour at the toe of the wall.

Rakha & Kamphuis (1997) investigated wave-induced sediment transport in front of a seawall using a 3D wave basin to validate a numerical model. Of particular interest were measurements of wave setup, which was found to be strongly dependent on the seawall toe water depth. At shallow water depths, wave breaking occurred in the surf zone, producing maximum setup and an increase in the toe water depth. When the toe water depth was raised further and waves were reflected (i.e. there was no surf zone), setup did not occur. This process has not been measured in any of the field or 2D flume seawall experiments, but is likely to occur as similar surf zone conditions would be present.

## 3.4. Numerical modelling

Through a series of computational approximations, numerical models aim to simulate the wave flow processes and their interaction with the seabed and structures. A model is setup by first defining a grid or mesh to represent the area of interest. These are typically 2D (e.g. a cross section though shoreline or plan section of coastline, where depth averaged values are calculated). The input conditions are then set at each boundary of the grid. This could be a tidal flow velocity or input wave height and period. Starting at the boundary the model iteratively solves the Navier-Stokes equations for each cell in the grid, thus calculating the propagation of viscous fluid flows within the model.

Due to the complex nature of the coastal zone, approximations and simplifications must be made to maintain reasonable computational times and model size. As a result numerical models require robust calibration and validation data to determine if the output solution is correct and the assumptions are justified. With regard toe scour, the general lack of large scale physical model tests and our limited understanding of the scour processes, limits the confidence that can be applied to current modelling techniques. However, numerical model enables rapid testing of a variety of different beach configurations, without the model or scale effects associated physical models. Therefore the key features of models currently in use by engineers and scientists were briefly reviewed. These include COSMOS, GENESIS (GENEralized model for SImulating Shoreline Change) and SBEACH (Storm-induced BEAch Change).

The COSMOS model (Nairn & Southgate, 1993) can be run as either a 2D cross shore beach profile model or as a 3D model where both cross shore and longshore sediment

transport can be predicted. The sediment transport module of COSMOS 2D, was validated using SUPERTANK model test data (McDougal *et al.* 1996) and limited field data from Blackpool beach. When modelling a simple beach without seawall, HR Wallingford (2001) noted that the model performance decreased due to difficulties in modelling changes in wave character close inshore, the key region of interest in toe scour research.

Powell & Whitehouse, (1998) used COSMOS-2D to simulate toe scour under a range of wave spectra and toe water depths. They found a correlation between the scour depth to wave height ratio ($S_t / H_0$) the relative water depth and the wave steepness, with the greatest scour occurring for steep waves close to breaking(Figure 3-8). However the results also suggested that toe scour can exceed the incident wave height, an observation not supported by numerous physical model sediment transport studies. The model was also unable to produce beach accretion for any of the water levels tested, contrary to the model tests of HR Wallingford (2006) and Xie (1981).

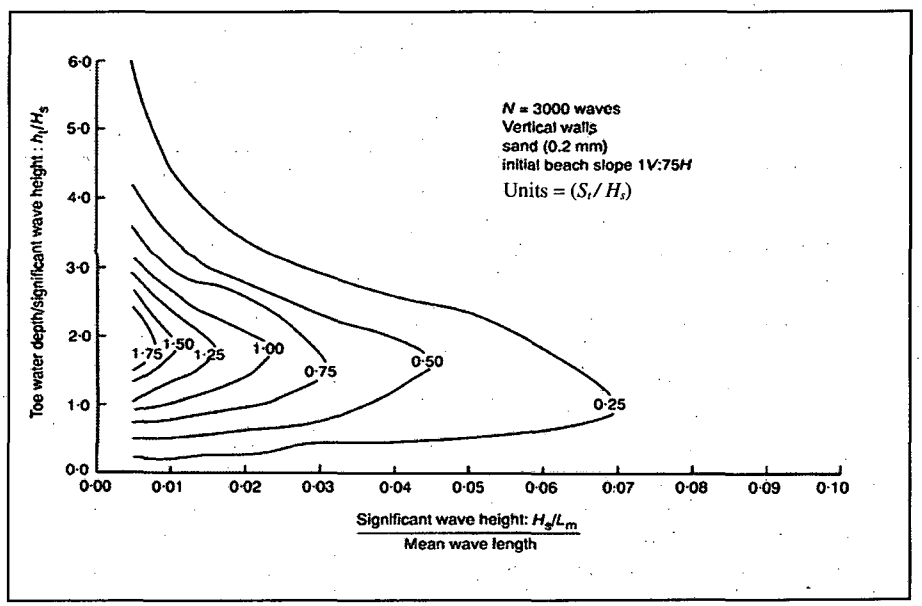


**Figure 3-8: COSMOS-2D scour prediction plot (from Powell & Whitehouse 1998)**

Other models include GENESIS, which is a shoreline response numerical modelling system (Hanson & Kraus 1989). However the model does not include the effect of reflected waves, the provision for tidal level changes and can is therefore only suitable for predicting larger scale morphological responses.

Another popular 2D modelling tool is SBEACH (Larsen & Kraus, 1989), which uses an energy dissipation algorithm to predict sediment transport across the beach profile. McDougal *et al.* (1996) modified the SBEACH model to include wave reflection and compared the results to three seawall tests conducted as part of the SUPERTANK series. The model successfully reproduced the laboratory tests, though these tests in themselves only produced limited toe scour. The researchers could find only a marginal difference compared to the SBEACH model without reflected waves. However these results were based on a small number of physical model results, dominated by wave breaking and are contrary to the clear evidence of reflection driven transport presented by other authors when the toe water depth is increased.

The latest numerical models assert their ability to simulate wave fields near coastal structures including the combined effects of shoaling, refraction, diffraction, reflection and wave breaking (e.g. Karambas *et al.* 2007). However it is doubtful whether these models can simulate the highly localised reflected wave flows and impact processes associated with seawall toe scour. These form part of much larger surf zone, which varies both spatially (wave heights in metres to sediment grains in millimetres) and temporally (from a storm durations in hours, to a wave period in seconds, to peak wave impact in milliseconds). These difficulties are compounded by the complex interaction and feedback mechanisms which link these processes.

For numerical modelling to succeed, a clear concept of the scouring mechanism must exist and be represented explicitly through numerical computation. This can only be achieved through detailed flume investigations of the toe scour process. Assuming the modelling challenges posed by these dynamic systems will be solved in the future, there remains a general lack of field data to validate the results (Kraus & McDougal, 1996).

## 3.5. Current scour guidance

When designing new seawall structures or assessing the scour risk of existing structures, the current guidance is largely based on the result of the medium scale 2D flume studies. In their reference book on scour in the marine environment, Sumer & Fredsøe (2002) reviewed toe scour processes and prediction methods, emphasising the correlation between toe scour and toe water depth. The authors suggested under deep water non-breaking reflective waves, breakwater research could be applied to seawall scour prediction. For breaking waves and near-reflecting conditions, the review

combined the scour prediction equations of Fowler (1992) and Xie (1981) on a single plot (Figure 3-9), using the same dimensionless variables, for the prediction of maximum scour.

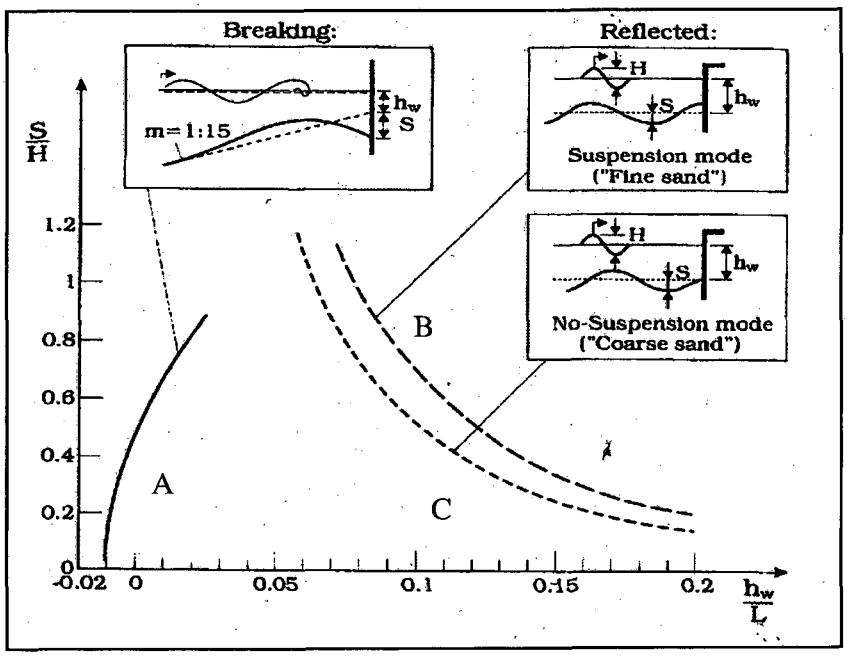


**Figure 3-9: Non dimensional scour (from Sumer & Fredsøe, 2002)**
**Eqn A: Fowler(1992), Eqn B & C: Xie (1981).**

The figure encompasses experiments conducted at medium scale using breaking waves *(-0.02 <$h_w/L_m$<0.04)* and reflected waves (0.06 <$h_w/L_m$<0.2). However does not however acknowledge that the results for Xie (1981) were collected using regular period waves and are therefore likely to overestimate the scour depth. Nor does it explain the disparity where the two lines would be expected to intersect (the area of most interest to engineers, as scour is deepest). Furthermore the insert diagram identifying the positions of the scour for Fowler (1992) is misleading, as some of his tests produced reflected waves, highlighting the weakness of applying the parameter $h_w/L_m$ to define wave breaking.

Though useful for visualising the toe scour processes, further model test research is required to unify these datasets in the critical scour region *(0.03 <$h_w/L_m$<0.06)* and to validate the scour depths under irregular period waves. The use of the maximum scour depth variable is also less practical then the maximum toe scour depth, which is more critical to wall stability and foundation damage.

The most recent guidance regarding seawall toe scour is available in the US Army Corps of Engineer Coastal Engineering Manual (ASCE 2006), a common source of reference for coastal engineers. Based on mostly physical model test results, the manual recommends that seawalls be considered as breakwaters in non-breaking wave situations; however the guidance is less clear for breaking waves. The manual suggests that breaking waves cause the greatest scour, by generating strong downward flows during impact, and that plunging waves can form rotating vortices at the wall toe. This statement is not supported by experimental data or reference. The manual goes on to tentatively suggest the Fowler (1992) scour prediction equation, but notes the limited number of model tests conducted and the lack variables describing the sediment characteristics.

## 3.6. Conclusions

### 3.6.1. Field studies

The review considered literature pertinent to localised scour at the toe of seawall structures with sand beaches. Existing field studies of unwalled beaches under storm waves revealed a range of complex nearshore processes, which occur in both longshore and cross shore directions. Of the numerous field studies completed, none have recorded evidence of toe scour in front of seawalls. As these results were collected at low tide during post storm surveys, it is suggested that the scour features were probably infilled with the falling tide. Post storm breakwater scour measurements were more frequent, however the offshore coastal environment is significantly different to the nearshore, where wave the wave heights are depth limited and the effect of tidal range more apparent.

The lack of field research literature supports Sutherland *et al.* (2003), who emphasised the need for further monitoring experiments and improved sensor designs to enable collection of data for validation of model results. The difficulties in sampling within the wave breaking zone suggest that beach imaging techniques such as ARGOS may be useful.

### 3.6.2. Physical model experiments

A series of physical model experiments were reviewed, these were mostly 2D due to the high cost and lack of suspended sediment transport in 3D model tests, limits their use to studies predicting coastal morphology. Of the 2D tests, most were conducted at small scale using regular waves. These are prone to scale effects due to the use of fresh water and problems in reducing the sediment size sufficiently to achieve suspended sediment transport and similitude with the prototype. As a result, the scour depth tended to be overestimated and reflection based scour process promoted. The small scale tests were however useful in observing the key scour processes, such as breaking wave flows and when planning medium scale experiments.

Only two medium scale sediment transport studies have been conducted with irregular waves and a planar initial beach profile. A third experiment using an equilibrium initial profile provided contrasting results, however without a consistent initial profile, comparison of this dataset to existing and future test results remains difficult. Additional

medium or large scale sediment transport tests are required to enable the existing datasets to be validated and extended to provide improved scour prediction guidance.

The 2D model tests suggested that toe scour depth increases with, but never exceeded the incident offshore wave height. The scour depth also correlated to the wavelength to water depth ratio, reaching a peak around $d_t / L_m = 0.01$. The model tests highlight the importance of wave reflection and wave impact flows to the scour process. In shallow water, toe scour would be expected to be dominated by wave breaking at the wall face, whereas in deep water, wave reflections would lead to sediment transport towards the reflected wave nodes and the seawall. However the parameter $d_t / L_m$ does not adequately represent wave breaking at coastal structures, despite the suggestion in Figure 3-9.

The structure of wave flows at the vertical walls with unbroken reflected waves has been researched extensively, with scour occurring in regions of high bed shear stress. However a study into breaking wave flows, which have been suggested anecdotally to generate high speed flow vortices, leading to increased scour, has yet to be completed.

Further investigations of the wave flows in front of the seawall, particularly during breaking wave impacts, should be conducted, to enable the hydraulics of the toe scour process to be better understood and to improve guidance.

### 3.6.3. Numerical modelling

Several popular numerical models were reviewed; however these models cannot fully reproduce the highly localised reflected wave and impact flows associated with seawall toe scour, which is complicated by the interaction and feedback mechanisms which link these processes. Further field and flume testing is required to provide suitable validation data for new numerical models.

### 3.6.4. Current design guidance

In the physical model studies, the toe scour depth has rarely been measured to exceed the incident wave height, with the exception being one experiment where excessively steep seabed slopes were used. It would appear that this "rule-of-thumb" remains a useful guide when designing emergency scour protection at coastal structures with natural beaches. However this is of limited use when trying to optimise a seawall design

to reduce cost or to estimate the risk of scour for a specific event and location. The reliability of this statement also requires validation through field monitoring.

A series of empirical predictors have been proposed, which provide a more robust assessment of scour depth. However, they all fail to include an elementary understanding of the scour process, particularly the type of wave breaking, which can change significantly due to the variation of tide height and its effect on the toe water depth. The leading predictors include Fowler (1992) which represents shallow water toe scour, and the Xie (1981) equation which represents deepwater reflected wave conditions. The region between these two equations has yet to be studied in model tests of suitable scale.

The layout and design of Figure 3-6 and Figure 3-9 are helpful in presenting engineers and scientists with an understanding of both the empirical scour depth and the key factors driving the scour process. They highlight the need for an integrated approach, combining both cause and effect, to produce improved scour prediction equations, figures and guidance. In particular and unlike these diagrams, it is also important to indicate the scoured beach profile shape without exaggerating the vertical scale, to avoid confusion over the geometry and steepness of the scour bedform.

# 4. Field study: Blackpool and Southbourne

In this section the results of the scour field study conducted at Blackpool and Southbourne beaches are examined. The chapter is divided into seven sections; the first two introduce the rational and study aims. Section three discusses the experimental method and equipment. Sections four and five discuss the result of the respective Blackpool and Southbourne beach deployments. Section six discusses the experimental results and accuracy to draw conclusions, which are presented in section seven.

## 4.1. Introduction

The literature review demonstrated that field measurements of toe scour are limited to anecdotal evidence and speculation following post storm beach visits. This suggested that toe scour could be infilled as the storm intensity reduces and water levels receded. It is therefore important to establish the likelihood and magnitude of toe scour under field conditions. This was achieved through two field experiments designed to collect evidence of beach level changes in front of beach structures under storm conditions, as part of a Department of Environment, Food and Rural Affairs (Defra FD1927) funded project in partnership with HR Wallingford and the University of Southampton.

The first experiment was conducted between 1995 and 1999 in front of a vertical seawall at Blackpool on a sand beach as part of an existing HR Wallingford study for Blackpool Borough Council. This dataset was recovered from archive and investigated further. The second experiment was conducted using similar instrumentation, at a 1:2 sloping seawall on a sand beach in Southbourne, Dorset in 2005 over a one month period. Site selection was based on the author's research into historic beach levels and anecdotal evidence from local coastal mangers that scour features had been observed.

## 4.2. Aims and objectives

As part of the project team, HR Wallingford was responsible for supplying and deploying the instruments and converting the raw data into a useable format. Wave and tide gauge records were also obtained by HR Wallingford. The author took forward these datasets to achieve the following aims and objectives:

- Develop a dataset for comparison to laboratory datasets and numerical models;
- To determine the wave height, water depth and peak scour during storm events;
- Determine the parameters and conditions most likely to cause scour.

## 4.3. Equipment and methods

In 1995 Blackpool Borough Council commissioned HR Wallingford to monitor beach levels on a fine sand beach in front of a vertical seawall at Blackpool. The study involved deployment of three HR Wallingford Tell-Tail scour monitors, two at the wall toe and one approximately 10m offshore (Figure 4-1 & Figure 4-2). The instrument configuration and cross sectional beach layout are shown in Figure 4-3 and Figure 4-4.

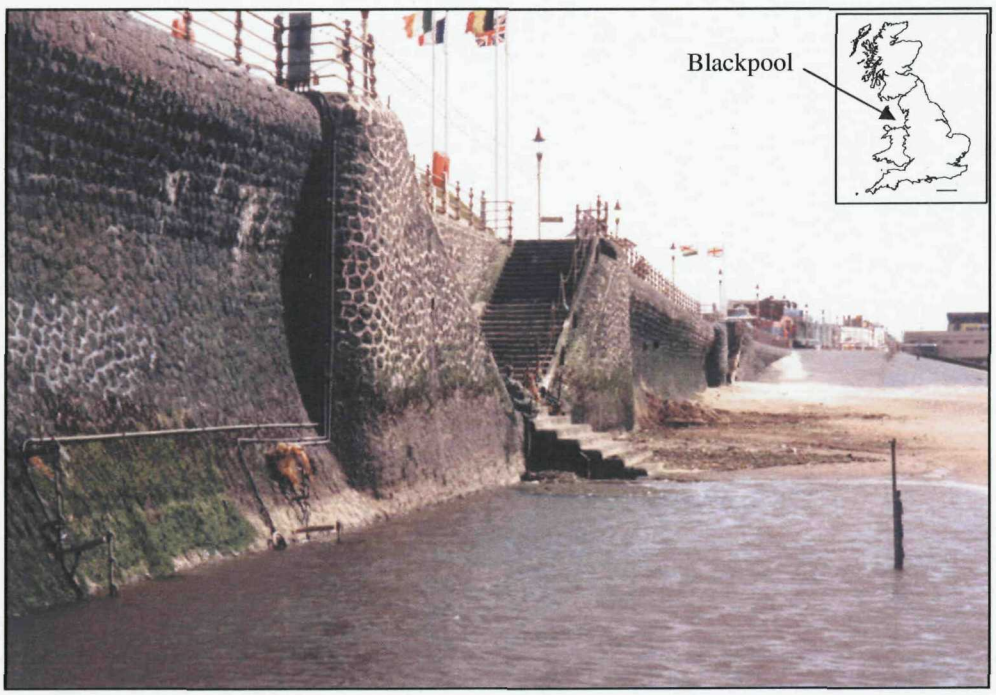


**Figure 4-1: Blackpool seawall and Tell-Tail monitors (from HR Wallingford, 2005)**

**Figure 4-2: Offshore Tell-Tail scour monitor at Blackpool (from HR Wallingford, 2005)**

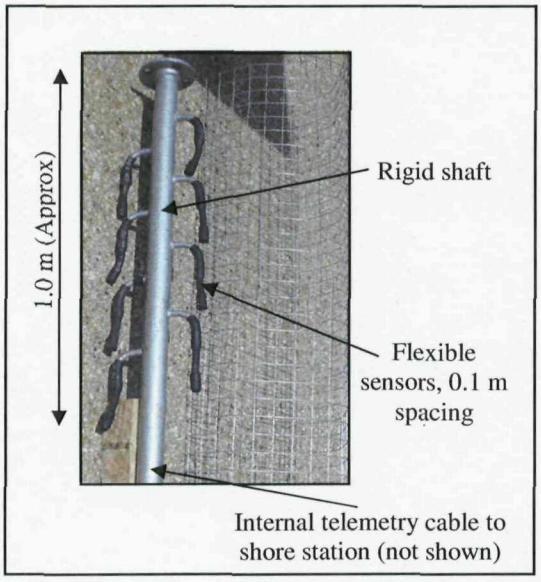


**Figure 4-3: Tell-Tail scour monitor components**

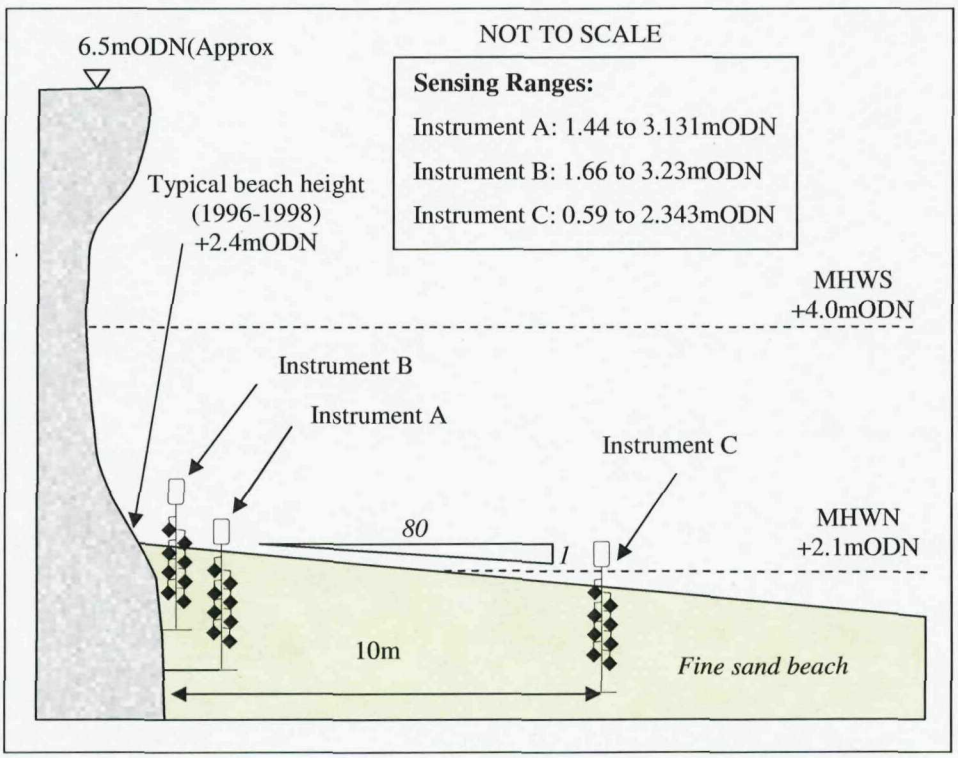


**Figure 4-4: Cross section of seawall and instrument position**

The instruments consist of an array of eight flexible movement sensors mounted on a rigid steel shaft. When buried beneath the beach the sensors remain static. However, when beach levels fall, successive sensors become exposed to wave flows, triggering sensor pulses, which are logged internally every 15 minutes. The height of each sensor was determined, allowing beach level to be inferred and continuously monitored at any

state of the tide and under storm conditions. Throughout the deployment, staff from Blackpool Borough Council routinely downloaded the data, which was forwarded to HR Wallingford for storage. This continued beyond the initial deployment contract duration (12 months), up to the year 2000 when the instruments finally ceased to function. The most complete years which were from January 1996 to December 1998, were taken forward for detailed analysis.

Similar instruments were deployed at Southbourne in 2005 (9th May to 7th June) on a sand beach ($D_{50}$ = 0.3mm), with a typical slope 1:28, to observe beach levels in front of a 1:2 sloping seawall. In this experiment only two instruments were used, one bolted to the sloping seawall the other positioned at the wall toe in vertical orientation (Figure 4-5). During the deployment conditions remained relatively calm, except for a low pressure weather system between the 22-25th May, which caused increased wave heights and beach level changes. Beach level measurements were therefore only analysed for this period.

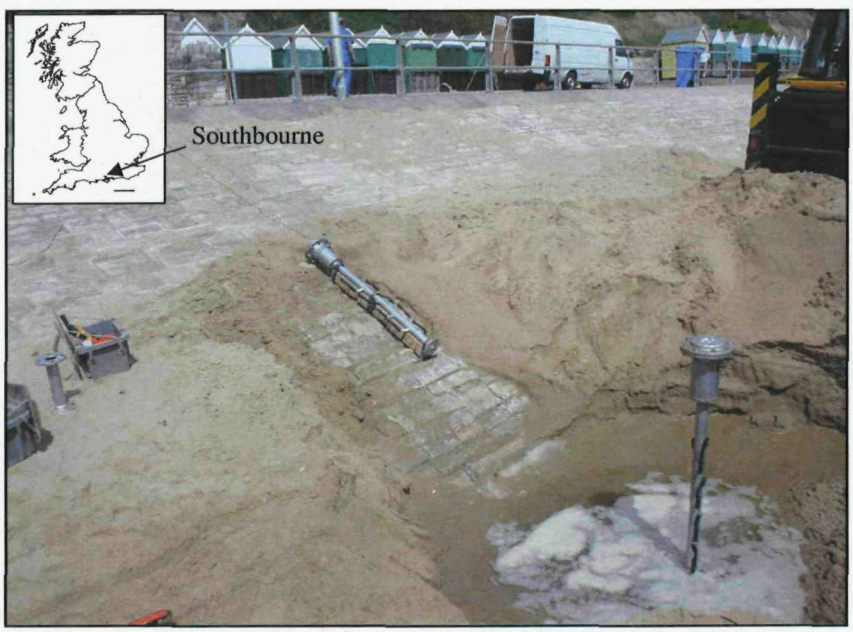


**Figure 4-5: Tell-Tail sensor deployment at Southbourne May 2005**

### 4.3.1. Additional data sources

**Blackpool deployment**

At Blackpool, Met Office wave data (hindcast from wind observations) was obtained for a position 27 km offshore of the beach instruments in 16 m water depth. Similar wave return period conditions occurred in 1996 and 1997, with a wave height range of 0.5m to 3.5 m, which was repeated in 1998, but with a slightly higher percentage of waves greater then 1 m. The data indicated that over the deployment period the site was limited to a maximum significant wave height ($H_0$) of 3.5 m and a mean period ($T_m$) of 7 s. The Blackpool seawall is orientated to the west; the dominant wave direction for the duration of the deployment was 240° to 270° and therefore near normal to the shore.

Observed tide height data was obtained at 15 minute intervals from the British Oceanographic Data Centre (BODC) for the Liverpool gauge. The tidal range was significant, with a mean spring range of 8.2 m. The Liverpool data was corrected using the Lennon method for Blackpool; further details of this method are contained in HR Wallingford (2005). Due to the proximity of the sites, the tide time was not corrected.

Cross shore beach profile data have been collected along the Blackpool frontage since 1956, with the closest profile being BBCSEC 9A, approximately 170 m south of the deployment site (HR Wallingford, 2005). The average beach profile slope at BBCSEC 9A during the deployment period (1996 to 1999) was 1:80, indicating a relatively flat sandy beach. The average beach height at the toe of the wall during the deployment was between 2.4 and 3.9 mODN, just above mean high water neaps.

**Southbourne deployment**

At Southbourne, Channel Coastal Observatory data was made available from a wave buoy located 2.0 km west-south-west of the deployment site at Bournemouth and tide data obtained from the Proudman Oceanographic Laboratory gauge at Bournemouth pier, 4 km west of the deployment site. Given the close proximity of the wave and tide sources, no corrections were made to the data. In contrast to Blackpool, the mean spring tidal range was considerable smaller (1.8 m), and included an unusual tidal prism, with a distinct stand during the ebb tide.

Seasonal beach profile measurements were also supplied by the Channel Coastal Observatory, and were used in planning the deployment location and reviewing historic beach level trends. The lowest measured beach level in front of the wall occurred in January 2004 at a level of +0.3 mODN, a similar level to that shown earlier in Figure (2-1a). During deployment the beach level at the wall toe was around +1.4 mODN.

### 4.3.2. Data sorting and filtering

At Blackpool the instrument data files were first assigned their respective wave and tidal parameters. Due to the limited resolution of the wave model data (every three hours), linear interpolation was used to match the $H_0$, $T_m$ and wave direction to the corresponding tide and sensor data which was collected every 15 minutes. This was not necessary at Southbourne, as the instrument, wave and tide data were all collected at fifteen minute intervals or shorter.

During the matching process some of the archived files were found to be incomplete due to battery failure or memory limitations, resulting in gaps and overlaps in the dataset. Furthermore over the 5 years of deployment the aggressive environment caused failure of the individual sensors, therefore only the most complete years (1996, 1997 & 1998) were taken forward for detailed analysis. This amounted to 820 days of data from 24 separate channels logging every fifteen minutes. This dataset is unique and to the author's knowledge is the only continuous record of beach levels in front of a seawall.

The short deployment at Southbourne produced a high quality datasets without the interruption of instrument damage or power failure. Through the frequent site visits made by the author and a good understanding of the site's characteristics, the dataset was relatively simple to interpret and processes. Furthermore, only one significant storm event occurred, enabling simple graphical analysis.

When inferring beach levels, detailed inspection of the datasets revealed that the Tell-Tail sensors were susceptible to noise and the pattern of sensor channel exposure could be misleading, e.g. when senor activation occurred out of sequence or appeared to fluctuate rapidly. Therefore a more sophisticated technique was adopted at Blackpool using MATLAB and a series of filter rules, which are described in detail in Appendix B, and summarised in Table 4-1.

**Table 4-1: Summary of filter criteria and values at Blackpool**

| Filter Criteria | Value |
|---|---|
| Minimum sensor pulse threshold | 3 pulses per minute* |
| Minimum offshore significant wave height ($H_0$) | 0.75 m |
| Minimum sensor immersion | 0.1 m below SWL |
| Maximum scour rate | 2 cm per minute |
| Minimum and maximum incident wave angle | 225° to 315° |

** This was the only filter to be applied at Southbourne, as the site was closely supervised during deployment*

Events where the filter criteria were satisfied and the beach level fell and recovered over a tidal cycle, with no relic scour features, were sampled for Blackpool and Southbourne beaches. A graphical plot of each event confirmed that the correct wave and tide conditions were selected at the point of initial and maximum scour. During this process, events where the change in beach level still remained unclear, or fluctuated rapidly, were excluded from analysis. These were typically data points on the fringes of the filter criteria.

## 4.4. Results- Blackpool deployment

The most severe erosion events from each year were plotted and examined to show the tide height and beach height at the wall and offshore instruments. The significant wave height ($H_0$), mean wave period ($T_m$) and wave direction (*Dir*) were appended to each event for the point of maximum scour.

### 4.4.1. Annual scour maxima - 1996

During the flood tide on the 27th October 1996 (A) the beach level fell in two distinct stages to 1.94 mODN, dropping below the beach level further offshore, which was between +0.15 m higher, and indicated a trough at the toe (Figure 4-6). At high tide the beach level at the toe of the wall recovered and accreted to a level of 2.42 mODN, though the beach level remained unchanged further offshore. With the ebb tide, the beach level at the wall fell slightly to a similar level as the initial condition.

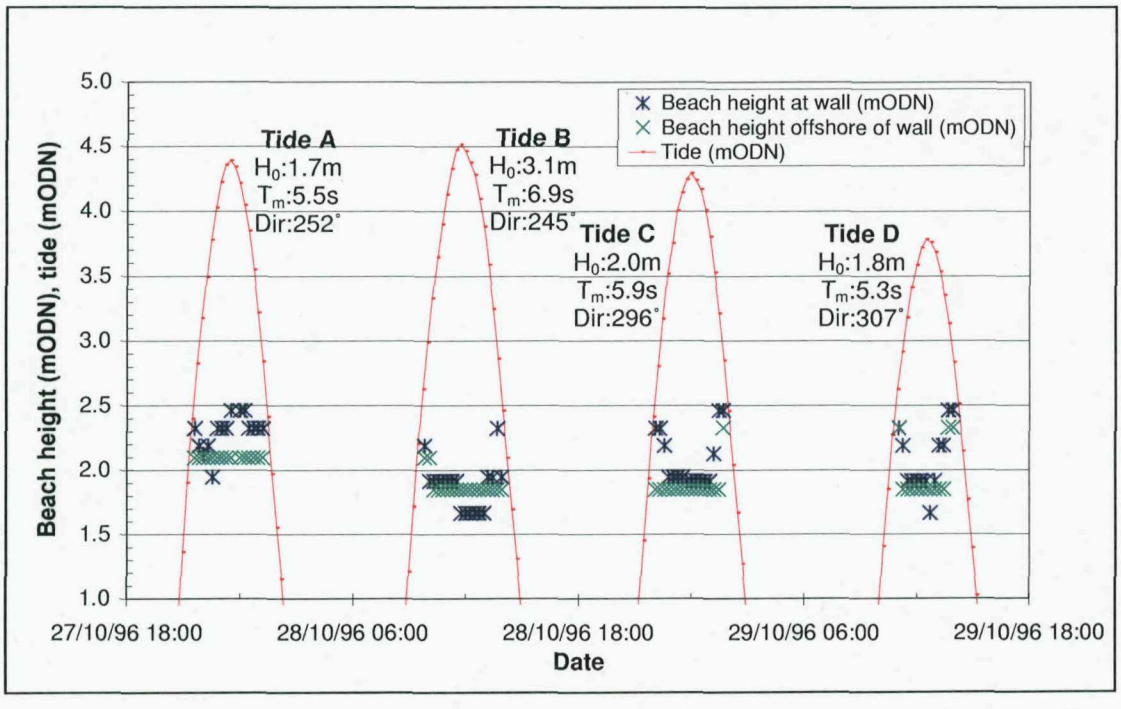


**Figure 4-6: Maximum scour events October 1996**

On the 28th October 1996 (B) the wave height and period had increased. As the water depth rose the beach level at both instruments fell rapidly and remained static until shortly after high tide, when accretion commenced. The beach level at the toe of the wall rose and dropped suddenly as the tide fell below 2.5 mODN, but had accreted to a similar level at the start of the next flood tide. Thus, this point appeared to be a false

reading. In comparison, these patterns differ to the afternoon tide on the 28th (C), where at high tide the levels at the wall remained above those offshore, before both the wall and the offshore levels recovered to a higher level then event (B).

The wave height and period continued to decrease on the afternoon of the 29th October 1997 (D), however the beach at the wall toe was eroded to a similar level as the morning tides on the 27th and 28th October. The erosion cycle was similar to the 28th October with erosion occurring at the peak of the tide, followed by rapid accretion with the ebb tide.

### 4.4.2. Annual scour maxima - 1997

Due to sensor damage in January 1997, the offshore beach instrument failed, leaving only the wall mounted sensors. During the flood tide on the 5th April 1997(A) the beach level dropped to 1.66 mODN briefly, before recovering by +0.5m at the peak of the tide (Figure 4-7). The accretion remained static for approximately 45 minutes and recovered to a height of 2.55 mODN as the tide ebbed. The wave height decreased to 1.8 m on the following tide (B), and the beach fell by -0.42 m before recovering to a similar level with the ebb tide. By the next tide (C), the wave height had decreased significantly and was excluded by the filter criteria, the raw instrument data revealed a static beach level of +2.55 mODN throughout this tide.

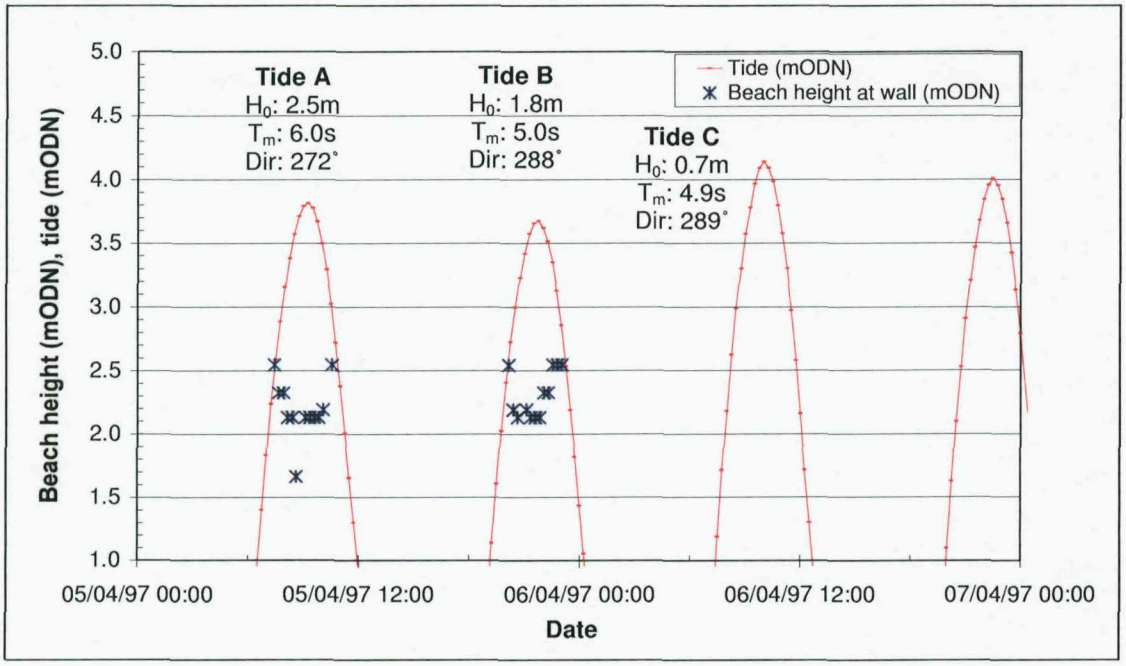


**Figure 4-7: Maximum Scour events April 1997**

### 4.4.3. Annual scour maxima – 1998

Several scour events occurred during 1998 and all reached a similar maximum scour depth of 1.44 mODN (Figure 4-8). The most interesting event occurred on the 15th and 16th October 1998 (A & B), where the tide only reached a depth of +0.14 m and +0.16 m at the wall respectively and did not cause a change in the beach level, even under a moderate wave height of up to 2.3 m. On the following tide (C) (17th October), high tide was 0.7 m greater in height; once the water depth exceeded +0.5 m, erosion occurred and continued in common periodicity with the flood and ebb of the tide. At high tide, the level at the toe of the wall remained constant, but as the tide fell the beach returned to its initial level.

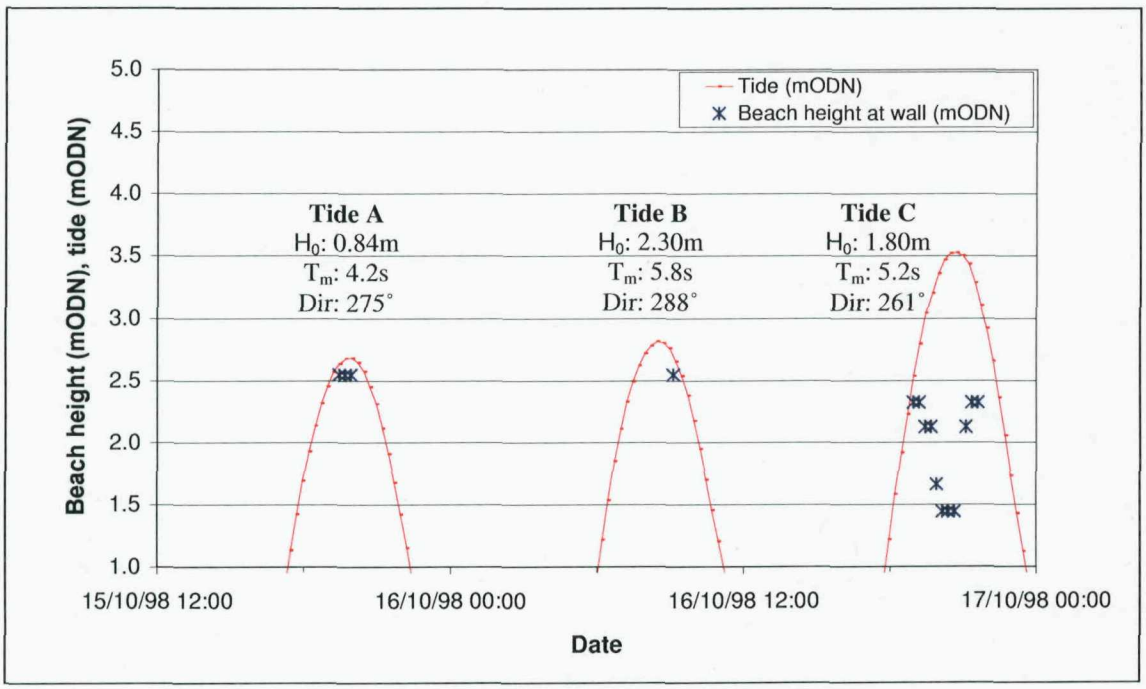


**Figure 4-8: Maximum Scour events October 1998**

### 4.4.4. Combined Data Analysis

In Figure 4-9 the maximum scour depth was compared to the ratio of the offshore wave height to toe water depth, and was considered an indicator of the potential wave breaker type.

The deepest scour occurs when $H_0 / d_t$ is between 1 and 2, when plunging type breakers (as shown in Figure 2-2) would be expected to break on or near the seawall. Significantly lower scour depths occur when $H_0 / d_t > 4$, where shallow water would cause waves to break offshore of the wall. No scour occurred when the toe water depth

was significantly deep ($H_0/d_t < 0.5$), this would cause reflective wave conditions. During the three years of deployment, the maximum toe scour depth remained less then the incident offshore wave height (Appendix C).

The 1996 data was analysed further to distinguish the height difference between the offshore and wall instruments at the point of maximum scour, and to determine if general beach lowering occurred or if a scour trough was present at the wall toe (Figure 4-9). Toe scour troughs tended to form when $1 < H_0/d_t < 2$, with deeper scour depths then events where erosion occurred at the wall and offshore simultaneously. Due to the failure of the offshore instrument in January 1997, this analysis could not be extended to the other deployment years.

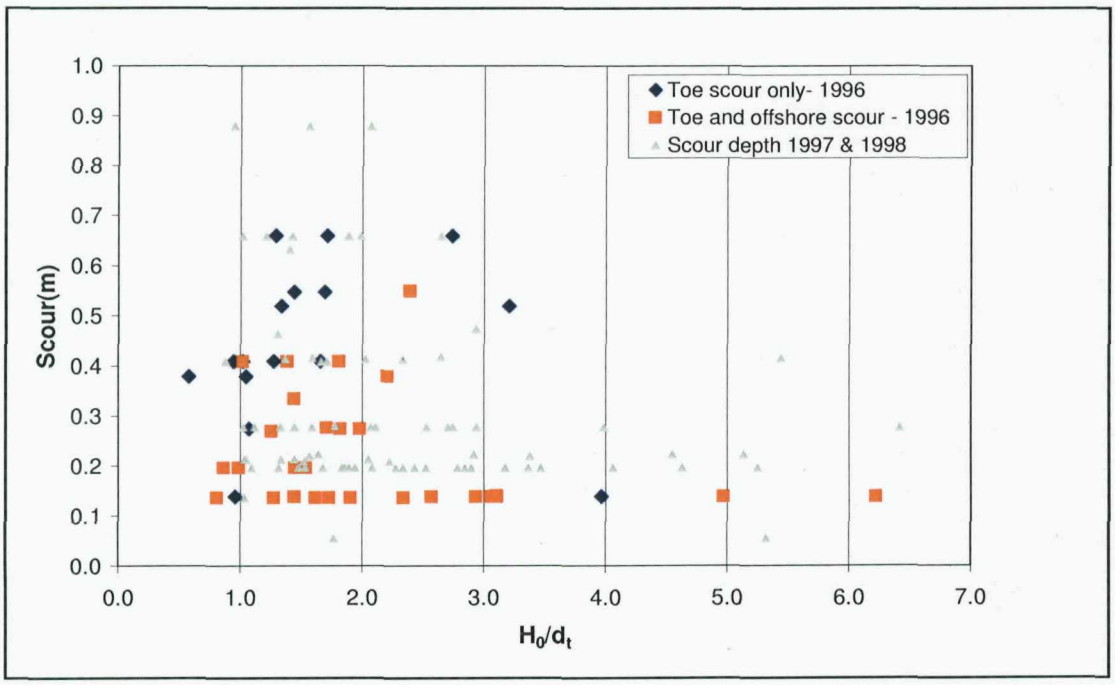


**Figure 4-9: Scour type and depth as a function of wave height and water depth**

Given the significant tidal range at the deployment site, the results were analysed to determine if the large tidal range had an effect on the scour depth. The field data was sampled into 1m bands of tidal range and the average, lowest and highest toe scour depths were extracted (Figure 4-10). Though the average scour depth increased by 60% between neap and spring tides, the significant variation the upper and lower scour depth values and correlation between the average wave height and average scour suggests tidal currents are not the primary scour process. Though it is noted that longshore currents could cause suspended sediment (as a result of scour) to be transport away.

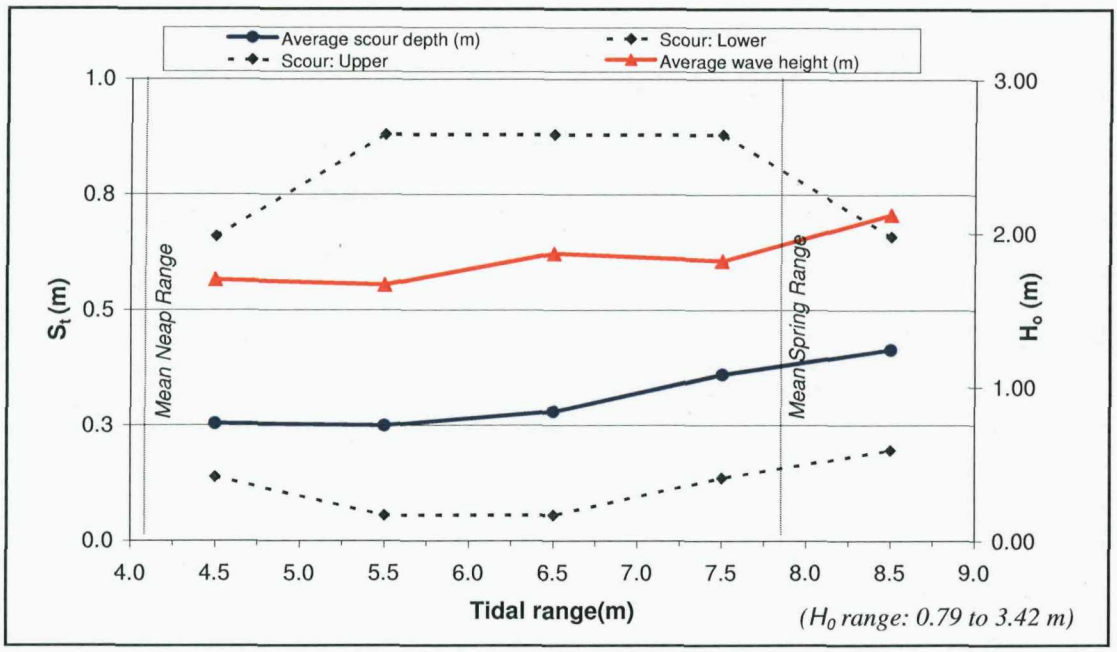


**Figure 4-10: Effect of tidal range on toe scour depth compared to offshore wave height.**

## 4.5. Results -Southbourne Deployment

Beach level data was collected over a five week period, during which time only one storm event occurred, which peaked on the 24th May, with a $H_0$ of 1.6 m. Despite the relatively small wave heights during the deployment, the beach level changes exceeded the wall mounted instruments' sensing range and prevented data collection. Therefore data was only available from the beach instrument, though at the peak of the storm event, the severe scour caused the beach level to drop further, which exceeded this instrument's sensing range for a brief period.

For each event, the initial beach level was determined by interrogating the beach instrument data to find the first sensor channel to be activated; this also provided an approximate water level elevation. When compared to the tide gauge, the activation of the beach sensors appeared to be consistently +0.9 m higher then the water level indicated by the gauge. Unfortunately removal of the instruments prevented investigation of this error, however the good correlation between the timing of changes in beach level and the unusual tidal prism at Southbourne, suggests this was probably a levelling error, not a local tidal anomaly.

For the beach level comparison plot below, the original instrument elevations and tidal heights were used. To enable comparison with other flume and field datasets the instrument elevations were decreased by 0.9 m for the remaining figures and tables. This led to sensor activation commencing as the tide height equalled the beach height, and was consistent with the sensor operation at Blackpool

Figure 4-11 shows the tide height and beach level at the offshore instrument, and the wave characteristics at the peak scour depth. With the flood tide and increasing wave height on the 23rd May (A) the beach level fell, with maximum scour occurring at high tide. The beach then recovered with the ebb tide. A similar pattern of erosion and accretion occurred on the afternoon tide on the 24th May (B), despite a smaller wave height. On the 25th May (C) wave conditions decreased significantly, only 0.3 m of beach lowering and recovery occurred. A total of six scour events occurred during the Southbourne deployment with a maximum scour depth of 1.1 m with a $H_0$ of 1.5 m.

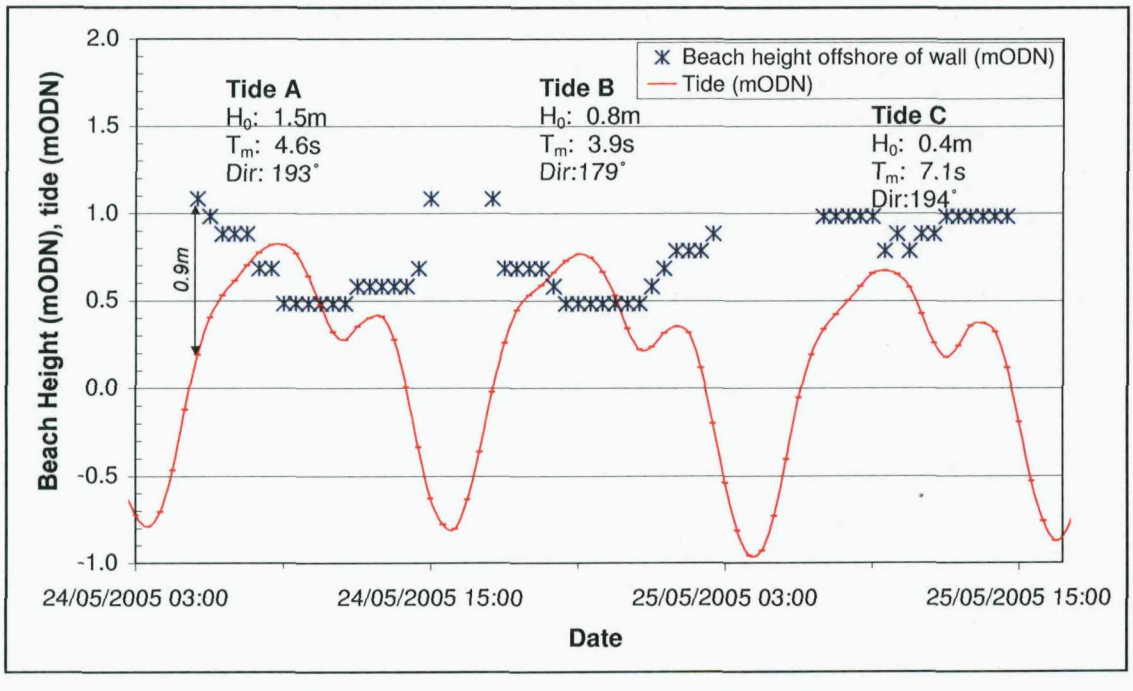


**Figure 4-11: Maximum scour events May 2005**

## 4.6. Discussion

### 4.6.1. Toe scour and beach level changes

Over the three years of sensor deployment at Blackpool, 119 separate scour events were identified. These followed a pattern of erosion and accretion in common periodicity with the tidal cycle, with the beach level returning to its original condition as the tide ebbed. Comparison of the time of maximum scour and high tide indicated a lag of +-15 minutes at Southbourne, and approximately 1 hour at Blackpool, suggesting a link between toe water depth and scour. It should be noted however that the tide data at both sites had limited temporal resolution (15 minutes), and at Blackpool was based on interpolation of data from the Liverpool, therefore these values should not be used to infer the rate of scour.

In general, scour depth increased with wave height, though the final scour depth often varied significantly, but never exceeded $H_0$. The variation in scour depth may be due to the change in the tidal range or other nearshore processes e.g. wind strength, offshore beach profile or nearshore circulation flows, the tidal range was found to have little effect, except where high tide fell below the beach level.

Due to the limited number of beach profile sampling points, it was not possible to determine where the eroded beach material was transported to, nor the extent of the scour feature at the wall. From the offshore instrument data available for 1996, during sixteen of the forty four events the offshore beach height was above the level at the wall, indicating a toe scour trough. During the remaining events, the offshore beach height varied between 0 to -0.48 m below the beach height at the wall, indicating a sloping beach profile or a trough > 10 m wide. Trough formation, and the deepest toe scour both tended to occur when $1 < H_0/d_t < 3$, where wave breaking conditions would be expected at the wall, enhancing turbulence and subsequent sediment suspension and transport.

Under shallow water conditions ($H_0/d_t > 4$) and deep water conditions ($H_0/d_t < 0.5$), relatively little scour occurred, suggesting energy dissipation occurred on the offshore beach profile at low tide and energy was reflected at high tide. Furthermore, under reflective wave conditions, fine sand sediment would not be expected to scour from the seawall toe, which coincides with a reflective wave antinode (Xie, 1981).

The 1:2 sloping wall results for Southbourne produced evidence of significant beach level changes. The maximum scour depth was similar to those observed in the Blackpool study, despite the wave height remaining significantly smaller. This could be a result of sloping seawalls being more prone to scour; the steep beach slope (c.1:28 and significantly greater then Blackpool c.1:80) reducing the surf zone width and increasing energy dissipation near the seawall; or the tidal range which was also significantly smaller, and would cause the seawall to be exposed to the most intensive scour conditions ($1 < H_0/d_t < 2$ at Blackpool) for a longer duration.

### 4.6.2. Experimental accuracy and limitations

The collection of continuous beach level data from in front of a seawall has been achieved for the first time using electronic measuring equipment and combined with wave and tide records. Unfortunately *insitu* wave and tide records were not available, therefore hindcast and extrapolated tide data was used. These are the best available and though they represented the general wave and water level conditions during the deployment, they should be used with caution when comparing the results to other field studies.

The advantages of collecting wave and tide data close to the deployment site are evident in the Southbourne dataset, which was simpler to analyse and interpret following the frequent site visits. However careful equipment setup is still required to ensure the instruments are levelled correctly and that their elevation corresponds to the expected changes in beach level over the deployment period. This could be improved by conducting frequent post storm surveys to build a history of beach profile trends.

Though limited in sensing range, memory size and battery life, the simple design and operation of the Tell-Tail sensors enabled data collection at Blackpool for over four years. The same equipment also worked successfully at Southbourne, though the significant beach levels drop nearly caused one of the instruments to be lost. The use of motion sensors to detect beach level required significant filtering to exclude erroneous data points. Further work is required to improve the equipment and techniques available to monitor toe scour as suggested by Sutherland *et al.*(2006), enabling more detailed field monitoring.

Both field datasets contained significant variability in depth of maximum toe scour, indicating that other factors such as wind, local bed slope, offshore bathymetry and nearshore currents may work either in opposition or synergy with the scour processes. The variability may have also been due to the tidal range and relative speed of tidal rise and fall, both of which depend on spring and neap tidal range. These alter the duration of the incident wave conditions at the point most critical to scour.

## 4.7. Conclusions

A unique field dataset measuring beach lowering and toe scour was collected at both a vertical and sloping seawall. The Tell-Tail instrument provided a robust method for collection of continuous beach level measurement under all conditions. However, careful filtering was required to remove erroneous data points.

Scour depths varied significantly in both studies and closely followed the flood and ebb of the tide, which controlled the toe water depth, but showed weak correlation to the tidal range. Scour at the wall tended to infill with the ebb tide, suggesting these features would not be detected by post storm beach surveys. The variability of the scour depth suggested that in addition to an optimal water depth and wave height, other variables (e.g. wind and bathymetry) may have limited scour reaching maximum depth.

At both locations, the maximum scour depth never exceeded $H_0$, a rule-of-thumb for scour prediction. At Blackpool, the deepest scour occurred in the range $1 < H_0/d_t < 2$, this was also the region where a trough tended to form at the wall toe in the data available for 1996. It was suggested that this was a result of waves breaking near to or onto the seawall.

The Southbourne dataset was too short to draw firm conclusions for sloping walls. However, significant changes in level scour occurred under relatively small waves, suggesting they are equally prone to toe scour.

The field datasets can be applied to verify the results of physical and numerical model studies, though caution is required when using the Blackpool wave data results, which were based on hindcast wind data. Future seawall monitoring studies require improved measurement techniques and should include local wave and water level sensors, and collect beach level measurement from across the surf zone.

# 5. Sediment transport study: scour prediction

A sediment transport study was conducted to investigate toe scour processes at vertical and sloping seawalls. In this chapter, the results are reported, analysed and a scour prediction formula developed. The chapter is divided into seven sections, section one introduces the study and examines the existing prediction equations. Section two presents the experimental aim and section three reviews the materials and methods. In section four, the scour depth results and beach profile results are presented. Section five tests existing scour prediction equations and develops new prediction equations. Section six discusses these results which are concluded in Section seven.

Conclusions with respect to these tests, the literature review, and the field studies are discussed and presented in Chapter 7.

## 5.1. Introduction

The field studies conducted at Blackpool and Southbourne demonstrated that significant beach level changes can occur in front of seawalls under wave attack. While providing evidence of scour, the results were complicated by temporal and spatial variations in the wave climate and beach configuration. The data therefore lacked sufficient detail to predict toe scour and no cause-effect relationship could be established. In order to establish a causal relationship, variables must be systematically controlled. This is only possible using physical model experiments, which as shown in Section 2.3.1, should be of at least medium scale (e.g. $H_0 > 0.1$ m).

A 2D sediment transport experiment was conducted by HR Wallingford staff and the author as part of a Department of Environment, Food and Rural Affairs (Defra FD1927) project. The author assisted in the running of the model tests and analysis of the resulting dataset. The key overall study conclusions were reported in HR Wallingford (2006) and Sutherland *et al.* (2006). These documents focused upon the beach profile measurements, the maximum scour depth and the scour protection tests.

The experimental results, specifically the scour depth measurements, beach profile response at the wall, and wave breaking characteristics were contrasted; then taken forwards for comparison to the scour predictors short-listed in the literature review section.

### 5.1.1. Existing scour prediction equations

As discussed in Section 3, medium scale scour tests conducted by Xie (1981), using a flat sand bed ($D_{50}$ = 0.11mm), exposed a breakwater structure to both regular and irregular period wave conditions, and demonstrated sediment transport under non-breaking reflected waves. A maximum scour prediction equation (Eqn 5.1) was produced by fitting a curve to the data. Though based on regular wave tests, the results were compared to irregular wave tests, suggesting the predictions were conservative.

Fowler (1992) conducted a series of 2D seawall scour tests on a steep 1:15 beach slope using regular or irregular period waves 0.2 to 0.3 m high, with a fine sand bed ($D_{50}$ = 0.13mm). The test proceeded with bursts of waves until a stable equilibrium profile was achieved. A tentative prediction equation for maximum scour was generated based on non-dimensional analysis (Eqn 5.2). Both Equations 5.1 & 5.2 predict the maximum scour on the beach profile, which may not necessarily occur at the wall. Highly reflective wave conditions can lead to reduced scour or accretion at the wall toe.

As part of the SUPERTANK test program, Kraus & Smith (1994) conducted three 2D model tests with a vertical seawall and fine sand beach ($D_{50}$ = 0.22mm). Using the existing beach profile from the previous test run, short bursts of either constructive or destructive irregular period waves ($H_0$ = 0.7-0.8 m) were generated. However distinguishing between each test remains complicated, as the initial beach profiles were different. As a result, the toe scour prediction equation (Eqn 5.3), only predicts changes between each equilibrium profile. The prediction equations, wave and sediment characteristics are summarised in Table 5-1.

**Table 5-1: Medium scale seawall scour experiments and scour predictors**

| Author | Best fit equation | Sand $D_{50}$ (mm) | Wave height range(m) |
|---|---|---|---|
| Xie (1981) | $\frac{S_m}{H_0} = \frac{C}{[\sinh(kd_t)]^{1.35}}$ (5.1) | 0.11 | 0.71 – 0.91 |
| Fowler (1992) | $\frac{S_t}{H_0} = \left(22.72\frac{d_t}{L_0} + 0.25\right)^{0.5}$ (5.2) | 0.13 | 0.20 – 0.30 |
| McDougal *et al.* (1996) | $\frac{S_t}{H_0} = 0.41\cot\alpha^{0.85}\left(\frac{L_0}{H_0}\right)^{1/5}\left(\frac{d_t}{H_0}\right)^{1/4}\left(\frac{H_0}{d_{50}}\right)^{1/3}$ (5.3) | 0.22 | 0.70 – 0.80 |

$S_m$ = Scour in the vicinity of the seawall
$S_t$ = Scour at the toe of the seawall
$k$ = Wave number = $(2.\pi).L_o^{-1}$
$C$ = Constant 0.4 (fine) 0.3 (coarse) sand
$d_t$ = Toe water depth
$L_o$ = Offshore wavelength
$H_o$ = Offshore wave height
$D_{50}$ = Sediment diameter
$cot\ \alpha$ = Beach gradient

In reviewing the variables within the Xie (1981) equation, the Hyperbolic Sine function was found to have a small effect on the predicted scour depth (<5 % when $d_t/L_m$ = 0.08). It is not clear why this parameter was included. The equation also includes a coefficient for sediment grain size, with fine grained sediments leading to a relative increase in the scour depth. The Fowler (1992) equation is based on a statistical fit to laboratory data collected with arbitrary coefficients. The equation appears to bisect the higher scour values within the dataset, providing an upper estimate of toe scour.

The McDougal *et al.* (1996) equation includes additional parameters to describe the beach sediment and geometry and is a first step towards a processes based prediction equation. Equation 5.3 suggests scour is proportional to increases in wavelength, toe water depth and beach slope. In contrast to Xie (1981), and despite only testing one sediment size, Equation 5.3 suggests that scour is inversely proportional to grain size. The literature review identified that turbulence and wave reflected transport to be critical to scour, these would be expected to cause increased suspension of finer grained sediments.

As noted by Sumer & Fredsøe (2002), when the Xie (1981) and Fowler (1992) predictors are plotted together using the non-dimensional units $S/H_0$ and $d_t/L_m$, a scour depth envelope is produced, with maximum scour peaking at both 0.030 & 0.075 $d_t/L_m$ (Figure 5-1). In this plot the Fowler (1992) equation represents toe scour, the Xie (1981) equation maximum scour, which tends to occur further offshore. However, neither researcher collected data from the critical region (0.03 <$d_t/L_m$ <0.075), where scour depths appear to be greatest and of most interest.

Fowler (1992) attempted to extrapolate the curve (as shown on Figure 5-1) using small scale, regular wave period tests from Chesnutt & Schiller (1971) and Barnett (1987). This suggests the equations intersect at a point close to $d_t/L_m$ = 0.07. The errors associated with experiments at this scale were illustrated in Chapter 2.3.1, reducing the confidence that can be placed on scour depth predictions in this range. In particular, the values of $S_m/H_0$ appear >1. This is not supported by the existing literature, or recent field experiments.

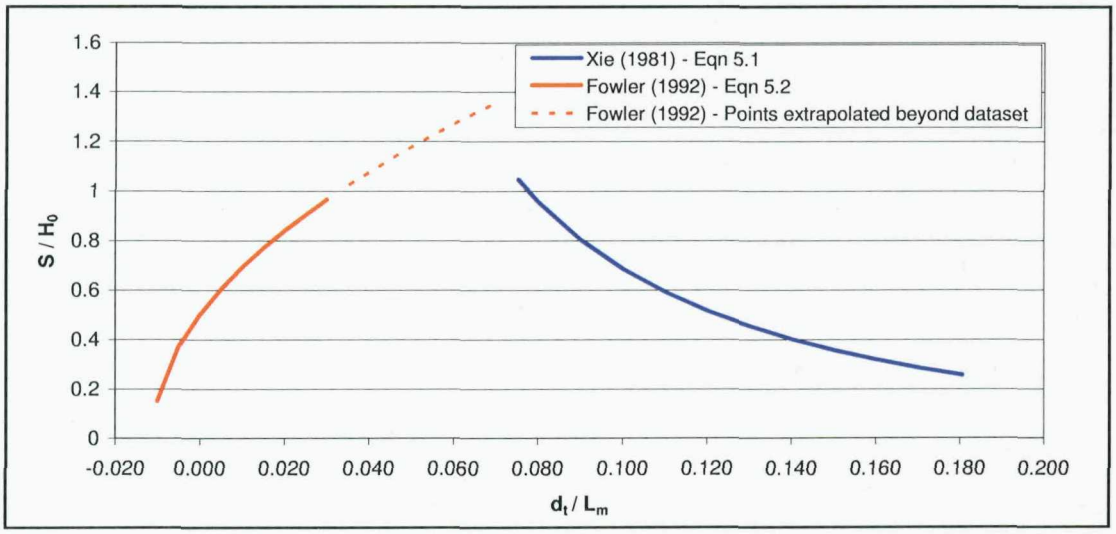


**Figure 5-1: Non-dimensional plot of scour prediction equations 5.1 & 5.2 for a sand beach, $H_0$ = 0.2 m , $d_t$ = 0.2 m, $T_m$ =2.5 s, $L_m$ =10 m.**

### 5.1.2. Summary

A review of three scour prediction equations based on medium scale laboratory test suggests that existing methods for prediction scour are limited to either breaking or non-breaking conditions. There is no reliable guidance in the region $d_t / L_m = 0.07$ where scour appears deepest. This is the region of most interest to engineering and scientists. All the equations rely on empirical fits to laboratory datasets, with arbitrary coefficients. Equation 5.3 from McDougal. *et al* (1996) is the only one to include some of the key scour parameters.

The following sections present the methodology and results of the latest medium scale flume experiments conducted at HR Wallingford. These straddle the range of both the Xie (1981) and Fowler (1992) datasets. The results are used to test the existing prediction equations and take forward Figure 5-1 to enable development of improved scour prediction methods.

## 5.2. Aims and objectives

The existing field and flume measurements improve our understanding of the toe scour process; however when designing structures, engineers and scientists require guidance for a range of full scale conditions, which may not correspond to a specific test. Producing a statistical best fit line to a test series enables empirical equations to be developed, and a causal relationship to be established. Together these improve understanding and quantify the scour in the prototype environment. For this study the following experimental aims were established:

- Examine the latest experiments to define a causal relationship;
- Investigate the conditions when $0.04 \leq d_t / L_m \leq 0.08$, a region of interest defined by earlier scour predictors;
- Test the existing scour predictors of Xie (1981), Fowler (1992) and McDougal *et al.* (1996) using the latest results;
- Produce a new prediction equation, suitable for use by coastal engineers to predict maximum and toe scour for a range of seawall conditions;
- Establish the principle mechanisms leading to maximum toe scour.

## 5.3. Materials and methods

Physical model tests were conducted in the new 40 m, 2D wave flume within the Froude Modelling Hall at HR Wallingford, UK. The flume, 1.2 m wide by 1.7 m high, consisted of concrete side walls and a 4 m long glass side window opposite the seawall (Figure 5-2). Irregular period JONSWAP spectrum waves were generated using a piston-type wavemaker, with stroke length +-0.6m and maximum operating depth of 1.6 m. An integral absorption system was used to absorb wave energy reflected by the seawall.

A 19.2 m long, 1:30 smooth concrete slope was constructed from the flume floor up to an elevation of 0.64 m, to form a test basin 5.14 m long which was filled with Redhill 110 sand with $D_{50} = 0.111$ mm, and a settling velocity of 0.0077 $ms^{-1}$ (based on Soulsby, 1997). In tests 1 to 14 a 1:30 beach slope was used, tests 15 to 34 used a 1:75 beach slope. Before each run the sand was re-profiled using a screeder and screed boards to provide a smooth finish.

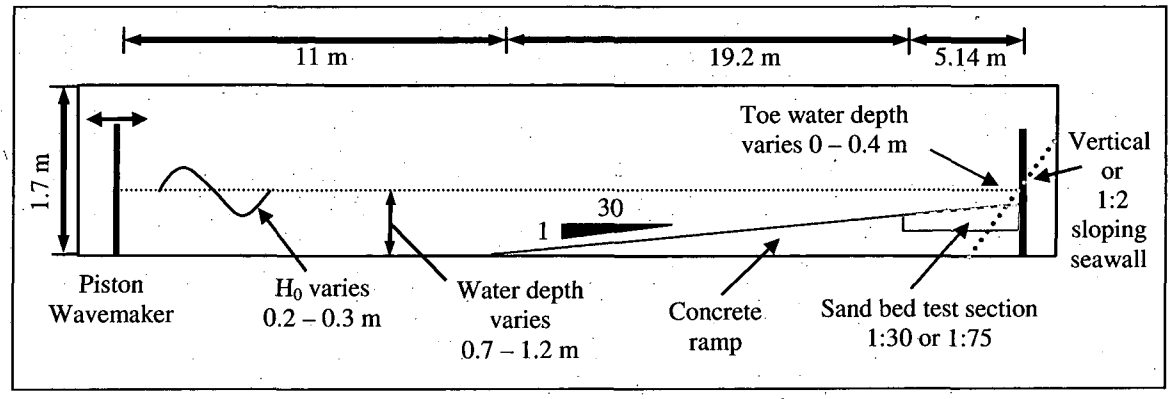


**Figure 5-2: Flume cross section schematic**

Beach profile measurements were collected using a touch sensitive profiling system (HR Wallingford, 2007), which caused only slight deformation (approximately 1 to 2 mm) of the sand bed. The specified system resolution was ± 1 mm in the horizontal direction and ± 0.5 mm in the vertical direction. This data was interrogated to determine the magnitude of scour at the toe of the seawall ($S_t$) and the maximum scour on the beach profile ($S_m$). In the sloping wall tests, scour at the wall caused the toe position to move seaward, as the buried element of the seawall became exposed; therefore $S_t$ was measured where the new beach level intersected with the wall at the end of the test.

A group of four wave probes was situated at the offshore end of the flume and additional probes were placed over the sand bed and near the seawall. During the tests the vertical seawall created reflected waves, there were removed at the end of the flume by the absorbing wave paddle. In the wave probe records, the incident and reflected waves were separated by performing reflection analysis using the Goda & Suzuki (1976) least squares method on the data from the three offshore wave probes. The wave height records were analysed using a Fast Fourier Transform to derive the wave energy spectrum for comparison to the specified input spectrum. Statistical analysis was then conducted to determine the offshore significant wave height ($H_0$), offshore peak wave period ($T_p$) and reflection coefficient for each test.

Further details of the test procedure and equipment setup are described in HR Wallingford (2006). The tests conducted with variable water levels and rock toe protection are reported in Sutherland *et al.* (2006).

## 5.4. Results

### 5.4.1. Scour depth results

Test results were obtained for a vertical and 1:2 sloping seawall with a significant wave height ($H_0$) of 0.20 m or greater, for a range of irregular wave periods ($T_p$) and seawall toe water depths ($d_t$). The pre-test setup and calibration runs indicated that a duration of 3000 peak period waves would produce scour conditions consistent with the tidal exposure duration in the UK. Beach profile measurements were taken at the end of each test to determine the toe scour ($S_t$), the maximum scour ($S_m$) and the position ($X$) of maximum scour relative to the seawall toe (Table 5-2 & Table 5-3). The tables include the Iribarren number ($\xi$), an indication of wave breaker type.

**Table 5-2: Vertical seawall test results**

| Test no. | Beach slope | $H_0$ (m) | $T_p$ (s) | $\xi$ | $d_t$ (m) | $d_t/L_m$ | $S_t$ (m) | $S_m$ (m) | $X$ (m) |
|---|---|---|---|---|---|---|---|---|---|
| 1 | 1:30 | 0.193 | 1.55 | 0.15 | 0.200 | 0.087 | 0.057 | 0.057 | 0.031 |
| 2 | 1:30 | 0.193 | 1.87 | 0.18 | 0.200 | 0.060 | 0.065 | 0.065 | 0.031 |
| 3 | 1:30 | 0.198 | 2.29 | 0.21 | 0.200 | 0.040 | 0.130 | 0.130 | 0.031 |
| 4 | 1:30 | 0.194 | 3.24 | 0.31 | 0.200 | 0.020 | 0.158 | 0.158 | 0.031 |
| 5 | 1:30 | 0.197 | 4.58 | 0.43 | 0.200 | 0.010 | 0.140 | 0.143 | 0.049 |
| 6 | 1:30 | 0.204 | 1.87 | 0.17 | 0.000 | 0.000 | -0.031 | 0.025 | 0.731 |
| 7 | 1:30 | 0.196 | 3.24 | 0.30 | 0.000 | 0.000 | -0.011 | 0.032 | 1.513 |
| 8 | 1:30 | 0.197 | 1.87 | 0.18 | 0.100 | 0.030 | 0.110 | 0.111 | 0.006 |
| 9 | 1:30 | 0.202 | 1.87 | 0.17 | 0.400 | 0.120 | -0.013 | 0.035 | 0.327 |
| 11 | 1:30 | 0.217 | 3.24 | 0.29 | 0.400 | 0.040 | 0.040 | 0.117 | 0.414 |
| 12 | 1:30 | 0.197 | 3.24 | 0.30 | 0.100 | 0.010 | 0.088 | 0.114 | 0.469 |
| 13 | 1:30 | 0.295 | 2.29 | 0.18 | 0.150 | 0.040 | 0.093 | 0.125 | 0.415 |
| 14 | 1:75 | 0.280 | 1.87 | 0.06 | 0.300 | 0.090 | 0.036 | 0.052 | 0.354 |
| 15 | 1:75 | 0.196 | 1.87 | 0.07 | 0.200 | 0.060 | 0.027 | 0.048 | 0.295 |
| 16 | 1:75 | 0.197 | 3.24 | 0.12 | 0.200 | 0.020 | 0.089 | 0.102 | 0.404 |
| 18 | 1:75 | 0.191 | 4.58 | 0.17 | 0.200 | 0.010 | 0.062 | 0.119 | 0.495 |
| 19 | 1:75 | 0.215 | 3.24 | 0.12 | 0.400 | 0.040 | 0.050 | 0.100 | 0.417 |

**Table 5-3- 1:2 sloping seawall test results**

| Test no. | Beach slope | $H_0$ (m) | $T_p$ (s) | $\xi$ | $d_t$ (m) | $d_t/L_m$ | $S_t$ (m) | $S_m$ (m) | $X_{sm}$ (m) |
|---|---|---|---|---|---|---|---|---|---|
| 26 | 1:75 | 0.190 | 1.87 | 0.07 | 0.200 | 0.060 | 0.063 | 0.068 | 0.165 |
| 27 | 1:75 | 0.192 | 3.24 | 0.12 | 0.200 | 0.020 | 0.104 | 0.105 | 0.232 |
| 28 | 1:75 | 0.194 | 1.55 | 0.06 | 0.200 | 0.087 | 0.062 | 0.072 | 0.155 |
| 29 | 1:75 | 0.241 | 1.87 | 0.06 | 0.300 | 0.090 | 0.063 | 0.052 | 0.203 |
| 30 | 1:75 | 0.243 | 3.24 | 0.11 | 0.400 | 0.040 | 0.043 | 0.064 | 0.124 |
| 31 | 1:75 | 0.201 | 1.87 | 0.07 | 0.000 | 0.000 | -0.001 | 0.010 | 2.480 |
| 32 | 1:75 | 0.206 | 3.24 | 0.12 | 0.000 | 0.000 | -0.006 | 0.023 | 2.640 |
| 33 | 1:75 | 0.192 | 1.87 | 0.07 | 0.400 | 0.120 | 0.014 | 0.024 | 0.066 |

### 5.4.2. Scour beach profiles

Figure 5-3 shows typical beach profiles, for similar wave conditions, over a range of water depths, for a vertical seawall. The profiles were plotted with axes of equal scale to represent the scour shape. The shallow gradient of the beach profile shape differs greatly from the typical examples provided in coastal engineering books, which are frequently presented with an exaggerated vertical scale which can be misleading. For example Figure 3-6 taken from Loveless (1994).

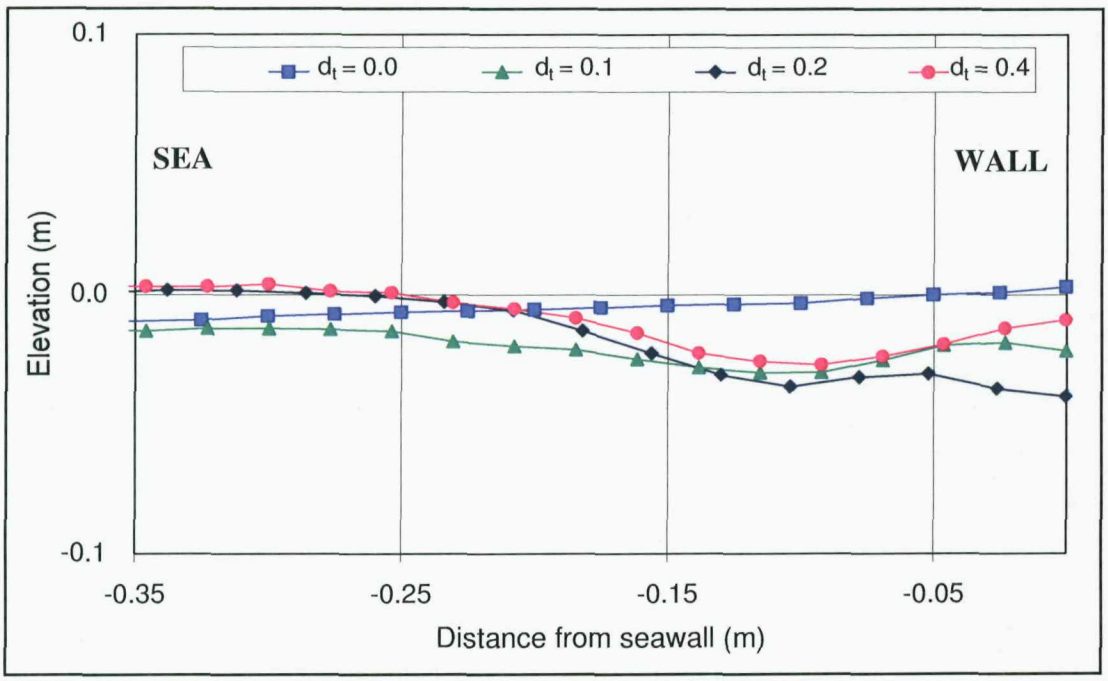


**Figure 5-3: Beach level at 3000 waves, Tests 4, 7, 11 & 12 for a vertical seawall. $H_0$ = 0.2 m, $T_p$ = 3.24 s**

The scour depth peaked when the water depth was sufficient to allow breaking waves to impact onto the seawall. This typically occurred when $H_0 / d_t \approx 1$ and led to sediment suspension by reflected and turbulent flows. These conditions also produced high velocity jets and spray, which were directed up the wall, before plunging down into the flume and mobilising sediment. As a result the rippled bed forms at the wall toe were washed away. This bed feature is discussed further in Chapter 5.8.2 and shown in Figure 5-13.

The velocity of the downrush was estimated at 4.3 $m.s^{-1}$ from analysis of video images and was approximately ten times greater then the critical threshold for sediment transport, demonstrating the importance and dominance of these flows to the scouring process when the wave conditions enable their formation.

When the water depth was very shallow, ($H_0/d_t > 4$), waves broke offshore and only small swash waves reached the beach, leading to accretion at the toe of the wall. When the toe water depth was increased significantly ($H_0/d_t \leq 0.5$), turbulence associated with wave breaking was localised at the water surface and only occasionally reached the bed. Sediment transport appeared to be dominated by flows associated with the wave orbital motion, moving the position of greatest scour offshore of the seawall.

## 5.5. Toe scour prediction

In the sediment transport test, the interaction of the incident waves and the seawall demonstrated that the toe water depth was critical in determining the type of wave breaking, which dictated the position and magnitude of sediment transport at the wall toe. This suggested that analysing the dataset using the non-dimensional parameters in Figure 3-9, would be beneficial. Non-dimensional analysis can be used to identify causal relationships in different physical model experiments, without the need to establish the precise model scale.

This approach was developed and a refined prediction equation produced by the author in cooperation with Dr James Sutherland- HR Wallingford and Dr Gerald Müller- University of Southampton.

### 5.5.1. Non-dimensional analysis

The datasets were compared using the units $d_t/L_m$ and $S_t/H_0$, similar units to those used by Sumer & Fredsøe (2002), however the peak wave period was converted to the mean period, by multiplying by a factor of 0.781 to enable later comparison with regular wave tests results and the field data presented in Chapter 4. The initial analysis focused on scour at the wall toe ($S_t$), as opposed to maximum scour across the beach profile ($S_m$), as toe scour is considered more critical to seawall damage and failure.

Figure 5-4 and Figure 5-5 combine the scour results for the 1:30 and 1:75 bed slopes, with Fowler (1992) 1:15 bed slope for a vertical seawall. Both toe scour and maximum scour followed a similar pattern, increasing to a point where $d_t/L_m \approx 0.017$ and decreasing either side. Additional data points from Xie (1981), who used a flat bed profile, fine sand and irregular period waves, confirmed that maximum and toe scour decreases when $d_t/L_m > 0.04$. In the case of toe scour, the Xie dataset highlights the

potential for accretion to occur under reflective wave conditions. However, it is likely that the flat beach profile used in these tests contributed to the significant height of these accretions compared to the results of HR Wallingford (2006). The single test from Kraus & Smith (1994) appears to fit the scour depth trend, despite being modelled with an equilibrium beach profile.

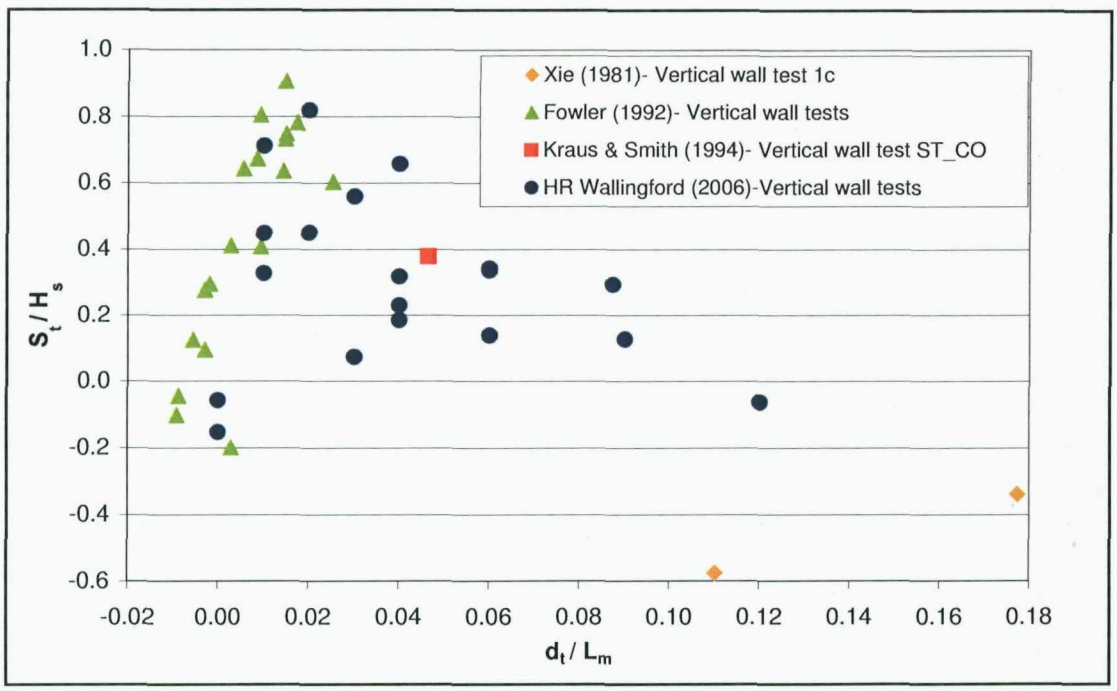


**Figure 5-4: Combined medium scale flume tests -Toe scour**

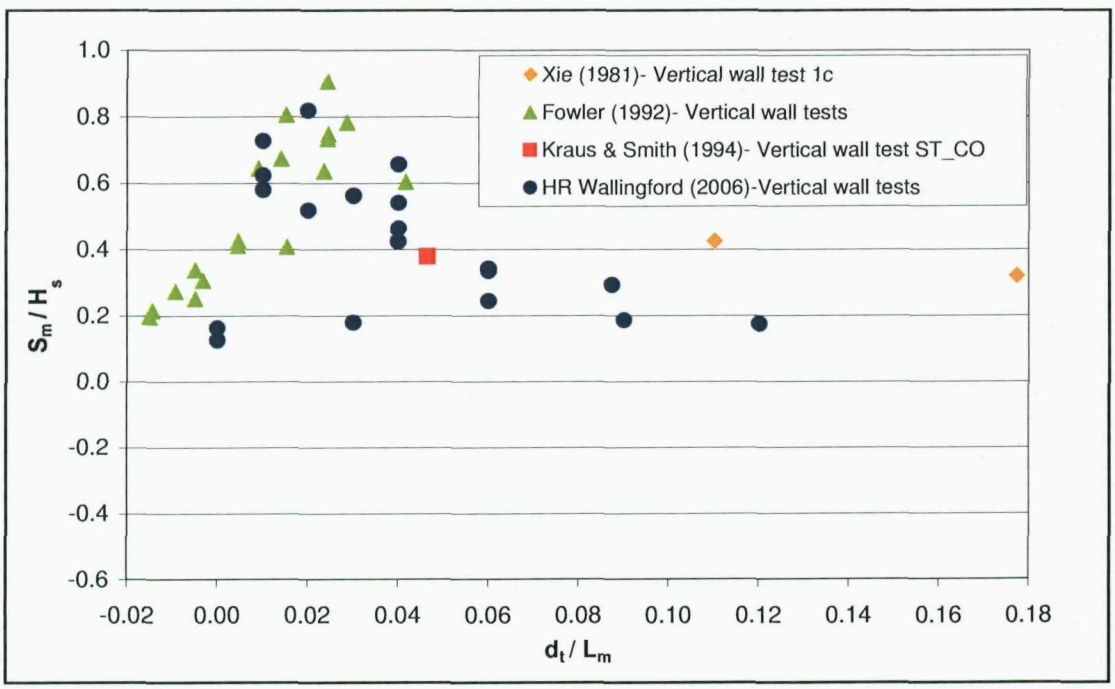


**Figure 5-5: Combined medium scale flume tests -Maximum scour**

Due to the flat beach profile and equilibrium profiles utilised in the Xie (1981) and Kraus & Smith (1994) test, these datasets were not taken forwards. Based on there similar methodology and concurring result, the HR Wallingford (2006) and Fowler (1992) datasets were combined for further analysis and comparison to the existing scour prediction equations for toe scour.

### 5.5.2. Vertical seawall scour predictor comparison

The maximum toe scour results from the combined Fowler (1992) and HR Wallingford (2006) datasets were used to test the fit of Equations 5.1 as shown in Figure 5-6.

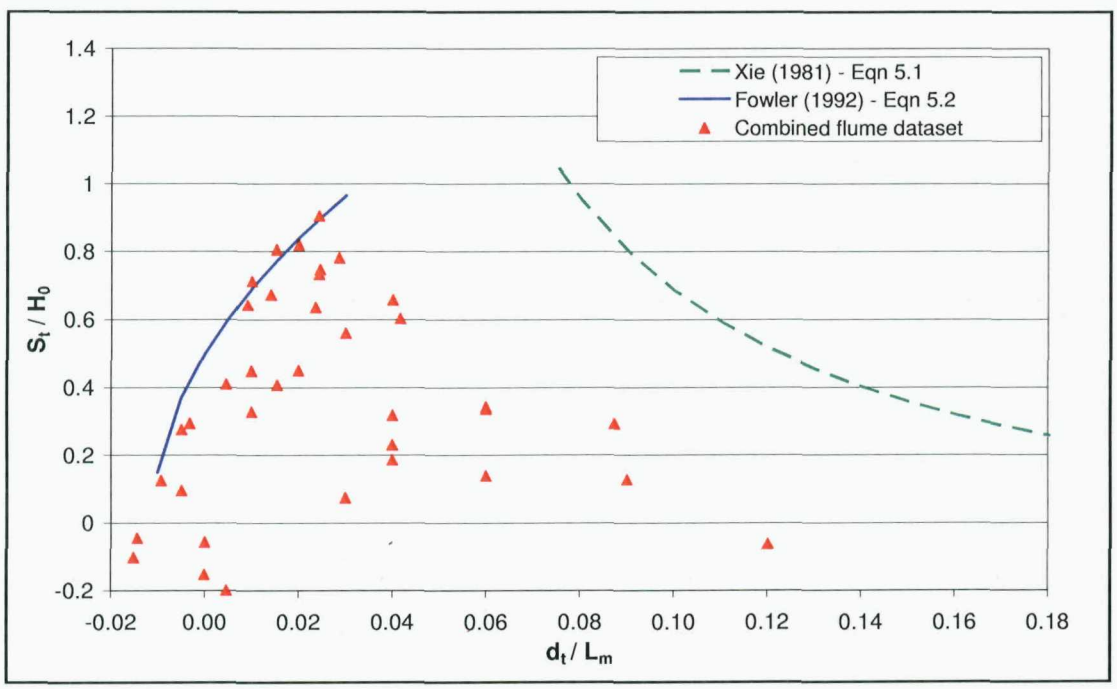


**Figure 5-6: Comparison Xie (1981) and Fowler (1992) scour predictors to the combined dataset**

Given the similarities of Figure 5-4 & Figure 5-5, Equation 5.1 from Xie (1981) for prediction maximum scour on the beach profile was applied to predict toe scour. The curve represents the approximate shape of the scour envelope for events where $d_t/L_m > 0.04$, but significantly over estimates the toe scour depth. This would also occur when plotted against values of maximum scour. Equation 5.2 from Fowler (1992) was found to fit the upper extreme and general shape for $d_t/L_m < 0.03$, though this is where most of the Fowler test results occur. However, the equation is limited to values of $d_t$ >-0.1m, therefore cannot cross zero on the ordinate axis.

Predictions based on Equation 5.3 from McDougal *et al.* (1996) are dependent on the beach slope and sediment size. Therefore three test cases were predicted: 1) Fowler (1992), 1 in 15 slope, $D_{50} = 0.11$ mm; 2) HR Wallingford (1996) 1 in 30, $D_{50} = 0.11$ mm; 3) HR Wallingford (1996) 1 in 75 slope, $D_{50} = 0.11$ mm. The predictions and corresponding elements of the combined datasets are shown in Figure 5-7.

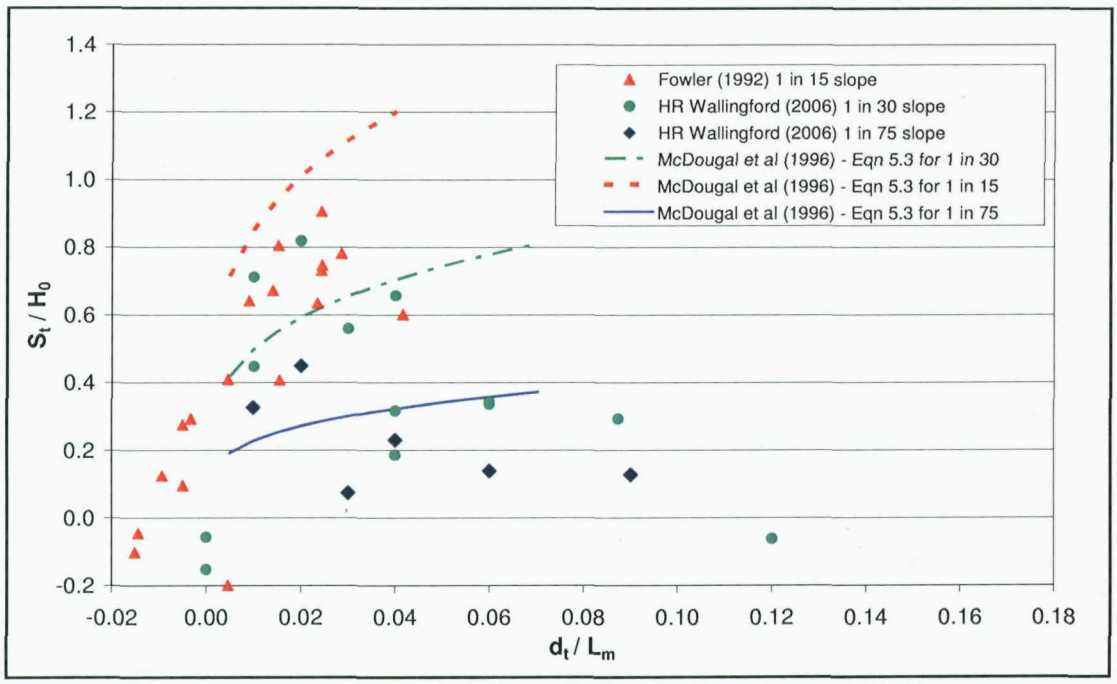


**Figure 5-7: Comparison McDougal *et al.* (1996) scour prediction equation to specific tests in the combined dataset**

Equation 5.3 highlights the effect of beach slope, with the results for each slope peaking around 0.02 $d_t/L_m$. The 1 in 30 and 1 in 75 curves fall significantly below the peak scour depth and do not acknowledge the significant decrease in scour for $d_t / L_m > 0.04$. The predictions for the 1 in 15 slope exceed the test results of Fowler (1992). They do however follow a similar gradient and provide an upper estimate of predicted scour depths. However, the equation returns a complex number when $d_t < 0$, therefore values in the range cannot be predicted.

In summary, the combined flume dataset show that a significant change in hydrodynamics occurs at 0.02 $d_t / L_m$ irrespective of beach slope. The existing equations do not consider this process adequately; therefore a series of new equations were fitted to the dataset for both probabilistic and deterministic prediction of toe scour.

## 5.6. Development of scour predictor for probabilistic application

The dependency of scour depth on wave height, wavelength, beach slope, Iribarren number, reflection coefficient and a range of other variables was first approximated by plotting each variable against the scour depth data and observing the correlation (Appendix D). These results suggested that the toe water depth and wavelength were the most significant. However given the scatter in the plots, it was acknowledged, that these variables do not represent the physics of toe scour, but simply constitute a key element of the processes at work; potential for wave breaking.

At this stage a more rigorous numerical definition of the type of wave breaking in front of the seawall was not tested, due to a only a qualitative assessment of wave breaking being available. However this aspect was explored in greater detail in Chapter 7

The dataset was split into two halves around the points of maximum toe scour ($0.015 < d_t / L_m < 0.035$). Applying an iterative approach, each breakpoint was tested by fitting a second order polynomial trend line to the dataset using a least squares fitting technique. The optimum fit was obtained, as detailed in Equations 5.4 and 5.5 and Figure 5-8 below. For Equation 5.4, the coefficient of determination ($R^2$) and the standard deviation were determined as 0.57 and 0.249 respectively. Equation 5.5 obtained similar values with an $R^2$ value of 0.69 and standard deviation of 0.237. The equations are valid in the range $-0.013 \leq d_t/L_m \leq 0.018$ for the prediction to toe scour at seawalls with beach slopes between 1 in 15 and 1 in 75.

$$\frac{S_t}{H_0} = 362.95\left(\frac{d_t}{L_m}\right)^2 + 20.55\left(\frac{d_t}{L_m}\right) + 0.18 \qquad d_t/L_m \leq 0.021 \qquad (5.4)$$

$$\frac{S_t}{H_0} = 84.064\left(\frac{d_t}{L_m}\right)^2 - 19.11\left(\frac{d_t}{L_m}\right) + 1.118 \qquad d_t/L_m > 0.021 \qquad (5.5)$$

Though the $R^2$ value is significantly less then 1, which would indicate an exact prediction, the equations represent the key trends in the dataset and are an approximation of the complex hydrodynamic and sediment processes occurring in front of the wall. To verify the key parameters were represented by the equations, the prediction residuals($S_{predicted}$ - $S_{observed}$) were plotted against $L_m$, $d_t/L_m$ and the Iribarren

number (Appendix E). The residual values were highly scattered compared to the Iribarren number and the $d_t/L_m$ ratio, however a clear correlation to these parameters was not observed.

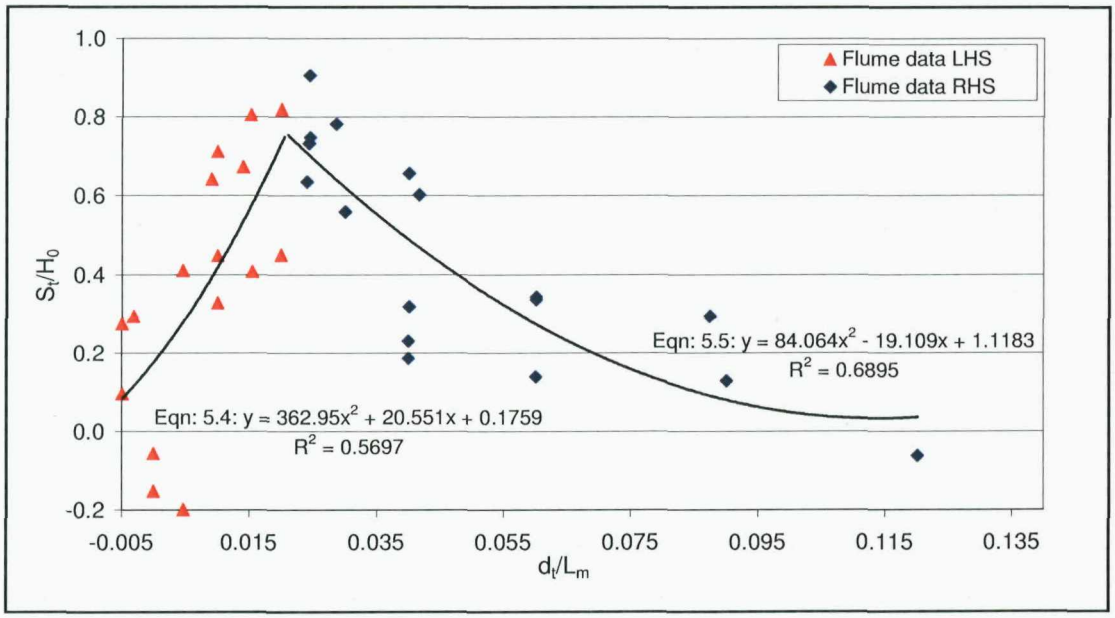


**Figure 5-8: Plot of prediction Equations 5.4 and 5.5 to the combined laboratory dataset.**

## 5.7. Scour predictor development for deterministic application

### 5.7.1. Approach 1: HR Wallingford (2006a)

As part of the Defra funded research project, Dr J Sutherland of HR Wallingford combined the medium scale toe scour model datasets with the field results from Blackpool and Southbourne. His aim was to develop a conservative estimate of toe scour over a range of relative water depths, beach slopes and sand grain sizes which could be applied to develop design tools and be incorporated into risk based asset management software. Equation (5.6) predicts the maximum toe scour ($S_{tm}$) for a vertical seawall. The curve, shown in Figure 5-9 below from (HR Wallingford (2006a), was fitted by eye to provide a conservative estimate scour depth, and is valid for the range $-0.013 \leq d_t/L_m \leq 0.018$ and $0 \leq \xi \leq 0.43$.

$$\frac{S_{tm}}{H_s} = 4.5e^{-8\pi(d_t/L_m+0.01)}\left(1-e^{-6\pi(d_t/L_m+0.01)}\right) \qquad (5.6)$$

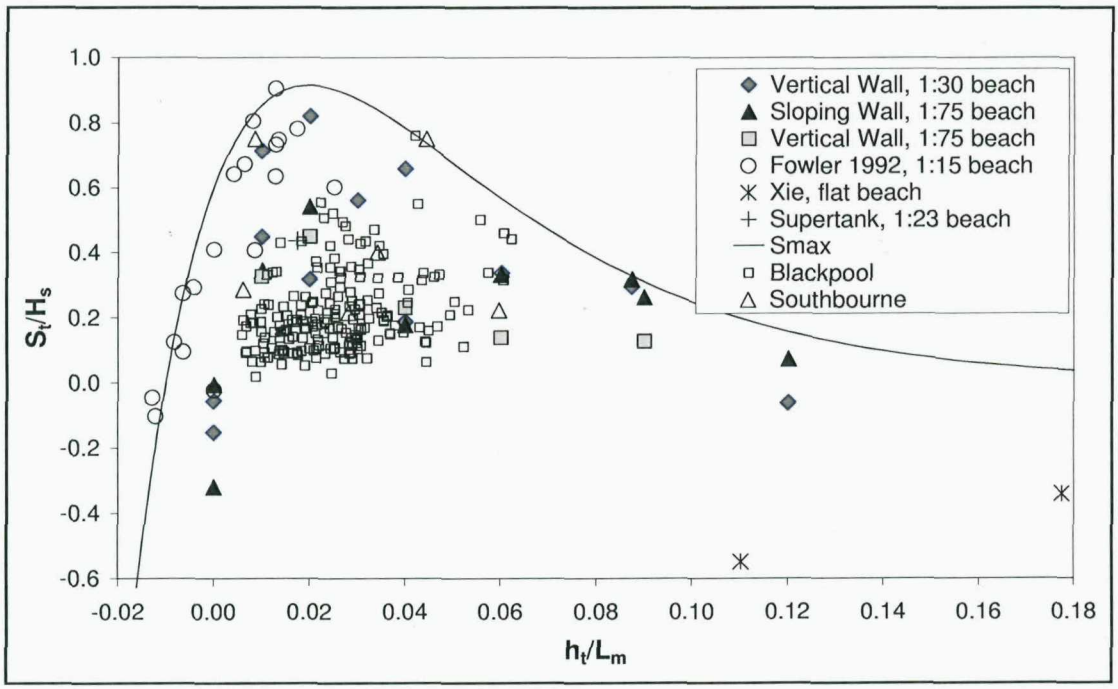


**Figure 5-9: Equation (5.6), conservative predictions of maximum toe scour compared to medium scale flume and field data**

The curve above can be applied to provide a simple first estimate of toe scour risk at a seawall and conservative values of scour depth. However, similar to the prediction equations 5.1 to 5.5, the curve does not indicate the significant changes in wave

breaking conditions occurring within different regions of the prediction. Furthermore, extrapolation of the curve beyond, $d_t / L_m = 0.12$, suggest that toe scour continues to occur, under these conditions toe scour will be expected to decrease and be replaced with toe accretion due to reflective wave conditions.

### 5.7.2. Approach 2: Pearce *et al.* (2008)

To provide a more accurate prediction of mean toe scour depth, the dataset was split in half at the peak toe scour depths and a curve fitted to each side of the dataset. To ensure the resulting equation remained practical for deterministic applications, the following additional criteria were established:

1. Be relatively simple with few fitted coefficients, to enable the user to interpret the effect of different variables;
2. The predicted scour depth should tend towards zero for high and low relative water depths to prevent erroneous results;
3. The peak predicted scour depth should always remain below $S / H_s \leq 1$, as shown in recent scour field and laboratory measurements;
4. The curves should be tested using statistical analysis to minimise human bias and error;
5. An upper envelope should be generated to enable conservative scour depth estimates for design.

**Statistical methods for developing the predictor**

The judge the reliability and success of each new equation the systematic and unsystematic root mean square error (RMSE) and the bias statistical tools were used to quantitatively measure the fit and provide guidance on how each equation could be improved to reduce the error. This procedure assumed that the observations were error-free and therefore all errors were a result of the prediction equation. This approach was adopted due to the relatively simple parameters collected during the experiment (e.g. toe water depth, wave height, scour depth etc).

The systematic error ($RMSE_s$) represents the success of the equation in making the right prediction for each data point, a systematic error of zero would represent a perfect fit (i.e. $Y=X$). The results of the scour prediction equation were plotted versus the observed values and a linear trend line fitted using a least squares algorithm. The difference

between the observed value and the corresponding prediction on the trend line were squared, summed and square rooted.

The unsystematic error ($RMSE_u$) is a measure of random errors in the experimental method or procedure (i.e. scatter); and was only considered briefly to evaluate the data quality. The prediction bias was also measured. This provided an indication of the offset of the trend line prediction when zero scour occurred, i.e. graphically a well fitting trend line would be expected to cross at the intersection of the $X$ and $Y$ axes. The systematic and unsystematic RMSE equations are presented below (Eqn 5.7 & 5.8 respectively), where $X$ represents the observed value, $Y$ the prediction, and $\hat{Y}$ the trend line prediction for the least squares fit. For simplicity, when presenting the error results, the systematic and unsystematic were summed to calculate the total root mean square error. The effect of systematic error and bias are demonstrated in Figure 5-10.

$$RMSE_s = \left[\left(\hat{Y} - X\right)^2\right]^{0.5} \qquad \text{(Eqn 5.7)}$$

$$RMSE_u = \left[\left(\hat{Y} - Y\right)^2\right]^{0.5} \qquad \text{(Eqn 5.8)}$$

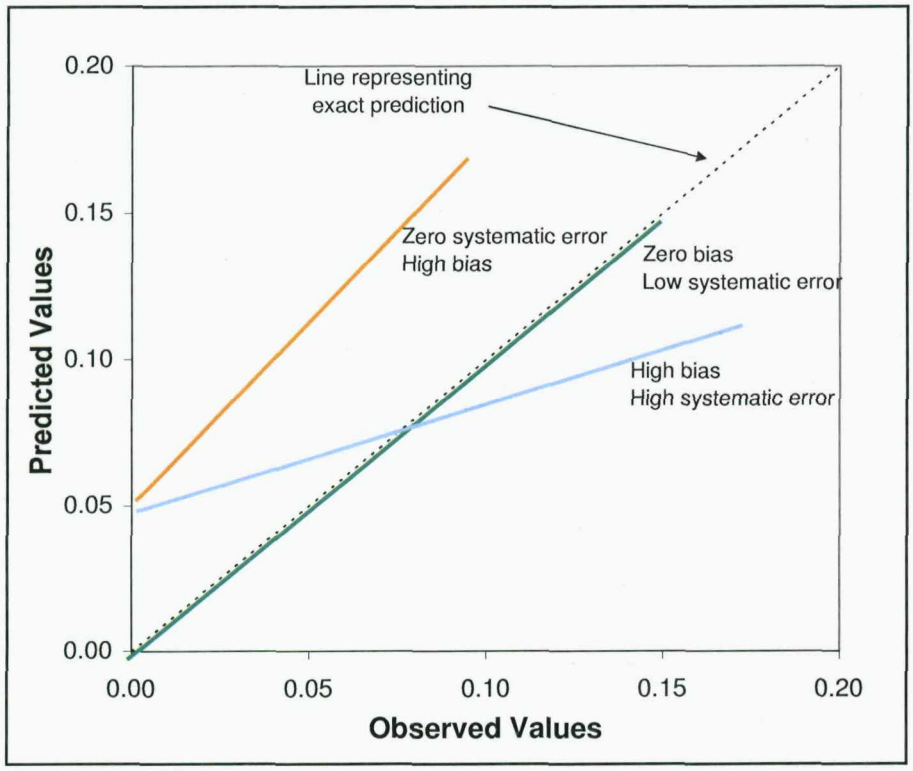


**Figure 5-10: Characteristics of the systematic & unsystematic error and bias**

By utilising a statistical measure of the error, the fit of the scour predictor to the dataset was obtained without including human bias from interpreting the results graphically.

**Predictor results**

To produce a best fit line, the dataset was split in two parts by iteratively selecting a break point between $d_t/L_m$ 0.0075 and 0.03 and deriving an equation to represent data lying on either side of the break. The success of each equation was determined empirically using the systematic and unsystematic root mean square error and bias.

Equations (5.9) and (5.10) below were found to satisfy the prediction criteria, maintain a low bias and systematic error for a break point at $d_t/L_m$=0.016.

$$\frac{S_t}{H_0} = \left(35\frac{d_t}{L_m} + 0.53\right)^{1.25} - 0.3 \qquad d_t/L_m \leq 0.016 \qquad (5.9)$$

$$\frac{S_t}{H_0} = 42\left(\frac{d_t}{L_m}\right)^2 - 15\left(\frac{d_t^*}{L_m}\right) + 1.03 \qquad d_t/L_m > 0.016 \qquad (5.10)$$

The best-fit lines for Equation 5.9 and 5.10 are shown in Figure 5-11, which have a total RMSE of 0.246 and 0.167 and bias of 0.0 and -0.004 for the left and right side equations respectively. Plots showing the goodness of fit for each equation are included in Appendix F.

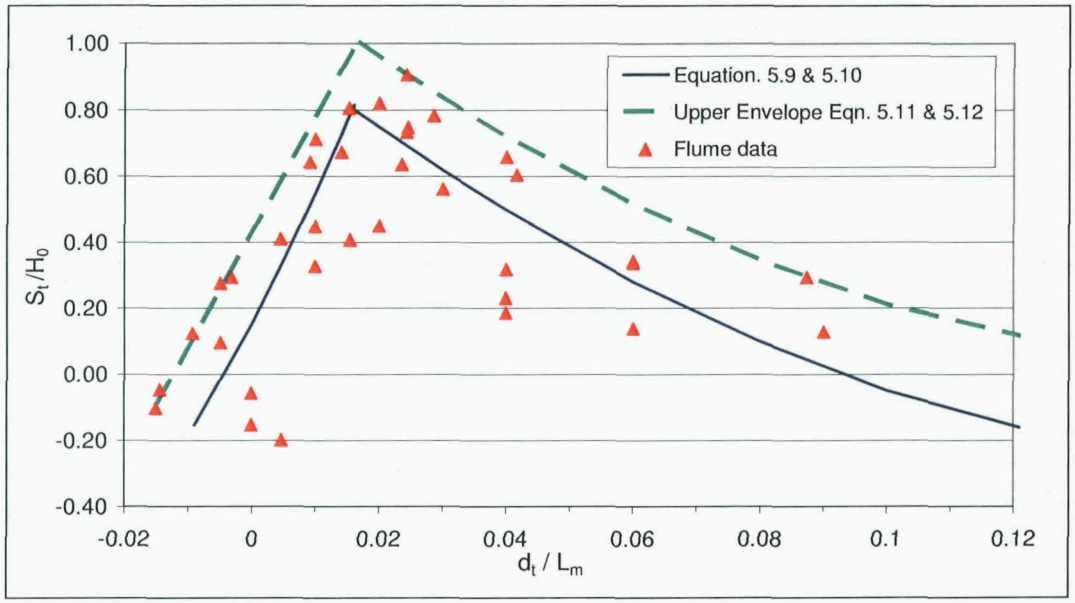


**Figure 5-11: Best fit toe scour Equations 5.9 and 5.10 plotted with upper envelope toe scour equations 5.11 and 5.12**

Equations 5.9 and 5.10 were developed further to derive an upper scour envelope as shown in Figure 5-11. Equations 5.11 and 5.12 were fitted by eye to predict the maximum toe scour for deterministic design.

$$\frac{S_t}{H_0} = \left(35\frac{d_t}{L_m} + 0.53\right) - 0.1 \qquad d_t/L_m \leq 0.0165 \qquad (5.11)$$

$$\frac{S_t}{H_0} = 42\left(\frac{d_t}{L_m}\right)^{1.95} - 15\left(\frac{d_t}{L_m}\right) + 1.24 \qquad d_t/L_m > 0.0165 \qquad (5.12)$$

Equations 5.9 to 5.12 are limited to $-0.015 < d_t / L_m < 0.12$ and peak at $S_t / H_0 = 1$. At the lower extreme, accretion is predicted at the toe of the wall. These equations remain valid for small values of $d_t$ including negative values, unlike the equations shown in Figure 5-7.

### 5.7.3. Sloping seawall scour prediction

Few medium scale irregular wave scour experiments have been conducted on sloping seawalls. The results of HR Wallingford (2006) showed that a 1:2 sloping wall could be as equally prone to toe scour as a vertical wall. The sloping wall flume results were plotted with the field results from Blackpool against the vertical scour prediction equations 5.9 to 5.12 (Figure 5-12). At the sloping wall, $S_t / H_0$ remains $<1$, and scour peaks at around $d_t / L_m = 0.025$. The results show that most of data points fit the general profile of the vertical wall best fit line, and with the exception of one point, all points fit the upper toe scour envelope equation.

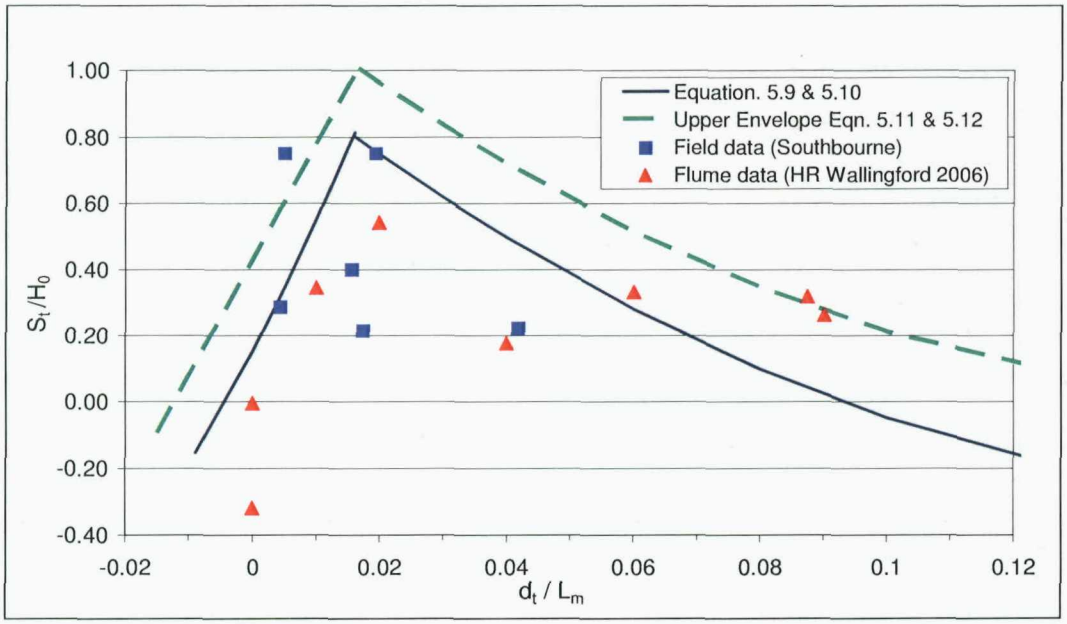


**Figure 5-12: Comparison of vertical seawall toe scour prediction equations to the 1:2 sloping seawall flume tests and field experiments at Southbourne**

## 5.8. Discussion

### 5.8.1. Limitations

The Fowler (1992) and HR Wallingford (2006) datasets were conducted at medium scale, using irregular period waves in a 2D flume. By using fine sand, suspended sediment transport dominated in both experiments, though was reduced in the tests conducted in very shallow water. Both experiments were conducted in similar sized flumes, and complement each other, despite being collected at different research institutions, demonstrating that laboratory effects were minimal. The combined dataset represents the best currently available for predicting scour at seawall structures.

The new dataset supersedes the reported small scale sediment transport tests, which have tended to be bedload dominated, often utilising regular period waves, which overestimated scour depths. However in both tests series, the significant wave heights modelled were in the range of 0.2 to 0.3 m for both experiments, therefore the dependence of scour depth of wave height has not been fully investigated, and requires further at modelling at medium or large scale. It could be speculated that the incident waves would be depth limited, therefore an increase in wave height may simply cause a shift in the breaker position and lateral shift in position on Figure 5-6, leading a change in the scour depth.

The combined datasets included beach profiles at 1:15, 1:30 & 1:75, all commencing from a plane bed slope to ensure consistent scour depths were recorded. The different beach profile slopes are likely to be the main cause of the scatter in the dataset, with steeper beaches tending to generate the deeper scour. Only Kraus & Smith (1994) conducted tests with an equilibrium beach profile, which was found to fit well with the other tests. An equilibrium profile would be expected to encourage wave breaking in the surf zone, however if the beach levels are low, there may be insufficient beach material to form the profile. Further research using a variety of beach slopes, and a repeatable equilibrium beach profile are required to fully understand this variable.

### 5.8.2. Model and scale effects

When designing the experiments a prototype scale was not chosen, instead the experiment was setup, using fine sand and high relative wave energy to ensure suspended sediment transport was achieved. For reference the medium scale test examples provided in Section 2, were based upon Test 4, and demonstrated suspended sediment transport would occur in most cases.

As the model tests results could be applied to prototype wall designs, it is important to investigate the influence of model and scale effects. At model scale the increased relative viscosity of the water and fine sediment grain size appeared to inhibit swash transport processes when the water depth was shallow ($H_0/d_t > 4$). Though the final beach profiles provided evidence that onshore sediment transport and infilling of scour features could occur, this was less then expected. This scale effect only seemed to affect the minority of tests where the toe water depth was < 0.05 m.

During tests where ($0.5 < H_0/d_t < 3$), breaking wave impacts and turbulence turned the water cloudy, with sediment plumes often persisting over one wave period duration. Given the high wave energy dissipation and the dominance of suspended sediment transport these test would be expected to suffer from the least viscous scale effects.

In the deep water tests ($H_0/d_t < 0.5$) sediment transport appeared to be dominated by flows associated with the wave orbital motion, though plumes of suspended sediment were also visible when reflected waves generated high speed flow accelerations. Based on linear wave theory the peak orbital velocity at the bed for a wave with $H_0 = 0.2$ m, $T_p = 3.24$ s, $d_t = 0.4$ m would be approximately 1 m.s$^{-1}$, which is approximately ten times greater then the threshold for sediment transport of the sand used in the experiment. This confirms that even the deepest tests were capable of generating significant sediment transport.

During the tests, sand ripples were observed in the bed and though consistent in form to ripples observed in the field, they appeared overly large compared to the model scale (Figure 5-13). This was assumed to be a consequence of the increased water viscosity, which caused the sediment boundary layer to increase and enable higher ripple growth

before becoming limited by drag. The net result was to increase the bed roughness, and hence energy dissipation of waves as they passed over the bed.

In a bedload dominated model, ripples could reduce the sediment transport rate, by resisting motion of sand particles. The dominance of suspended sediment transport in these experiments, suggest this would be less of a problem. Compared to the energy dissipation due to wave breaking and wave reflection, this source of energy loss was considered negligible. This was supported by a lack of bedforms at the toe of the wall when $H_0 / d_t = 1$, where high velocity downrush flows following the wave impact produced high levels of turbulence and sediment suspension.

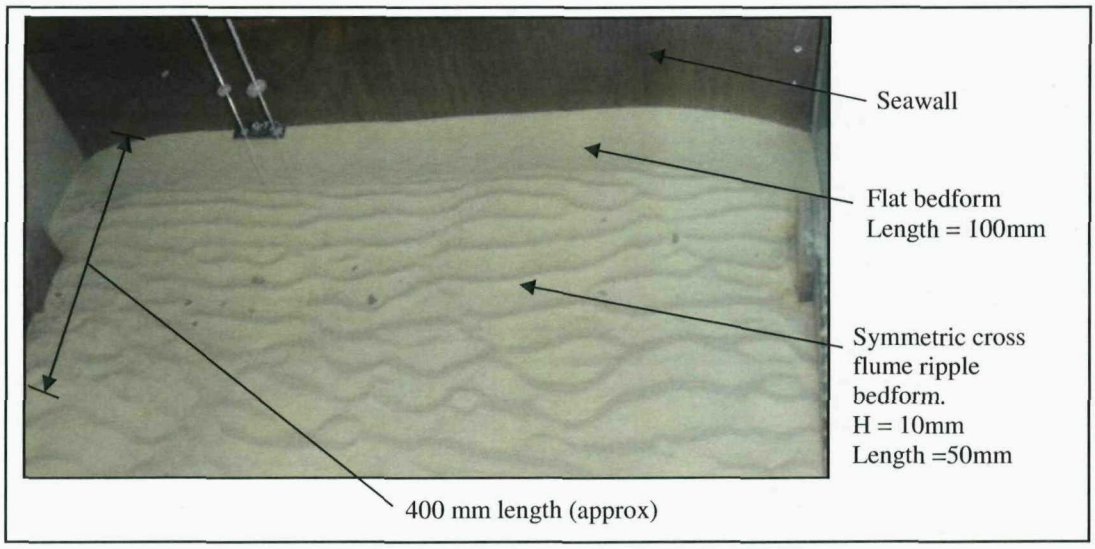


**Figure 5-13: Overhead view of flume sand bed, with evidence of ripples offshore of the seawall, and a lack of bedforms at wall toe**

Quantifying the effect of these scale effects and model effects such as wind, oblique waves and salt water remains difficult. There is a clear need for full scale physical model experiments and additional field measurements. Partial validation of these results was achieved through a comparison with the field data collected at Blackpool and Southbourne in Chapter 7.

### 5.8.3. Scour prediction

A non-dimensional plot of relative scour depth ($S / H_0$) and relative water depth at the toe of the model seawall ($d_t / L_m$) was found to illustrate the key factors affecting the variability of toe scour, of which wave breaking appeared the most important. Taking forward the simple comparison by Sumer & Fredsøe (2002), the scour predictors of Xie, (1981) and Fowler (1992) were applied to the data. These followed the shape of the dataset for mid values, but could not predict scour for shallow toe water depths. Therefore an improved probabilistic scour prediction equation was generated utilising the combined dataset.

The flume data indicated that both toe and beach profile peak at around 0.018 $d_t / L_m$. The break point coincided with the most intense wave breaking onto the seawall. By splitting the dataset and fitting two equations, the resulting curves demonstrate the key process controlling the toe scour. This is less obvious in the continious curve generated by Equation 5.6, though this equation would be easier to implement in computer models.

Using an iterative approach and set criteria, curves were fitted using a least squares approach. Equations 5.4 and 5.5 provide mean estimates of toe scour depth for a vertical seawall with beach slope between 1:15 and 1:75. These curves enable probabilistic predictions of toe scour.

To provide a deterministic estimate of toe scour depth a series of criteria were established. These included a requirement for the equations to tend towards zero for both very high and very low relative water, be relatively simple to apply with a low RMSE and bias. Using an iterative approach and applying the set criteria, a series of equations were fitted to each side of the dataset (Equations 5.9 & 5.10) to predict the mean toe scour depth. These curves were then modified to predict an upper maximum limit for toe scour at a vertical seawall (Equations 5.11 & 5.12).

Scour prediction equations 5.9 & 5.10 are simple to apply, with a low RMSE and bias, producing an average value for toe scour on beach slopes between 1:15 and 1:75, with sandy sediments and a relatively flat beach profile. Equations 5.11 & 5.12 provide and

upper maximum for these conditions when predicting toe scour for deterministic design. Both equations are limited to $-0.015 < d_t / L_m < 0.12$.

Based on limited laboratory measurements, the toe scour predictor for a vertical seawall was found to provide an estimate of toe scour at a sloping seawall, though further flume validation is required before using these for design purposes.

The prediction equations represent a simplification of the key variables affecting scour depth. Further research is required to understand the mechanics of seawall wave breaking and flows at the wall toe. This would enable future sediment transport studies to focus on other important variables, e.g. wave height, beach slope, initial beach profile, and clarify the scatter in the dataset.

## 5.9. Conclusions

A vertical seawall sediment transport experiment was conducted to provide improved understanding of scour at seawalls. Using a medium scale flume, irregular period waves and fine sand, realistic wave conditions and suspended sediment transport were achieved, the dominant process in the prototype situation.

At intermediate water depths, wave breaking was found to cause enhanced downward and seaward flows at the seawall face, generating turbulence and suspending sediment. This was evident in the increased scour depth and change in sediment bedforms.

By incorporating an existing laboratory dataset of similar scale and methodology, scour prediction equations were produced to represent this trend and predict toe scour and maximum scour at prototype seawalls. The non dimensional variables $d_t / L_m$ and $S_t / H_0$ were found to represent the treads in the scour dataset.

In general toe scour was found to increase up to a peak value of 0.018 $d_t / L_m$ ($S_t / H_0$ = 0.90) and maximum beach profile scour peaked at $d_t / L_m$ = 0.016 ($S_m / H_0$ = 0.96), coinciding with the most intense wave breaking impacts. $S_t / H_0$ always remained less then one. Either side of the peak, the scour depths tended towards zero, as the shallow water depth caused spilling breakers or large water depth tended to cause more reflective waves. In the prototype environment these conditions may induce accretion at the wall toe.

Based on this analysis probabilistic equations were developed to predict mean toe scour (Equations 5.4 & 5.5) using a least square fit. To enable scour depth predictions for design, a deterministic predictor was developed based on a series of criteria iterative approach to minimise the RMSE and bias. These were then extrapolated to produce an upper maximum prediction of toe scour (Equation 5.11 & 5.12). These equations are applicable to vertical seawalls, with smooth sloping foreshores between 1:15 and 1:75 and sandy sediment. These limited to the conditions where $-0.015 < d_t / L_m < 0.12$.

The toe scour prediction equations for vertical seawalls were tentatively suggested to estimate scour at 1:2 sloping seawall, though further measurements are required.

The effect of wave height on toe scour was not investigated in these tests, but is expected to be depth limited in most seawall locations. Additional experiments are required, ideally at large scale, to confirm this and the influence of scale effects. Further field data is also required to evaluate the effect of wind, beach profile shape and oblique waves.

The prediction equations provide useful probabilistic and deterministic guidance to estimate either mean or maximum scour depth at seawalls. However the equations, figures and parameter $d_t / L_m$ do not adequately represent the key scour processes, which were suggested to include the wave breaker type and wave flow velocity. To understand these processes and enable informed scour risk estimates, a more detailed investigation of seawall / wave interaction is required.

# 6. Toe scour hydraulic flow study

## 6.1. Introduction

In the previous chapter a series of physical model test results were presented which quantified the depth of scour under controlled laboratory conditions. Based on this dataset, the non-dimensional ratios toe scour depth over significant wave height ($S_t/H_0$) and toe water depth over the mean offshore wavelength ($d_t/L_m$) were found to predict maximum scour for a range on incident wave conditions.

For a fixed wave period and wave height, the deepest toe scour occurred when $d_t/L_m = 0.017$ and coincided with the incident waves breaking onto the wall, rushing up and then falling down towards the toe, causing sediment transport. ASCE (2006) suggested that these flows and their associated vortices may encourage sediment transport at the toe, though no guidance as to their structure or velocity was suggested. To find evidence of these flows and verify their importance, time sequence images were sampled from video collected during the sediment transport experiments (Figure 6-1 & Figure 6-2).

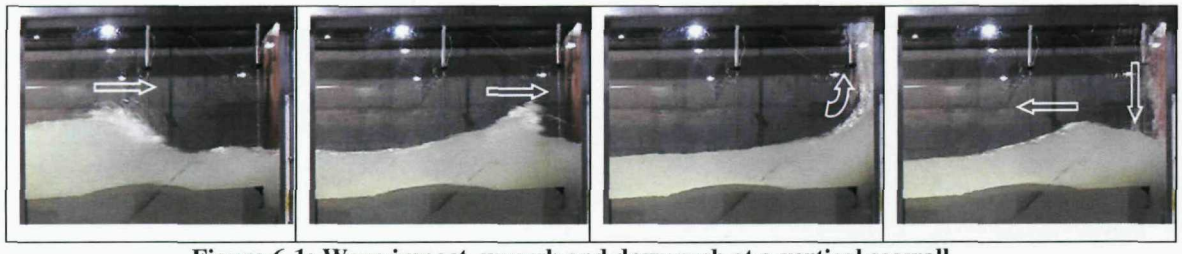

**Figure 6-1: Wave impact, uprush and downrush at a vertical seawall**

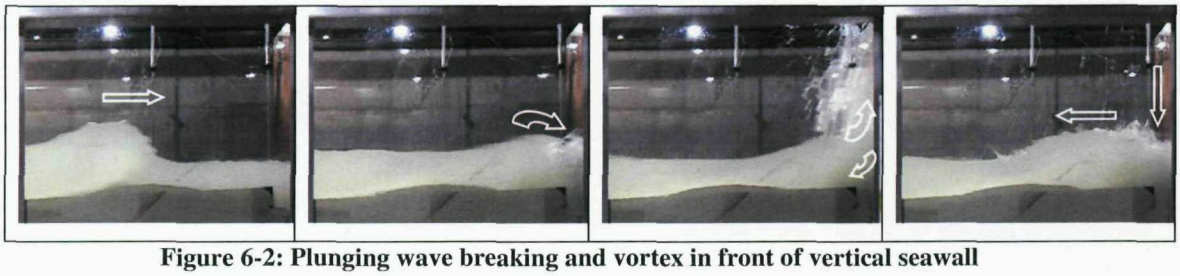

**Figure 6-2: Plunging wave breaking and vortex in front of vertical seawall**

In Figure 6-1, the first image shows the incident wave starting to spill as it approaches the seawall. On reaching the wall the wave flow is directed upwards and causes an uprush of water and significant spray approximately 0.5 m above the still water level. As the wave reflects from the seawall, the water rushes down the face of the wall and the spray falls down onto the water surface. Near the wall toe, the water becomes highly turbulent, with significant overturning and entrainment of air bubbles. In Figure 6-2, the wave breaks violently just before the seawall, and directs a plunging breaker towards the bed and spray towards the wall. These cause a chaotic wave uprush and a high velocity vortex at the toe of the wall; this is highly aerated and leads to significant suspension of sediment.

Close up samples of a wave downrush flow and a wave breaking at the wall toe are shown in Figure 6-3 and Figure 6-4 respectively.

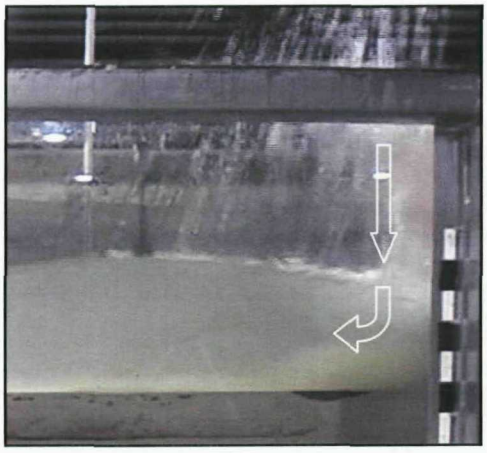

**Figure 6-3: Wave downrush inducing sediment suspension**

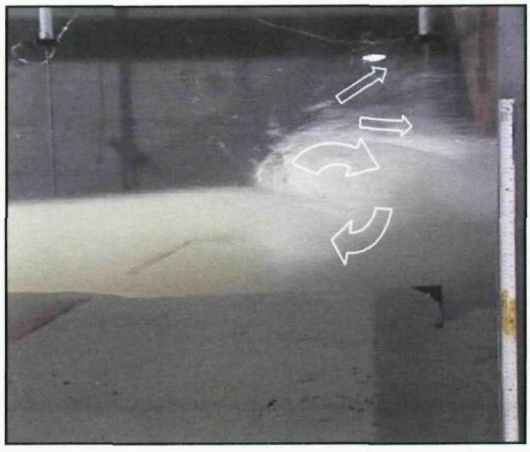

**Figure 6-4: Breaking wave causing turbulence and sediment suspension**

Neither the field measurements nor the sediment transport study were suited to carrying out a detailed analysis of these processes, which occurred within a couple of seconds and varied with each incident wave. Apart from the visualisation of broken clapotis waves at a breakwater by Gao & Inouchi (1998), the effect of breaking wave flows on sediment transport at a seawall have not been investigated. Therefore a series of hydraulic experiments were conducted to explore these processes in more detail.

## 6.2. Experimental aims

It was hypothesised that breaking waves generate fast moving flows at the face of vertical seawall, leading to enhanced sediment suspension and scour at the wall toe, in addition to orbital flows associated with reflected wave transport. The aim of the experiments was to answer the following questions:

- Can particle image velocimetry (PIV) be used to make observations and measurements of the scouring wave flows?
- If so, what are the flow patterns at the seawall and seabed?
- What effect do these flows have on sediment transport and toe scour?
- How does the flow structure change on a scoured beach profile?

This research will:

- Collect evidence of the flow regime in front of a vertical seawall;
- Establish the position and magnitude and flows associated with wave downrush and toe vortices;
- Compare the position of toe scour in the sediment transport tests to the flow velocities in the hydraulic study;
- Produce scaled models of the scour beach profile and observe the effect on wave flow.

## 6.3. Methodology

### 6.3.1. Limitations of existing flume study

The sediment transport study was used to simulate scour at a seawall using a movable sand bed exposed to 2D irregular period waves. In the tests a range of spilling, plunging and pulsating waves occurred, with the dominant breaker type dependent on the wave height and the toe water depth. When the conditions produced wave impacts at the seawall, flow velocities were observed to increase. Direct measurement of these flows would have required invasive current meters, which would have interfered with the sediment transport and sampled only a small region of the flow.

To sample the whole wave field without obstructing the flow, it decided to conduct a small scale hydraulic model study using regular waves and a fixed concrete bed. This enabled Particle Image Velocimetry (PIV) techniques to be utilised.

### 6.3.2. Particle image velocimetry

PIV is a non-intrusive method for simultaneously measuring the speed and direction of complex flows. The technique can be applied to fluids and gases and involves seeding the flow with reflective particles, then illuminating and observing their motion by collecting successive camera images at high speed. By using images pairs, the position shift of particles between frames can be determined and when combined with the image scale and frame rate, the flow speed and direction can be calculated.

The choice of seed particle is important and represents a compromise between several factors. Very fine particles would provide the highest resolution, but require high camera lens magnification to ensure they are represented by 2-3 pixels within the PIV image, otherwise distinguishing particles becomes difficult. The alternative approach would be to decrease with image size and increase the camera resolution. In this case the image would have been limited to only a small region of the flow field at the toe of the wall.

If larger diameter particles are used, they equate to a corresponding increase in the number of pixels in the PIV image. This decreases the resolution of the PIV system and prevents measurement of smaller flow features. PIV is also based on the assumption that the particles accurately represent the motion of water particles. The inertia of larger

particles can lead to the seed particles following there own trajectory within the flow field, inducing bias.

In this study, the hydraulic flow was seeded using neutrally buoyant, unexpanded polystyrene spheres of diameter c.0.75 mm. These are larger then those typically used in wave or current flow studies. The particles typically equated to 3-4 pixels diameter (0.07 cm) in the PIV image, but represent a compromise between the size of the flow feature, the camera resolution and the need to capture the entire flow field at the seawall. This was justified on the basis that the flow features were large (e.g. the toe vortex diameter was a minimum of 1.5 cm, though typically 2-3 cm) compared to the seed size. However, it would not be appropriate or accurate to derive the flow speeds of, for example, the near bed boundary layer or flow features smaller then 0.5cm diameter.

High quality digital images were collected using a high speed camera and a frame rate of 70 frames per second (fps). Despite achieving a lower resolution then traditional photographic film techniques, the digital images enabled experiment results to be previewed instantly, and the flume lighting and seeding to be optimised before each test was run.

Existing hydraulic flow PIV experiments have tended to use laser light sheets as a source of illumination (Adrian, 1991). However due to the configuration of the multiple flumes within the University of Southampton hydraulics laboratory, safety restrictions would have severely limited the experiment operation. The experiments also required frequent changes to the flume beach profile, therefore a more robust and transferable lighting source was constructed using halogen white spot lights and a narrow filter box. Compared to a laser system, this reduced the quality of the illumination and expanded the illuminated region in the direction of the optical axis, but represented the best compromise given the flume's position and the need to frequently modify the beach profile position.

Particle velocities were extracted using the Cross Correlation method, where the PIV image is subdivided into a grid, and each grid region is interrogated to generate a pixel intensity template. In the following image frame, the same grid region is located and a second pixel intensity template is generated. The Cross Correlation function statistically compares the two templates and iteratively shifts the first template until it matches the

second. When the images match, the product of the pixel intensity will be high, resulting in a high cross correlation value. The shift in pattern template between the frames is then assumed to represent the average movement of particles at the centroid of that grid region. This is then repeated at each grid point to determine the flow field.

The grid dimensions are therefore important. A fine grid provides highly detailed results, however if in a high velocity flow, a significant number of particles could leave the grid square, and it would not be possible to match the two templates accurately. Conversely a coarse grid prevents loss of particles, but some of the finer flow details can be lost. By testing various configurations, the optimum grid size was determined, as defined in the following section. Once the particle displacements were obtained, the image frame rate and image scale were used to calculate the velocity.

To determine the wave characteristics in the small scale model, gravity was assumed to be the dominant force inhibiting surface wave motions (Hughes, 1993), therefore Froude scaling similitude was applied. Using Equations 2.2 & 2.4, a length scale of 1:10 and 1:40 was calculated for the medium and small scale tests respectively, based on a prototype wave 2 m high. This resulted in a wave height of 0.2 m in the sediment transport study and 0.05 m high in the hydraulic flow experiments. The maximum toe scour depth recorded in the sediment transport test was -0.158 m (Test C), which scaled to a scour depth of 1.6m at prototype scale and 0.04 m deep in the hydraulic flow model. The PIV field of view was equal to a prototype beach profile 7 m wide and a seawall 4 m high.

### 6.3.3. Laboratory flume setup

A 1:30 plywood beach slope was set up in a 14 m, 0.4 m wide 2D wave flume and an impermeable vertical seawall installed. A section 0.65 m long was left open at the top of the beach slope closest to the wall, where concrete test sections could be installed. The test sections consisted of either a plane bed or a scaled model of the final beach profile shape from the sediment transport tests (Figure 6-5). These were constructed from a fine mix concrete with a wire mesh to provide additional strength and were limited to a ± 5 mm height tolerance due to the undulating profile.

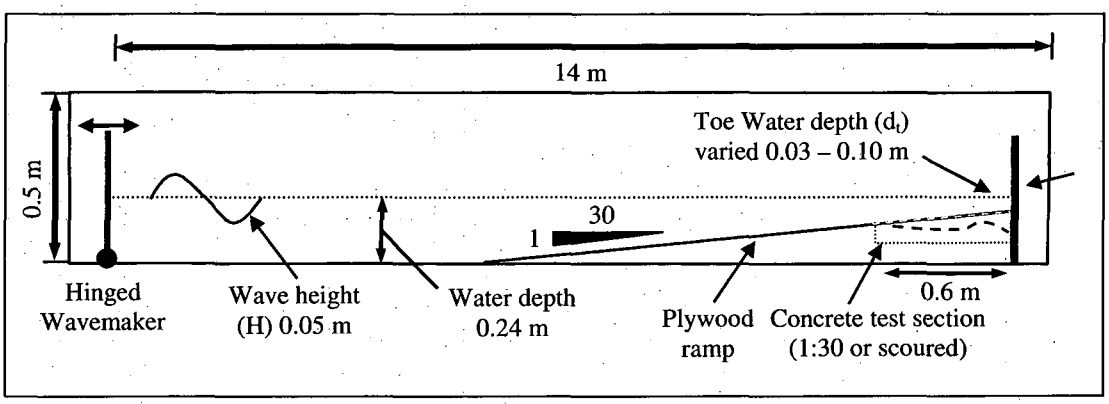


**Figure 6-5: Flume cross section**

A repeatable group of four regular period waves ($H$ = 0.05 m and $T$ = 0.7 or 1.3 s) were generated using a hinged wave paddle with internal wave absorption and recorded using a resistance wire wave gauge at the toe of the beach slope. The wave paddle and wave probes were controlled using a desktop PC and bespoke software via an analogue to digital converter and signal amplifier. An analysis of the wave paddle output found the wave height to vary between ± 2 mm, and wave periods between ± 0.02 s, though all test conditions were within two standard deviations of the mean.

The experiments were conducted using a Froude scaled wave height, mean wavelength and toe water depth to reproduce conditions in similitude with the corresponding sediment transport test. Before each test, the wave probe was calibrated and a sample wave series generated to enable small adjustments to be made to the wave paddle, thereby maintaining identical wave group characteristics for each test.

During the experiment the water depth at the toe of the wall ($d_t$) was set at either 0.03, 0.05 or 0.10 m by moving the rigid beach profile up or down, while the water depth at the paddle was kept constant. The beach gradient was maintained at 1:30, therefore the overall slope length was reduced as the toe water depth increased.

The tank was filled with fresh water and once the water level became steady, unexpanded polystyrene spheres (c.0.75 mm) were put into solution with a small amount of detergent to break the surface tension, and poured into the region of interest. The wave packet was generated and camera triggered as the wave group approached the seawall. The tests were repeated with different seed densities. The flume was then drained and test section replaced with the scoured beach profile, before the test was repeated following re-calibration of the wave gauge.

### 6.3.4. PIV setup and image collection

To collect the PIV images, a Basler 601F high speed digital camera was mounted perpendicular to the seawall and beach profile at a distance 0.95 m from the light sheet centre line (Figure 6-6). The camera was fitted with a high quality Moritex 35 mm lens, and achieved a frame rate of 70 fps, with a 5.3 ms exposure time. The camera was connected to a PC via IEEE 1934 FireWire connection, which controlled camera configuration, activation and frame grabbing. The digital images were sampled for a duration of 4 to 6 s with a resolution of 640 x 480 pixels.

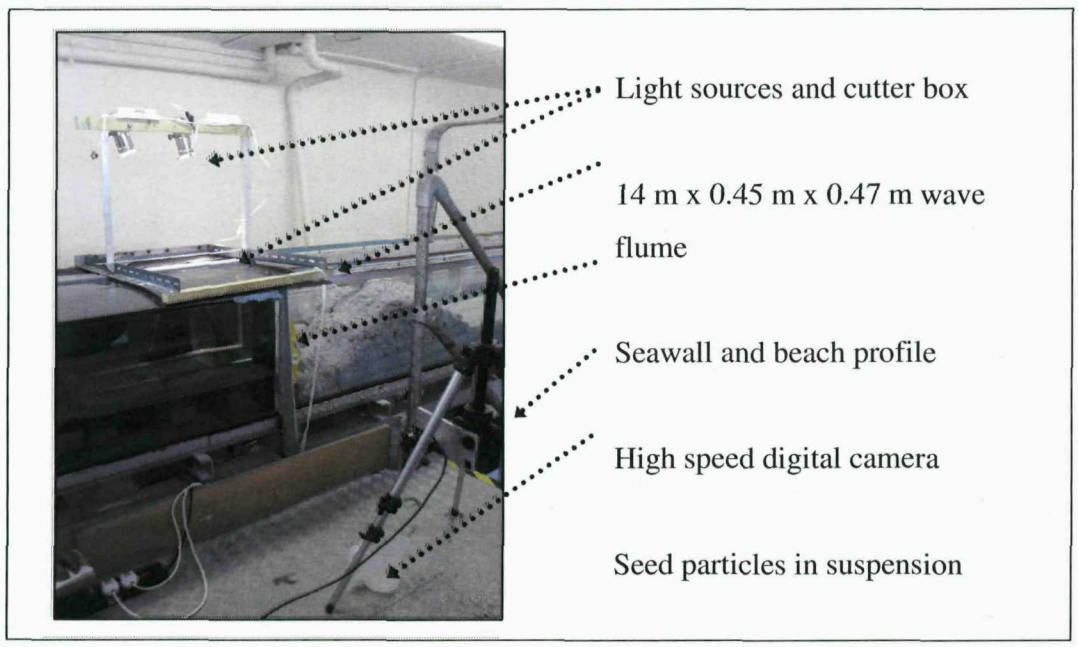


**Figure 6-6: Small scale flume setup for PIV measurements**

A 15 mm wide white light sheet was generated by a pair of 70 W halogen white spot lights with tunnel filters, which were positioned above the centre of the flume and directed though a 10 mm wide plastic slit (Figure 6-7). To eliminate reflections, sheets of matt black plastic were used to enclose the flume. The beach profiles and seawall were painted matt black and the camera tripod was enclosed with a black fabric sheet.

Prior to each test, the camera was focused manually on a removable reference scale at the centre of the light sheet and a calibration image obtained to determine the scale and hence number of pixels per mm. The sample images were also used to test for lens distortion, which was found to be of the order of $^{1}/_{10}^{th}$ of pixel between the image boundaries and therefore insignificant. The image plane measured approximately 0.15 m wide by 0.12 m high, this varied slightly between each test due the different beach profile elevations. The camera frame rate was verified using a digital stopwatch to ensure the camera and PC system achieved the target frame rate of 70 fps.

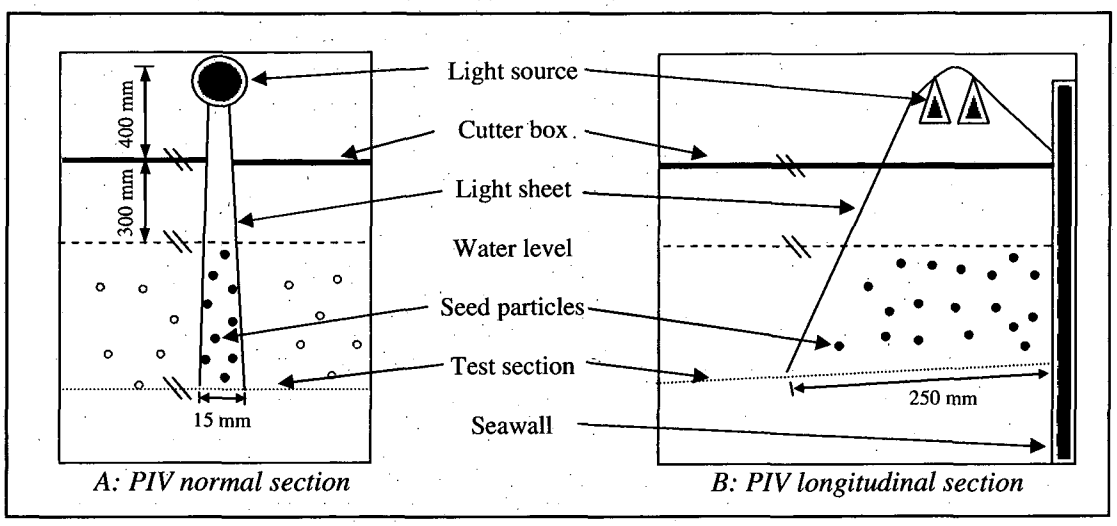


**Figure 6-7: Flume PIV cross and long sections**

### 6.3.5. PIV analysis

The best quality video records of the target wave were selected, based on light intensity and particle seeding density, and then split into individual frames. The duration of one wave cycle was determined using the orbital direction of the particles at the offshore boundary. The PIV analysis commenced and concluded when flow reversal occurred at the offshore boundary. Image pairs were then converted to 8-bit greyscale images and analysed using VidPIV v2.15 cross correlation software. The images were sampled using interrogation cells of 64 x 64 pixels with a 32 pixel square analysis grid, to provide an overlap and smooth the dataset.

Each image pair was then visually inspected to remove and interpolate spurious vectors, which were often generated near the water surface. Vectors exceeding 60 $cm.s^{-1}$, which were beyond the camera frame rate, and points where the flow could not be interpreted or interpolated were deleted. The analysis was repeated for each image pair for one wave cycle. The results files were processed using MATLAB to correct the image scale and produce scaled velocity plots in conventional units.

To verify the VidPIV velocity output, a sample point was selected from Test C, which included some of the highest particle velocities and caused the seed particles to streak in some of the images. To determine the effect of these particles on the PIV analysis, the position of the leading edge of the streak was identified in an image pair and the difference in particle position calculated over one frame cycle (0.0143 s). The velocity was found to be within 0.1 $cm.s^{-1}$ of that calculated by the Cross Correlation method, and demonstrated the ability of the software, when combined with the large grid size, to calculate the correct particle velocities (Figure 6-8).

| | Position X | Position Y | Velocity $cm.s^{-1}$ |
|---|---|---|---|
| VidPIV Cross Correlation | 96 | 352 | 46.8 |
| Pixel shift (Frame 139 to 140) | 81 | 353 | 46.7 |

**Figure 6-8: Particle streak velocity analysis, Test C, frames 139 & 140**

### 6.3.6. Test matrix

The following PIV tests were conducted (Table 6-1); the respective sediment transport tests numbers are shown for reference and the dominant wave breaker type. The position of each test relative to the scour prediction equations is shown in Figure 6-9. Tests in the range $0.01 < d_t / L_m < 0.04$ were most prone to wave impacts.

**Table 6-1: Test matrix**

| Test reference | Medium scale test reference | Breaker type | Model Specification | | | |
|---|---|---|---|---|---|---|
| | | | Offshore Wave height ($H$) m | Offshore Period ($T$) s | Toe water depth ($d_t$) m | Non dimensional $d_t / L_m$ |
| *A* | 12 | Spilling/ impact | 0.05 | 1.3 | 0.03 | 0.012 |
| *B* | 2 | Spilling/ impact | 0.05 | 0.7 | 0.05 | 0.058 |
| *C* | 4 | Impact | 0.05 | 1.3 | 0.05 | 0.019 |
| *D* | 11 | Near pulsating | 0.05 | 1.3 | 0.10 | 0.037 |
| *E* | 9 | Pulsating | 0.05 | 0.7 | 0.10 | 0.121 |
| *F* | 8 | Impact | 0.05 | 0.7 | 0.03 | 0.039 |

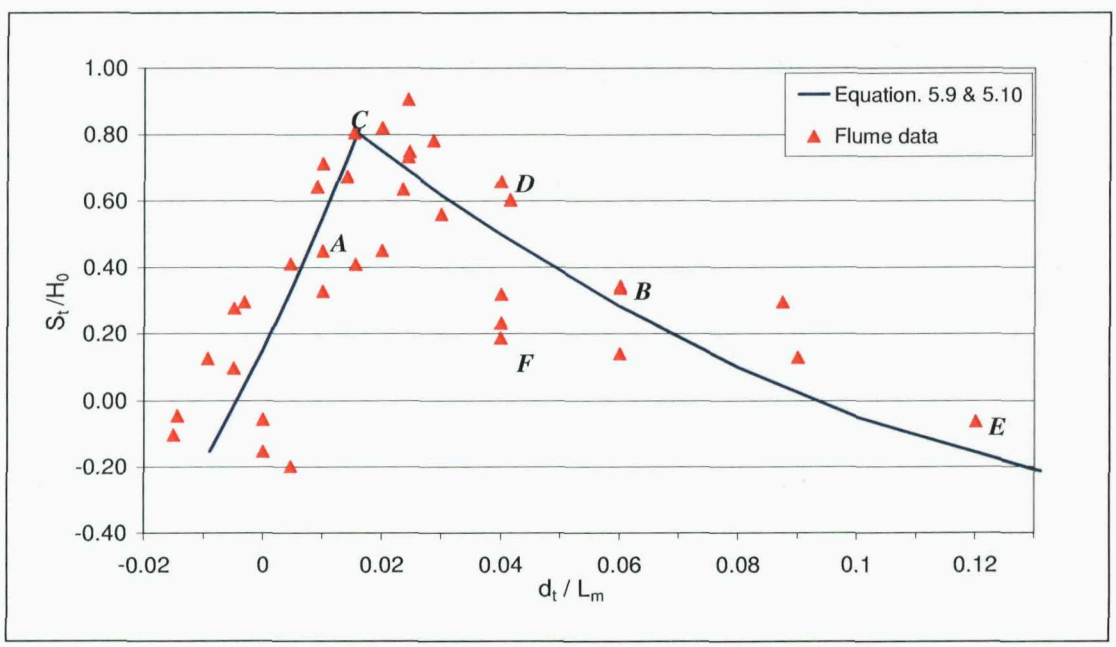


**Figure 6-9: Toe scour predictors and position of PIV tests**

## 6.4. Results

The results analysis included a comparison of wave flow observations, velocity measurements and sediment transport predictions for both smooth and scoured beach profiles. Sample images were included to illustrate the key flow patterns, supported by vector diagrams which present the flow velocity at each grid point. These were annotated with the still water level, beach profile and seawall position to aid visualisation.

### 6.4.1. Wave flows in front of a seawall

#### Key wave flow structure

In Test *A*, the toe water depth was shallow (0.03 m) and wave period long (1.3 s) leading to a spilling wave breaking approximately 0.5 m from the seawall. At the wall, the fastest flow speed (20-30 $cm.s^{-1}$) occurs at Frame 147 (Figure 6-10 & 6-11) as the reflected wave rushes back down the wall. This generates a significant offshore flow in front of the wall and forms a small clockwise rotating vortex at the wall toe, which persists for a period of 0.57 s over the full water depth.

For Test *B* (not shown) the water depth is raised to 0.05 m and period reduced, this causes the wave steepness to increase. As a result the incident wave spills approximately 1m offshore of the wall and continues spilling up to the wall. This leads to a small spilling impact at the wall, which dissipates quickly.

Test C maintained the same toe water depth but increased the period, producing a more intense wave impact and significant turbulence at the wall. The wave impact sequence is shown in Figure 6-12 and described below with references to key frames.

During the test, the incident wave remains unbroken until close to the wall (138), where it begins to throw forward (142). This produces a significant uprush flow up the wall (0.2 m high), and is followed by a high speed downrush (160) which causes streaking and shadows in the image, and makes PIV analysis difficult. The peak velocity was estimated at 80 $cm.s^{-1}$ from the particle streak lengths, though the flow decelerated significantly to 40-50 $cm.s^{-1}$ once below the water surface (Figure 6-13 & Figure 6-14).

As the downrush approaches the bed, the still water level was drawn down and an overturning breaker forms. This generates an intense clockwise rotating vortex at the wall toe (170 & 172), which occurs for a period greater then 0.5 s over the full depth at the wall toe (Figure 6-15 & Figure 6-16). The vortex appears to be constrained by the impermeable bed and the seawall to produce an extreme velocity gradient; only the direction of flow could be measured by the PIV software. The peak velocities were estimated to be in the range of 40-50 $cm.s^{-1}$ from particle streak lengths. As the wave reflects offshore, the vortex slowly dissipates and water droplets formed during the wave uprush, splash back down into the flume (178).

For Test *D* the water depth increased to 0.1 m and leads to a non-breaking pulsating wave at the seawall. The small downrush does not reach the bed, therefore the near bed velocities are reduced compared to tests *A* and *C* (Figure 6-17 & Figure 6-18). The same water depth was used in Test *E* (not shown), but with a shorter period, which causes the wave steepness to increase. The wave remains unbroken with the fastest flows confined at the water surface. The reflective flow structure appears visually similar to Test *D*, however early analysis of the peak velocities and net flow showed a significant offshore flow. This was inconsistent with the sediment transport results and the preceding flow tests and suggests either an experimental error or problem with the image capture process; therefore this test was not included in the flow analysis.

Test *F* maintains a similar toe water depth / wavelength ratio as Test *D*, by decreasing both the period and water depth. As the wave shoals it becomes overly steep and breaks approx 2.5 m offshore, before reforming into a smaller wave. This generates a near impact interaction with the seawall, with a small uprush, but significant downrush. The high downrush velocity was estimated at 85 $cm.s^{-1}$ from the particle streak lengths. Once at the bed the shallow water forces this flow offshore, and generates a small rotating vortex at the toe of the wall, for a period of 0.47 s (Figure 6-19 & Figure 6-20).

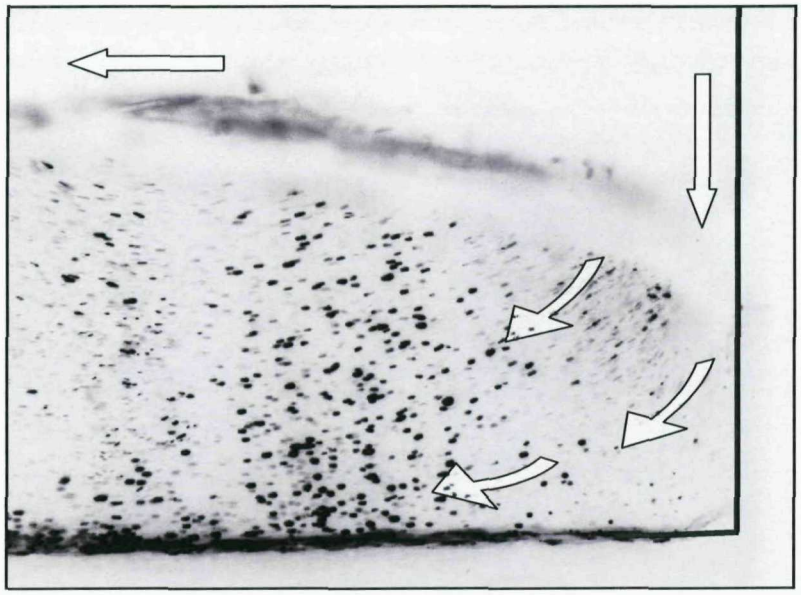

**Figure 6-10: Test *A*, frame 147-Wave downrush**

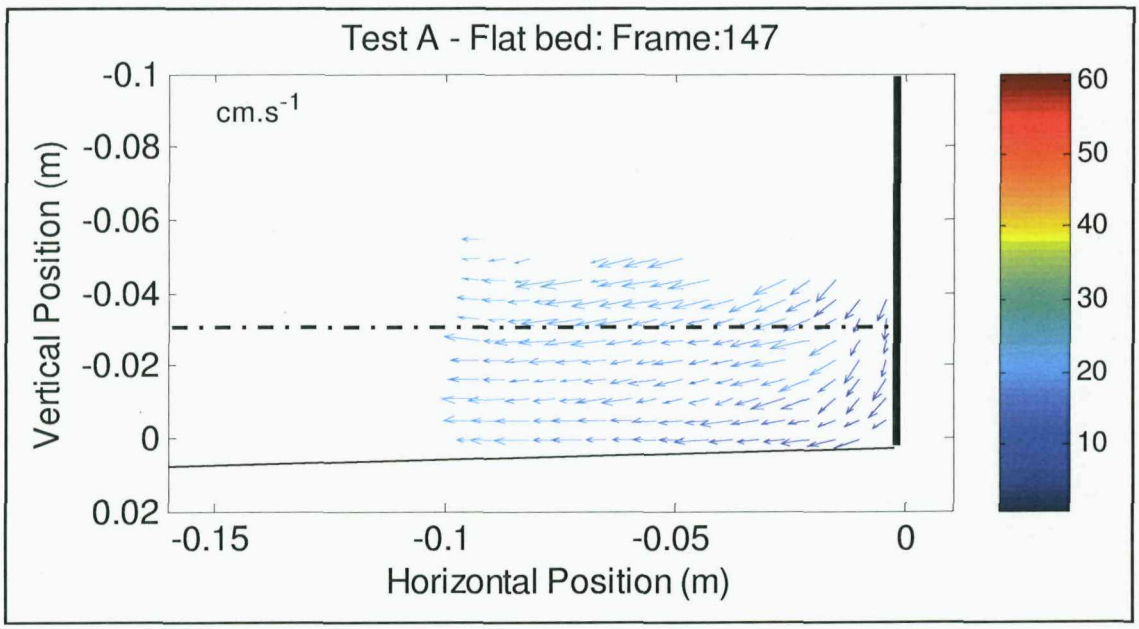


**Figure 6-11: Test *A*, frame 147-Flow velocities**

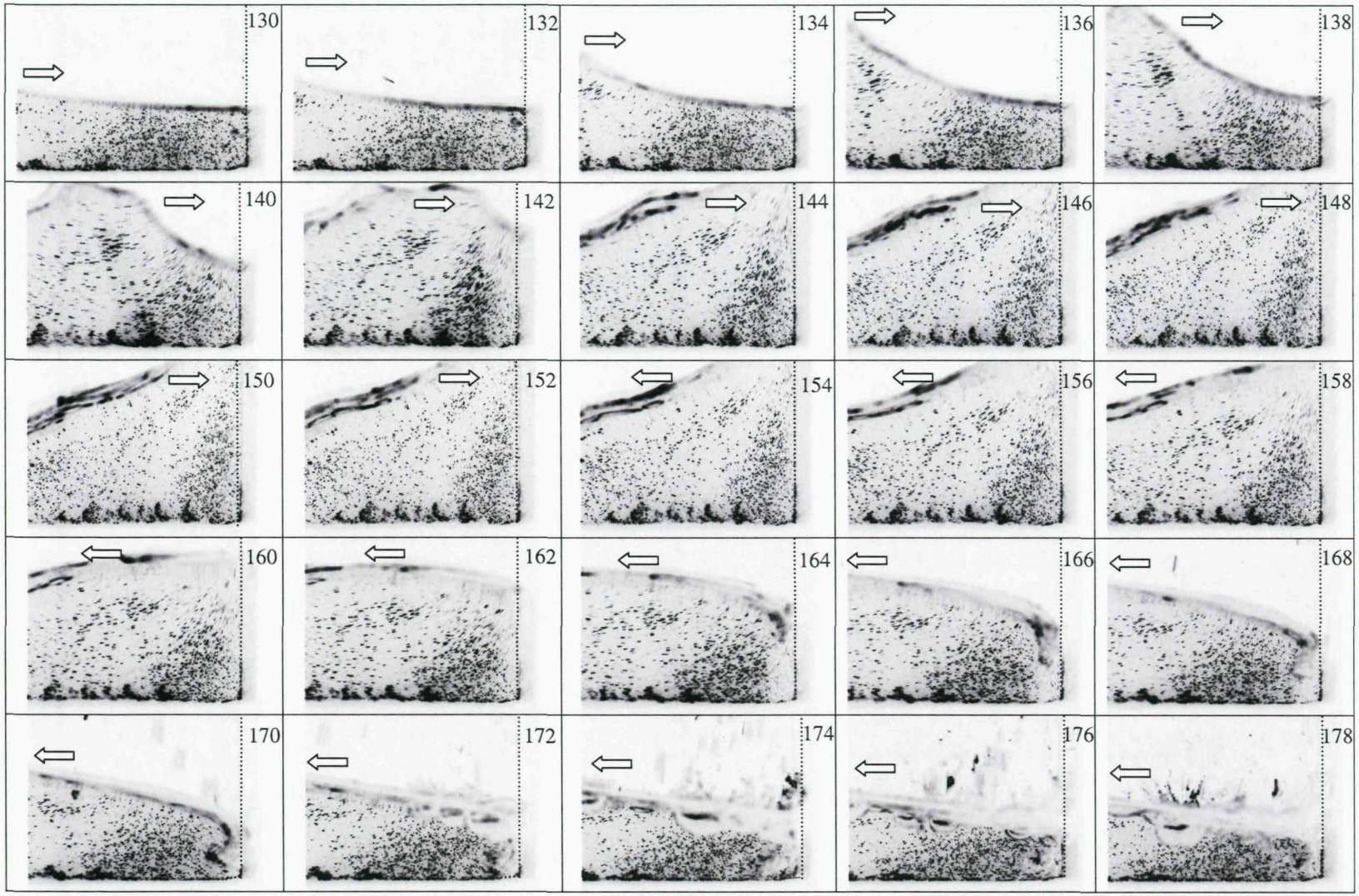


**Figure 6-12: Test *C*: Sequential images of wave impacting a vertical seawall, smooth 1:30 bed, $d_t$= 0.05m, $H$ = 0.05 m, $T$ = 1.3 s (Image separation 0.029 s / 2 frames).**

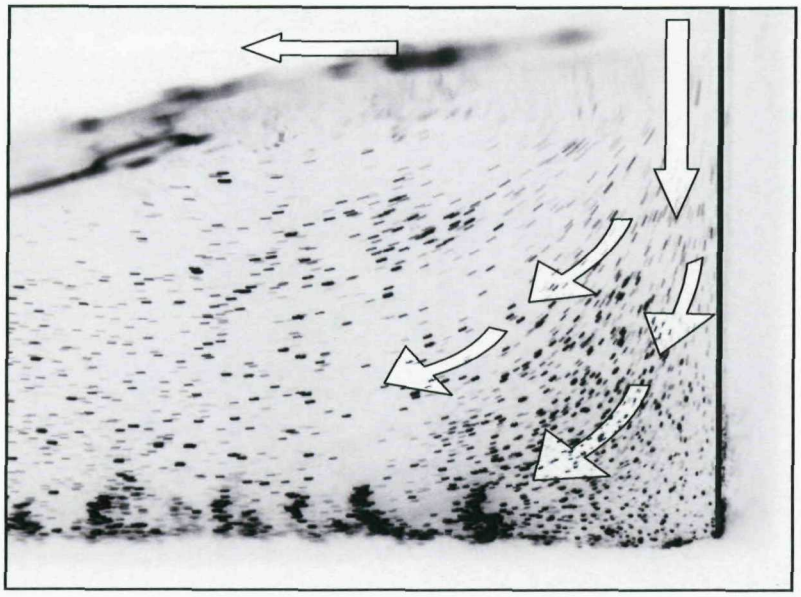

**Figure 6-13: Test *C*, frame 159- Wave downrush.**

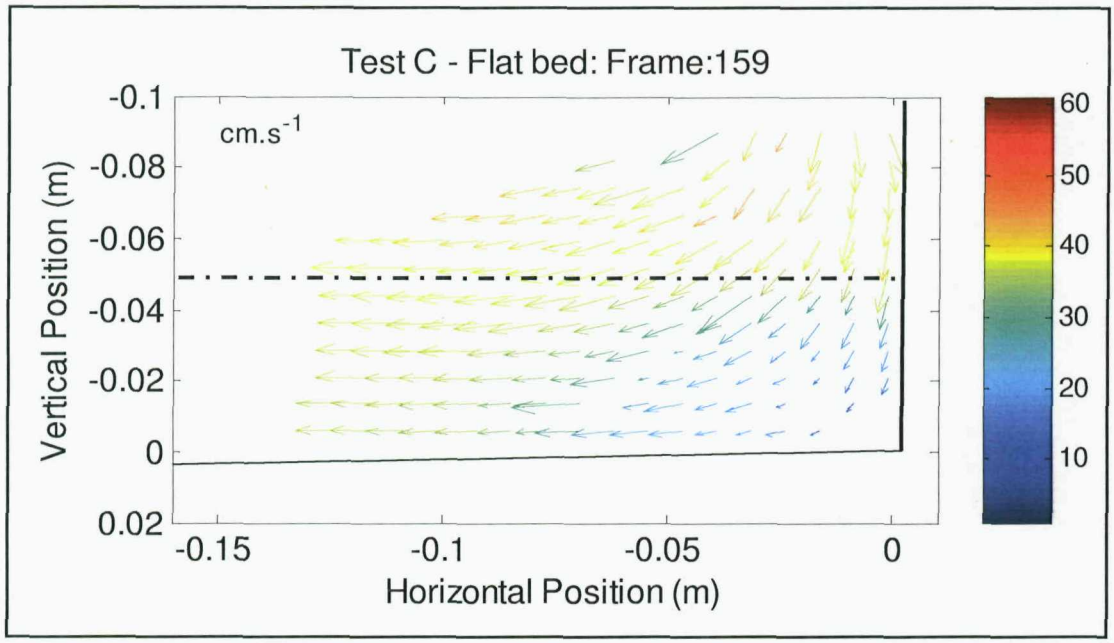


**Figure 6-14: Test *C*, Frame 159- Flow velocities**

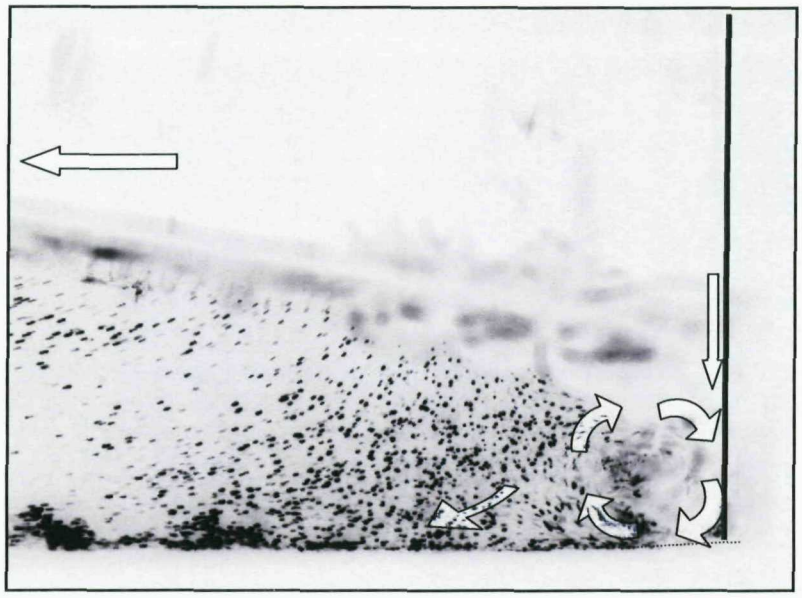

**Figure 6-15: Test *C*, frame 173-Vortex following wave downrush.**

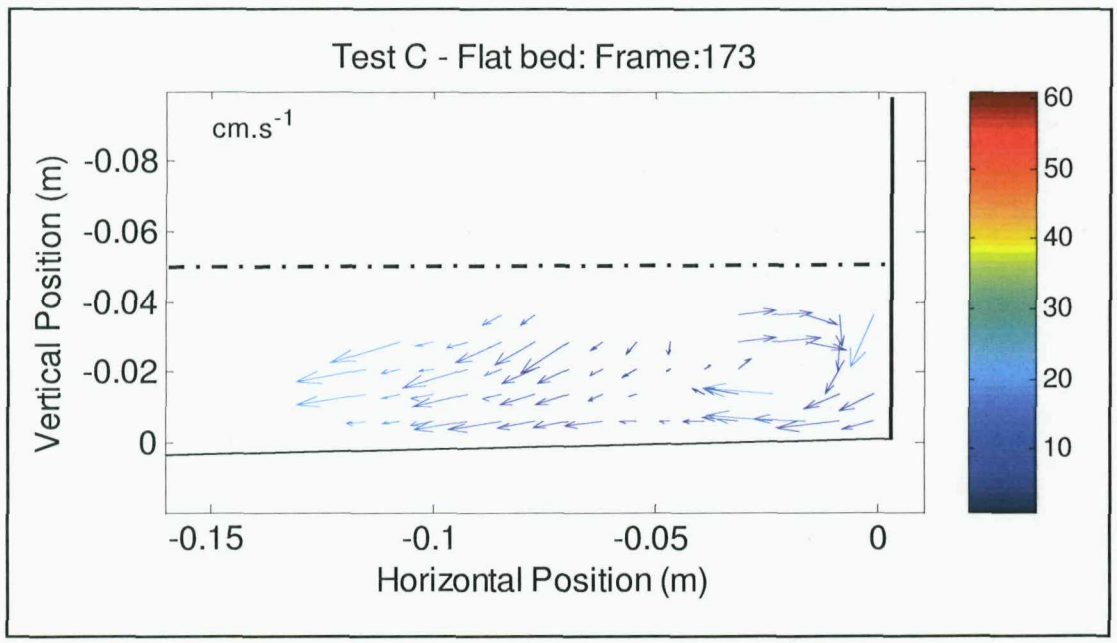


**Figure 6-16: Test *C*, frame 173- Flow velocities**

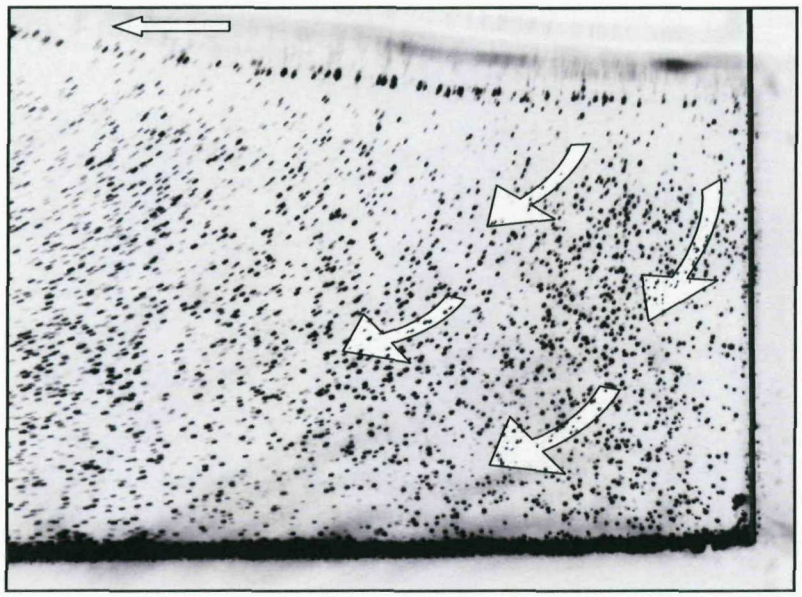

**Figure 6-17: Test *D*, frame 255- Small down rush, no vortex or flow acceleration at bed.**

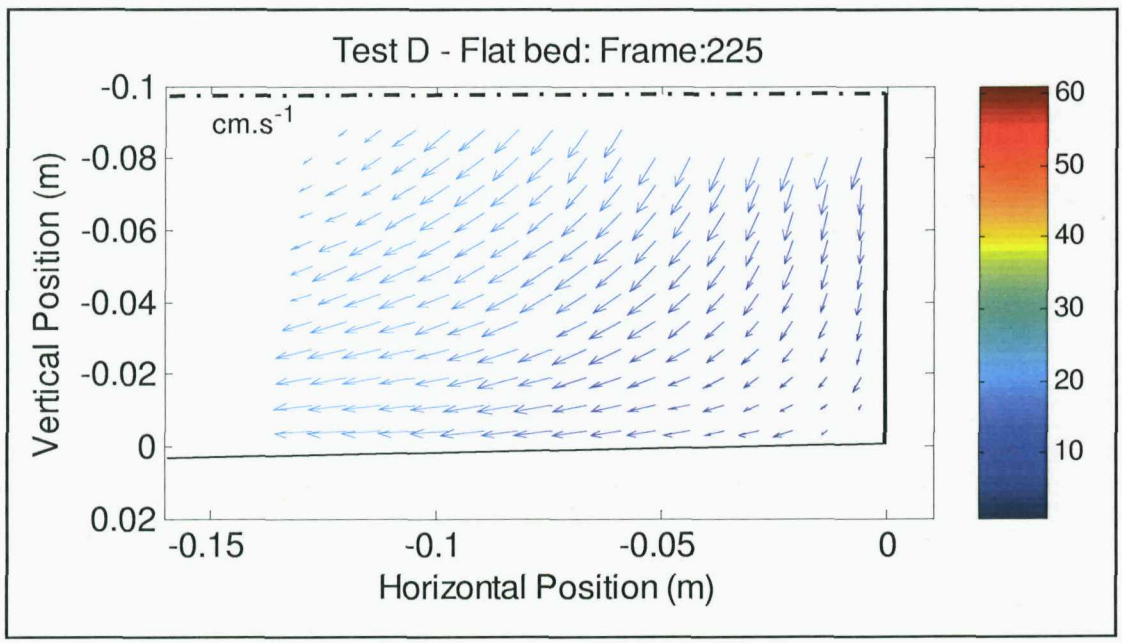


**Figure 6-18: Test *D*, frame 255- Flow velocities**

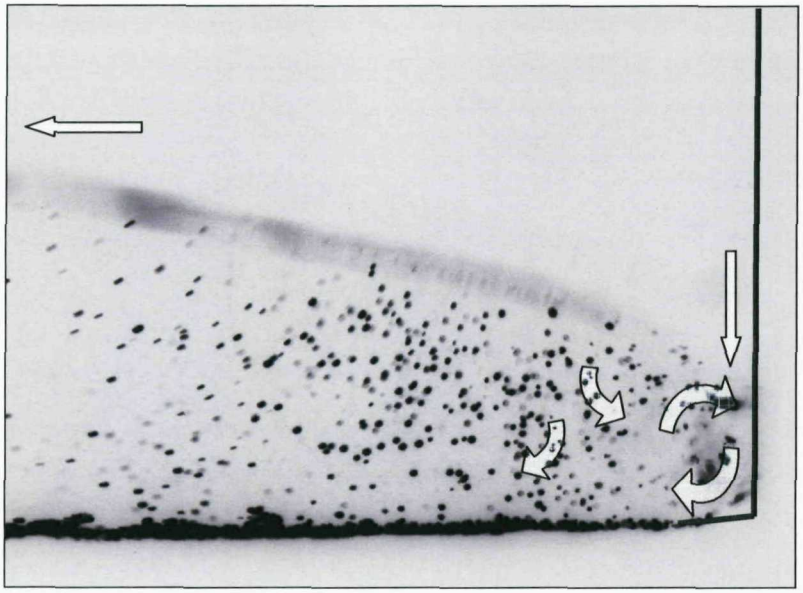

**Figure 6-19: Test *F*, frame 177- Vortex and draw down of toe still water level following wave downrush**

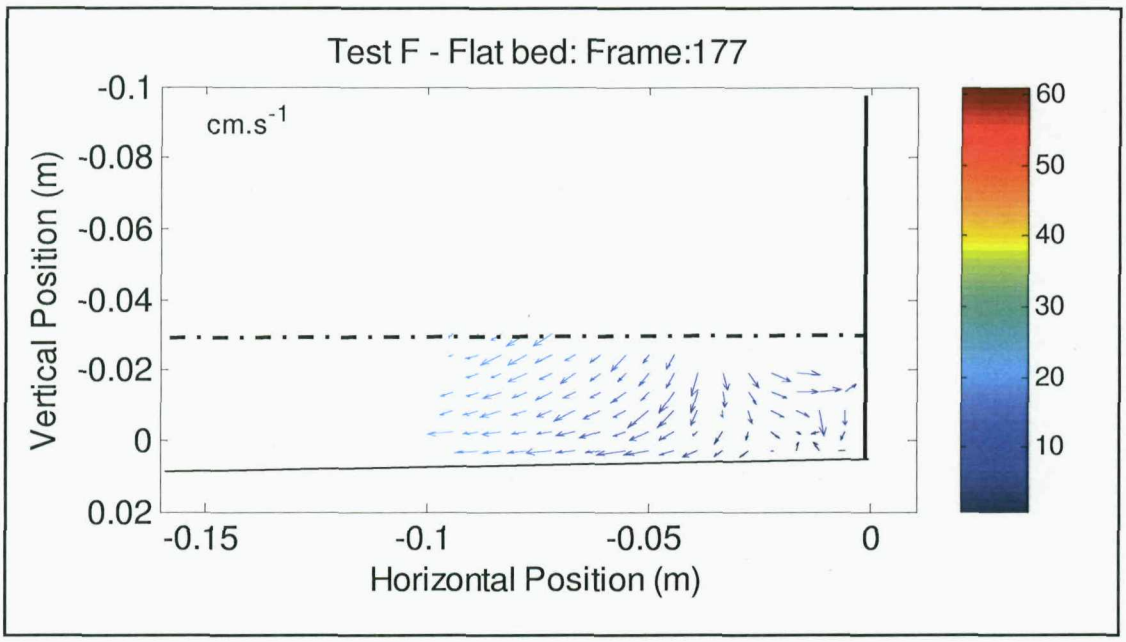


**Figure 6-20: Test *F*, frame 177- Flow velocities**

## Peak flow velocities

To interpret where the wave flows were most intense, the peak velocities during the wave cycle were determined for each test. In general the short period tests generated slower peak flow velocities then the longer periods, with the exception of Test *F*, where the flow speeds were increased by the wave downrush. The peak flow analysis focused on the tests with the most defined structure *A, C, D & F* (Figure 6-21 to Figure 6-24).

In Test *A*, the peak velocity was generally directed onshore at around 35 $cm.s^{-1}$, except at the toe vortex, which was directed offshore at 15-20 $m.s^{-1}$. Test *F* showed a similar peak flow pattern, with the flow directed onshore across the profile at around 25 $cm.s^{-1}$, but was reduced and directed offshore at the wall toe where the small vortex formed.

Test *C* showed a significant increase in peak velocity, with the fastest onshore flows (40-50 $m.s^{-1}$) occurring at the end of the profile and equally fast offshore flows occurring at the wall toe. At a position -0.04 m from the wall, the velocities were reduced, suggesting a point of convergence. In Test *D* the peak velocities remained < 25 $m.s^{-1}$ and were uniformly directed onshore.

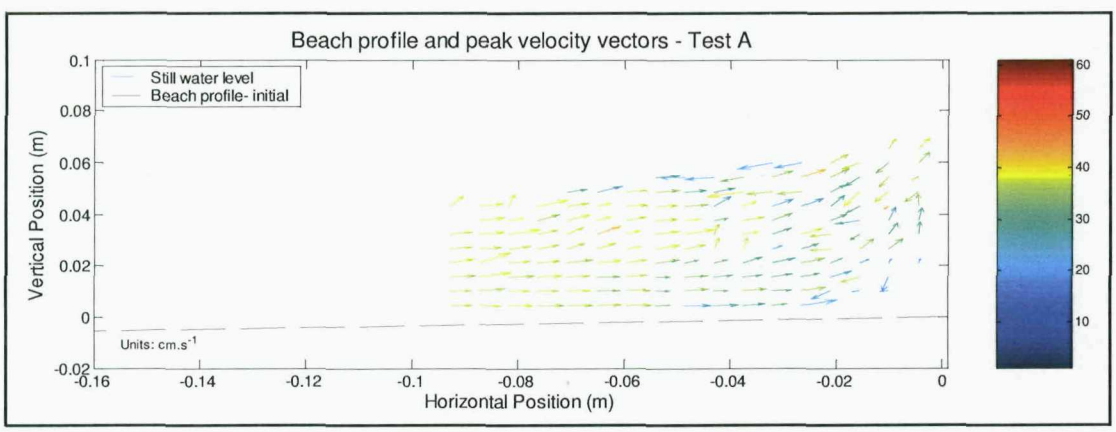


**Figure 6-21: Peak velocity results- Test *A***

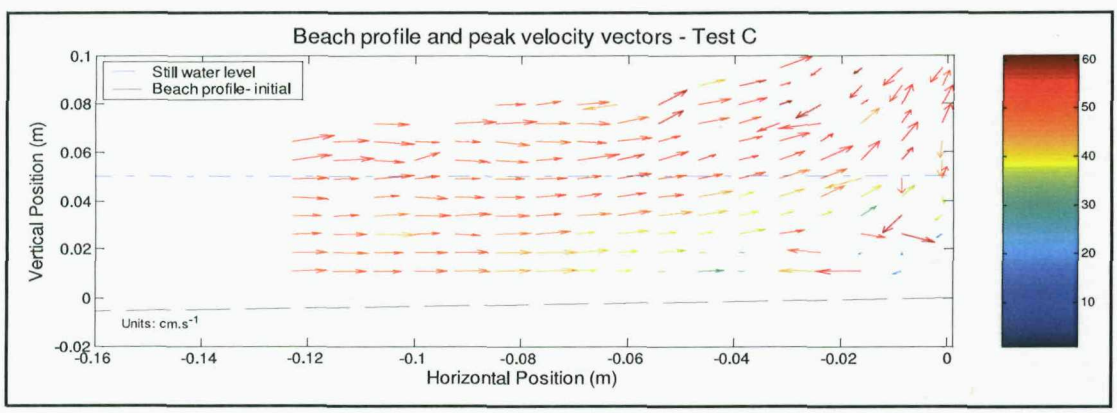


**Figure 6-22: Peak velocity results- Test *C***

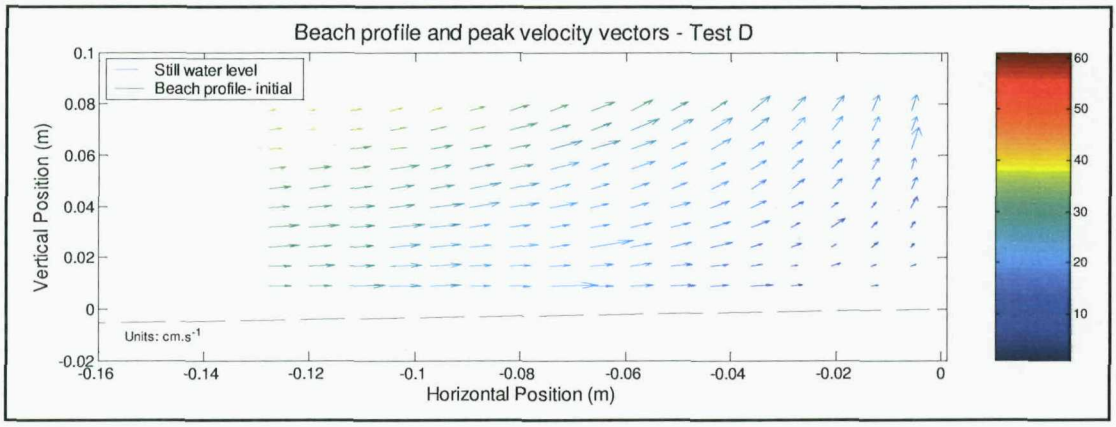


**Figure 6-23: Peak velocity results- Test *D***

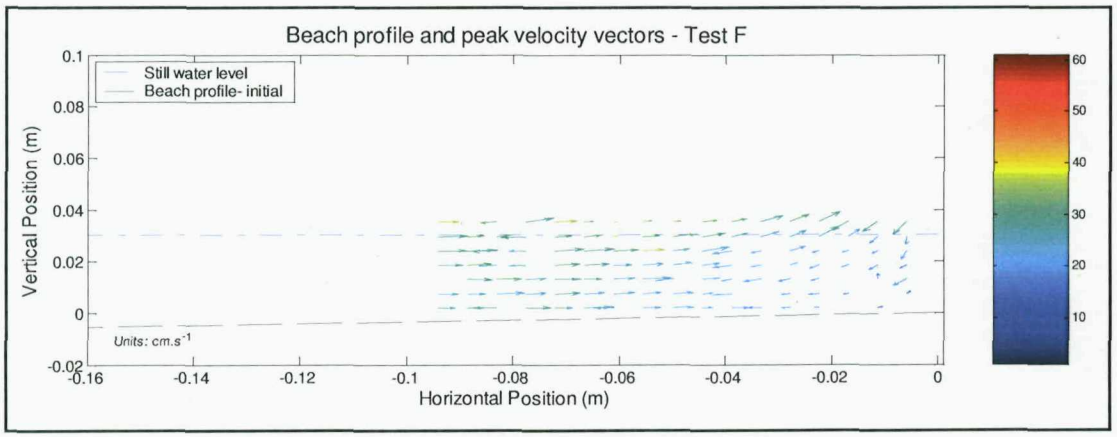


**Figure 6-24: Peak velocity results- Test *F***

## Summary

Utilising a smooth beach profile, the hydraulic flow pattern during wave impact and wave reflection was investigated. When waves broke at the wall, a significant uprush occurred and was followed by a flow down the face of the wall, termed the downrush. In tests *A*, *C*, & *F* the intersection of the downrush with the bed profile and it deflection offshore, led to the formation of a clockwise rotating vortex at the wall toe.

When the toe water depth was reduced or the wave steepness increased, the waves tended to break offshore, leading to a spilling wave impacts and reduced downrush, this also produced a smaller toe vortex. At the intermediate water depth and with a longer period (Test *C*), the waves broke at the wall. This produced a high velocity downrush, which drew down the still water level and generated an intense vortex at the wall toe. When the water depth was increased further, pulsating conditions occurred, and the waves were reflected, reducing the near bed flow velocities. Where the same $d_t / L_m$ ratio

was maintained (Tests *D* & *F*), the incident waves broke offshore in the shallow water test (*F*), but pulsated in Test *D;* this was not illustrated by the $d_t / L_m$ ratio.

An analysis of the peak velocities confirmed the position of the toe vortices observed in Tests *A*, *C* and *F*, and corresponded to an increase in the offshore near bed flow velocities. By contrast, over the remainder of the bed, the peak velocities were generally reduced and directed onshore. The highest peak flow velocities occurred in Test *C*, during the wave impact and wave uprush, except in the region of the wall toe, where the downrush and offshore vortex flows were greater. In the deep water test, the peak velocities followed the orbital direction of the incident waves and were significantly reduced. In general the peak flow velocities were reduced for the short period tests.

### 6.4.2. Effect of wave flows on sediment transport

The flow structure and near bed velocities were analysed in more detail to determine the likely direction of sediment transport and hence the risk of toe scour erosion. In linear flows, e.g. rivers, the water flow is orientated in one direction; therefore sediment transport follows that direction once the threshold velocity for particle motion is exceeded. Sediment transport under waves differs due to the water particles moving in an orbital trajectory as the wave progresses, with negligible net movement. In shallow water, the near bed orbital paths become flattened and represent a 'to-and-fro' motion.

When a seawall is introduced at the top of the beach profile, wave reflection occurs; therefore sediment particles are driven first by the incident then the reflected wave orbital motion, and then by the resulting boundary layer circulation. In addition, flows associated with the wave impact and downrush can oppose or complement the incident and reflected orbital flows, leading to flow asymmetry. This cannot be inferred from single PIV image frames or the peak velocity vector analysis.

To capture and interpret the wave flow, the concept of net drift will be defined by using a vector to represent the resultant movement a fluid particle at the bed over one wave cycle. The net drift is calculated by summing the velocity vectors at each grid point (though clearly only the grid points closest to the bed are the most significant to sediment transport) for each image frame, over one wave cycle. By dividing by the duration of each wave event, the net drift rate was calculated and represented the rate of transport with vector units $cm.s^{-1}$. It was assumed the particle would precisely follow

the flow of the water and not be adversely affected by either drag or gravity. To ensure that only a single wave was analysed, the flow direction at the offshore boundary was monitored. A reversal of flow direction determined the time and frame number separating individual waves. The net drift enabled the fluid particle motion to be linearized.

Given that the near bed velocities in the model (c.0.1 to 0.6 $m.s^{-1}$) were significantly greater then the threshold for transport of sand at model scale (c. 0.05 $m.s^{-1}$, Soulsby 1997), the drift rate was assumed to provide a good estimate of magnitude and direction sediment transport. Regions of high net drift were expected to scour, and low net drift regions expected to accrete.

## Sediment transport results

The sediment transport scour profile results were analysed for tests *A, C, D, F,* as these produced the most definitive results. Tests *B* and *E* both appeared to be dominated by offshore flows, despite producing different wave conditions and were not reviewed.

Figure 6-25 & Figure 6-28 show the scoured beach profiles for the short listed tests compared to the 1:30 initial smooth profile. The profiles were plotted using Froude scaling and the vertical and horizontal axes kept symmetric, to represent the true scour profile shape. Within the hydraulic flume a scour profile 0.60 m long was modelled, though the PIV study only focused on the region 0 to -0.17 m from the seawall, as this was the region most sensitive to profile change and scour. Figure 6-26 through to Figure 6-30 present the net drift results for the short-listed tests.

In Test *A*, moderate toe scour occurred at the wall, which peaked -0.1m from the wall, with the scour decreasing towards the end of the profile. The net drift was directed offshore up to a point -0.04 m from the wall, where offshore transport commenced at a rate of 1.1 to 1.8 $cm.s^{-1}$. This coincided with a change in the beach profile slope and an increase in the scour depth.

The wave conditions in Test *C* generated the deepest toe scour over a distance of 0.1 m, before the profile recovered and an accretion bar formed offshore. The impacting waves in this test resulted in a high offshore drift rate (2.5 -3.0 $cm.s^{-1}$) at the seawall toe. The

drift direction highlighted the vortex circulation seen in the flow results. The net drift further offshore was also directed offshore at a reduced rate of 1.0 -1.5 $cm.s^{-1}$.

The water depth was increased in Test *D* and the beach profile included slight scour at the seawall, which increased in depth further offshore, before forming a large accretion bar beyond the figures axis. The sediment drift rate was significantly smaller then the preceding tests, and was close to zero at the bed, slightly onshore close to the wall and slightly offshore at the end of the profile. The flow pattern in this test was highly reflective; calculation of the shallow water wavelength suggested that a ¼ wavelength reflected wave node would occur at a position -0.3 m from the wall. According to Xie (1981), accretion would be expected to occur at the node and the wall with scour in between. This pattern is confirmed by the sediment transport beach profile shape and the direction of the net drift towards the wall and node.

In Test *F*, the water depth was shallow and produced localised scour relatively close to the wall, and reduced with distance offshore. In the PIV tests the wave had broken offshore and reformed to cause a smaller near impacting wave with intense downrush flow. The net drift vectors confirmed these flows, and were directed offshore, at a rate of 1 $cm.s^{-1}$. This coincided with the extent of the toe vortex generated following impact. Offshore drift increased with distance from the seawall and reached a maximum rate of 2.3 $cm.s^{-1}$ at the end of the profile. This was contrary to the scour depth which decreased with distance from the wall and was lowest at the end of the profile. The net drift direction matched Test *C*, but at a reduced magnitude.

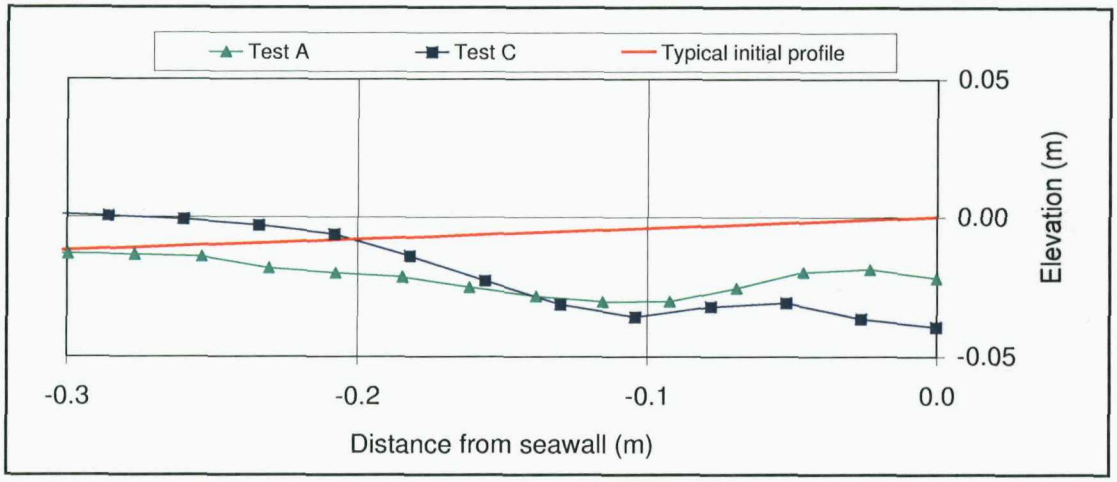


**Figure 6-25: Beach profiles- Tests *A* & *C***

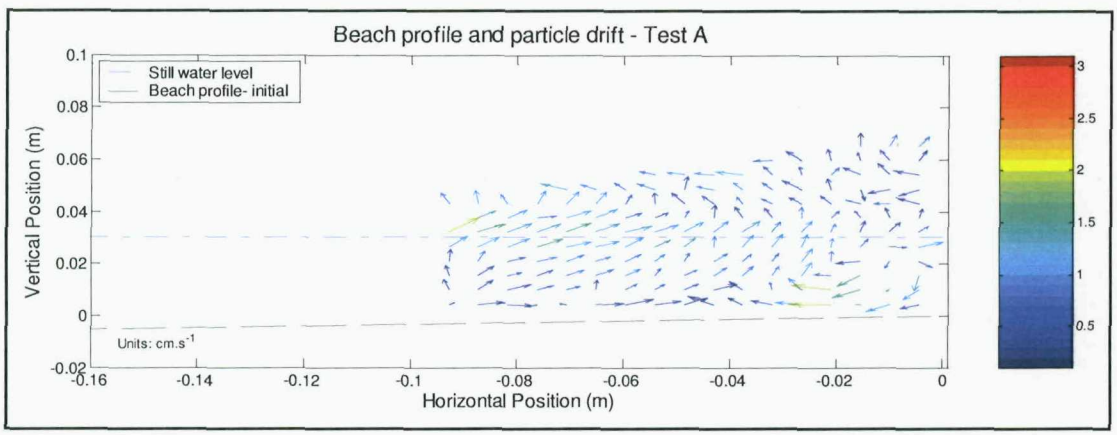


**Figure 6-26: Net drift results- Test *A***

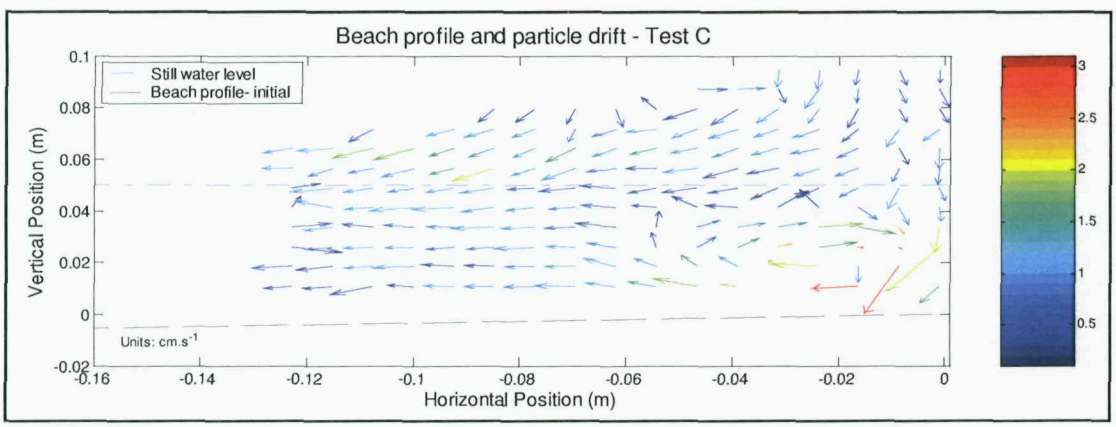


**Figure 6-27: Net drift results -Test *C***

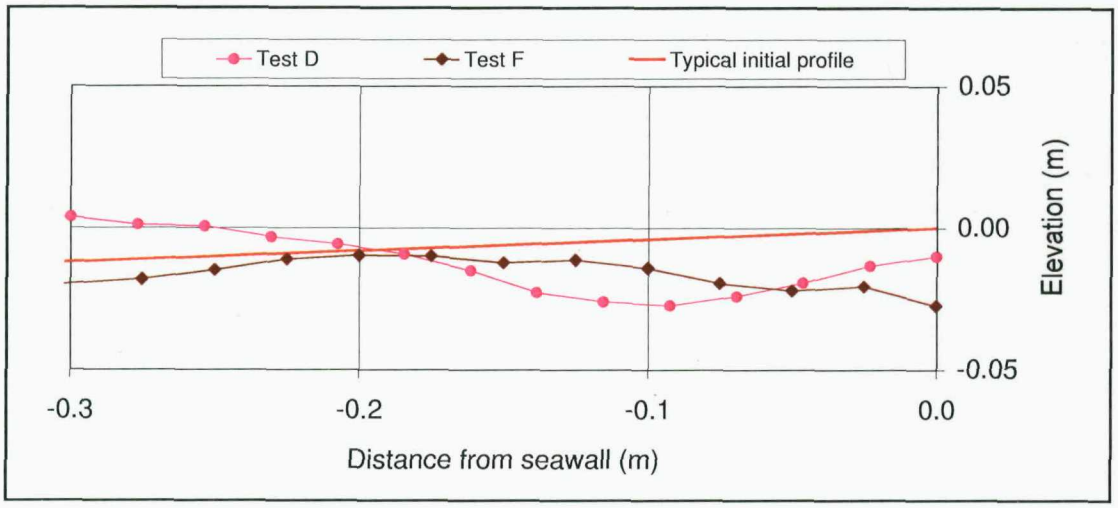


**Figure 6-28: Beach profiles- Tests *D* & *F***

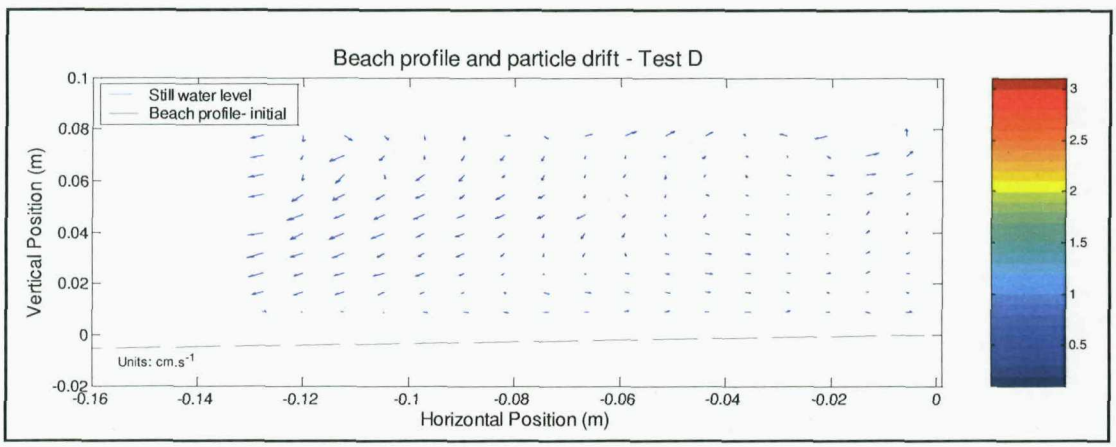


**Figure 6-29: Net drift results- Test *D***

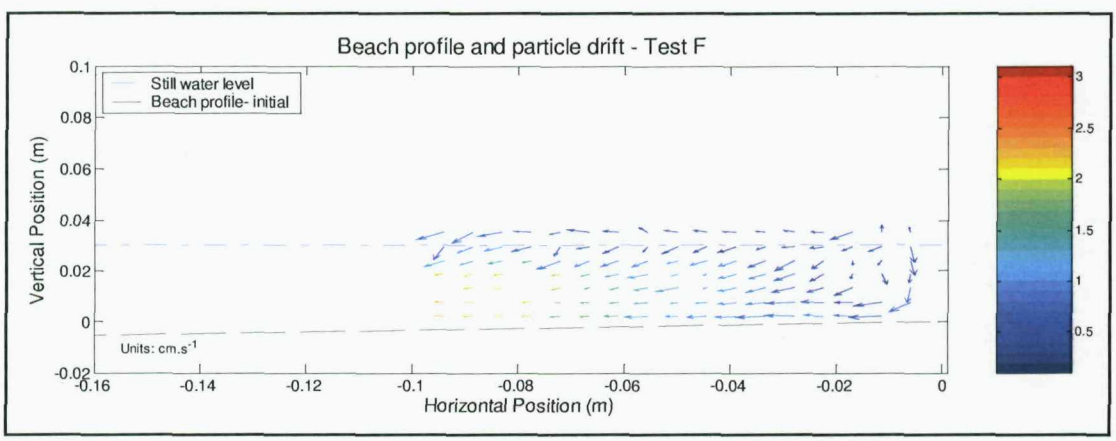


**Figure 6-30: Net drift results- Test *F***

## Summary

A series of hydraulic flow tests were conducted with a fixed bed slopes and regular period waves. The concept of net drift was defined which enabled the cumulative effect of the incident and reflected wave orbital flows and flows associated with wave impact to be assessed. The near bed flow velocities were found to significantly exceed the sediment threshold velocity, enabling the direction of sediment transport at the bed to be inferred from the net drift rate for the four short-listed tests.

The shape of the beach profile / scour profile in the in the sediment transport tests generally fell into three categories: 1) moderate scour localised near the seawall toe (Test *A* & *F*), 2) significant toe scour at the wall (Test C) and 3) nodal scour offshore of the wall (Test *D*). In shallow water (Test *A*), the drift confirmed onshore transport would occur over the beach profiles, except at the wall toe where the wave flows were sufficient to generate scour.

In the tests where wave downrush and a toe vortex occurred, (*C* & *F*) the net drift at the wall toe was directed offshore. This coincided with the position of maximum scour in Test *C*, which produced the highest net drift rate of all the tests, and the deepest scour. In Test *F* the toe vortex was smaller and corresponded to a smaller toe scour depth. In this test, the net drift increased towards the end of the profile, which did not agree with the sediment transport results, where scour reduced with distance from the wall. In the deep water Tests *D* the drift was significantly reduced at the toe and confirmed nodal transport relative to the shallow water wavelength.

### 6.4.3. Wave flow and drift on a scoured profile

The wave flow and net drift analysis was repeated using the scaled fixed bed scour profiles shown in Figure 6-25 & Figure 6-28, with identical wave conditions as their smooth profile equivalents in tests *A*, *C*, *D* & *F*. It was hypothesised that the scour beach profile would be in equilibrium with the wave flows and that a significant reduction in drift rate would occur.

In Test *A*, the incident wave again forms a spilling breaker and on impact at the wall a weak toe vortex occurs, this remains above the bed and reduces in intensity. The net drift results (Figure 6-31) confirm the position of the vortex and suggest offshore transport would occur, which increases towards the end of the beach profile. This coincides with an increase in scour at the end of profile. The magnitude of drift at the wall toe is reduced compared to the smooth profile test.

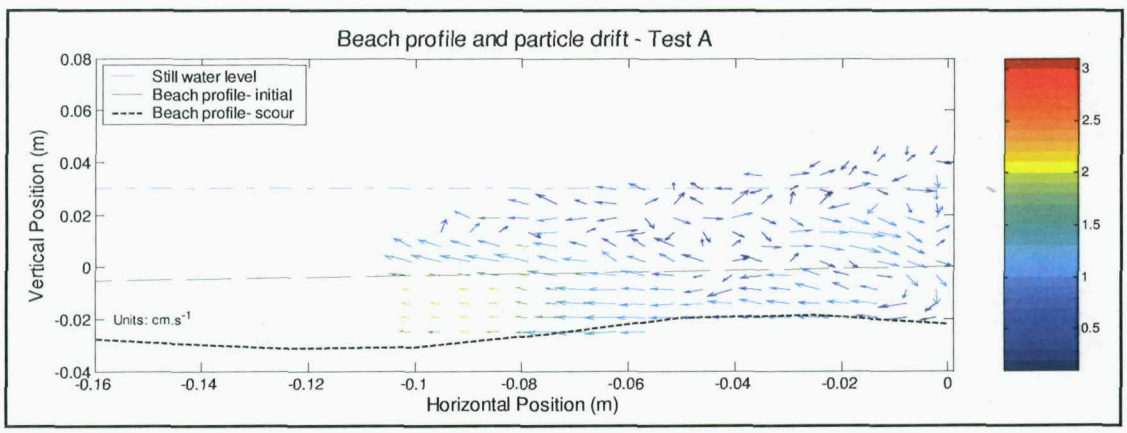


**Figure 6-31: Net drift results, scour bed- Test *A***

In Test *C* as the wave approaches the wall it comes close to breaking, however the scour profile increases the water depth by 41 mm, causing the impact to be less intense compared to the smooth profile case. Following impact a large downrush vortex forms, and remains above the bed, this produces the peak flow velocity (10-20 $cm.s^{-1}$) and drift rate at the wall toe (0.5-1.0 $cm.s^{-1}$). Beyond the wall toe, the net drift continues to be directed offshore, except at the end of the profile slight onshore transport seemed to occur as a result of the positive beach slope (Figure 6-32).

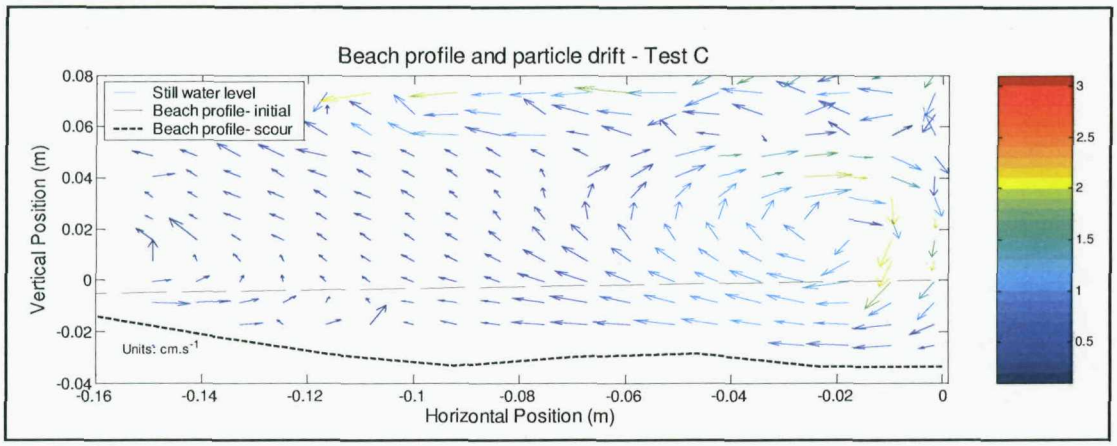


**Figure 6-32: Test C, Net drift and scour vortex above bed**

In Test *D* (not shown), a pulsating wave conditions occurs and the net drift rate increases compared to the smooth profile equivalent. This causes the direction of the peak velocities to switch from onshore to offshore. However the shape of the scour beach profile and wave form suggested that the test was dominated by reflection driven transport processes. It was not clear why the direction of drift did not follow the reflected wave pattern.

In Test *F* the wave again breaks offshore, and reforms to produce a small near impact / pulsating wave. The downrush velocity is significantly reduced compared to the smooth bed test and a toe vortex does not form. The drift rate near the wall also remains small. Further offshore the net drift directions are not clear, with alternating regions of slight onshore and offshore transport over the scoured bed. Figure 6-33 compares the seawall wave interaction at a similar point in the wave cycle for the smooth and scoured beach profile in Test F, and demonstrates the effect of the 28 mm increase in water depth and subsequent lack of toe vortex.

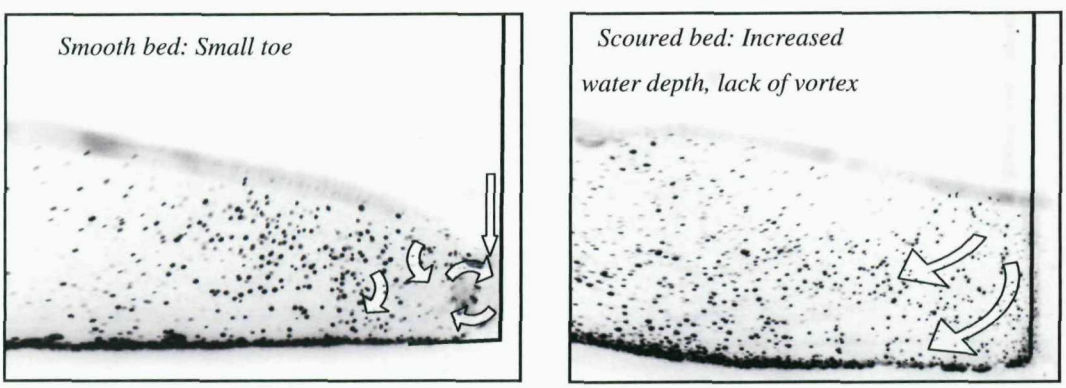


**Figure 6-33: Test F, comparison of flow following wave reflection on smooth and scoured beach profile**

### 6.4.4. Summary

In general, the toe scour caused the water depth in front of the wall to increase, which reduced the net drift intensity and peak flow velocity. This was most significant in Test *C* where the peak bed velocity reduced from 40-50 $cm.s^{-1}$ to 10-20 $cm.s^{-1}$. The increased water depth prevented the wave downrush from reaching the bed, and the associated vortex either did not form or remained above the bed, where it dissipated more quickly. In the deep water test (*D*) the flow structure followed a nodal sediment transport pattern within the flume, however the offshore direction of net drift did not support this pattern. It is not clear why this occurred or why the directions of the peak velocities were also reversed. For each test, the wave impact, vortex and drift characteristics were summarised in Table 6-2 for both smooth and scoured beach profiles.

**Table 6-2: Summary characteristics of wave impacts, flows and drift with smooth and scoured beach profiles.**

| Test | $d_t$ | $T$ | $S_t$ | Smooth bed profile | | | | Scoured bed profile | | | |
|---|---|---|---|---|---|---|---|---|---|---|---|
| | | | | Incident Breaker type | Bed vortex duration (s) | Drift at toe ($cm.s^{-1}$)# | $V_{max}$ at toe ($cm.s^{-1}$)# | Incident Breaker type | Bed vortex duration (s) | Drift at toe ($cm.s^{-1}$)# | $V_{max}$ at toe ($cm.s^{-1}$)# |
| *A* | 0.03 | 1.3 | -0.09 | Spilling | 0.57 | -0.5 to -1.5 | -10 | Spilling | - | -0.5 | -10 |
| *B* | 0.05 | 0.7 | -0.07 | Spilling | - | -0.5 | +10 | Spilling | - | -0.5 | -10 |
| *C* | 0.05 | 1.3 | -0.16 | Impact | 0.50* | -1.5 to -2.7 | -50 | Impact | 0.47 | -0.5 | -10 |
| *D* | 0.10 | 1.3 | -0.01 | Pulsating | - | +0.5 | +10 | Pulsating | - | +0.3 | +5.0 |
| *E* | 0.10 | 0.7 | +0.01 | Pulsating | - | -0.5 | -10 | Pulsating | - | -0.5 | -10 |
| *F* | 0.03 | 0.7 | -0.11 | Near impact | 0.47 | -0.6 to -1.0 | -10 | Near pulsating | - | -0.5 | -10 |

* The vortex generated during wave downfall continued to rotate beyond one wave cycle.

\# The toe was defined as the region 0 to -0.04 m from wall toe (- denotes offshore, + denoted onshore).

## 6.5. Discussion

### 6.5.1. The use of PIV in analysing seawall flows

The use of PIV in a small scale physical model experiment enabled the high speed flows and sediment transport in front of a seawall to be systematically analysed for a variety of wave and beach conditions. This would not have been possible using invasive current meters, which only provide point measurements. By summing the velocity vectors, the net drift of a sediment particle was inferred and applied to indicate regions of scour and accretion.

To ensure adequate exposure, a light sheet 15 mm wide was generated, this eliminated the need for complex optical equipment and overcame the laboratory restrictions. However this increased the depth of the sampling area, which should be less then the focal depth (Keane & Adrian, 1990). Through the use of a narrow 2D wave flume, shore normal wave approach and the limited depth of focus of the lens (< 5 mm, based on the lenses hyperfocal distance), the effect of the background particles did not appear to cause significant errors.

The experiments used a moderate camera frame rate of 70 fps, this was however insufficient to accurately record the fastest particles, which often appeared as streaks at the water surface and near the wall face, where their velocity was estimated at $\approx$100 $cms^{-1}$. A higher frame rate and laser illumination would be required to observe the point of wave impact at the wall and the wave uprush velocity. These features were also obscured by air bubbles entrained in the flow, suggesting analysis using Bubble PIV techniques (Ryu *et al*, 2005), where the bubbles are utilised as the seed particles, would be beneficial.

The particle velocities were significantly slower at the bed, the focus of this study, and were successfully captured by the PIV system. The use of a large 64 x 64 pixel interrogation cell ensured a good average velocity for each grid square, this also reduced leakage of particles beyond the cell boundary. However in the vicinity of the wall, where the strongest velocity gradients tended to occur, the interrogation cells were too large to accurately measure the detailed flow structure. In some cases the flow speed tended to be smoothed and averaged, though the direction remained true. Occasionally

the gradients were too severe for the PIV analysis software and produced erroneous results, these points were deleted.

In future studies, it could be possible to decrease the grid size and increase the camera lens magnification. By moving the camera to a different area of the flow each time and repeating the wave, the regions could be stitched together to provide a higher resolution PIV analysis. This technique would require accurate camera positioning and timing, with a highly repeatable wave.

Separation of the target wave was achieved by observing the orbital direction of the particles at the offshore boundary. Under some circumstances localised residual flows continued at the toe of the wall beyond this period. For consistency these were excluded, and were assumed to have small impact on the overall net drift as these velocities were low.

Though the use of fixed bed model overcame the limitations of sediment settlement witnessed in previous small scale experiments, other scale effects were witnessed during the test. These included large bubble entrainment, which tended to rise in the water column very quickly once the wave had reflected offshore, and an absence of smaller entrained air bubbles and foam, as witnessed in the field sites and medium scale flume experiments. These effects were not considered to adversely affect the speed and direction of flows at the bed at small scale, however the increased compressibility of air-entrained-water might affect wave impact pressures at prototype scale (Peregrine *et al*, 2004), though it is not clear how this might affect scour / sediment transport.

During the planning of the experiment, Test *C* was expected to reproduce the violent plunging breakers, spray and turbulence witnessed every couple of minutes in the medium scale tests. Though strong plunging breakers occurred in the small scale tests, these appeared less intense then the medium scale tests. This was attributed to the regular wave period which prevented a spectrum of incident and reflected waves being formed, which tend to interact to produce larger impacts. The use of irregular waves in the PIV study would severely complicate the experiment analysis; an alternative approach would be to generate a tuned wave group what would converge at the wall to generate a perfect impact, though this would be different to the prototype wave conditions. The increased surface tension in the small scale model would also be

expected to affect wave breaking (Miller et al. 1972) however the impact of this scale effect on sediment transport is very difficult to quantify.

### 6.5.2. Analysis of wave flows in front of seawalls

The key variable distinguishing each test was the type of wave breaking. When comparing the breaker type in each test to their respective $d_t / L_m$ ratios, and hence position on Figure 6-9, inconsistencies were apparent between the short and long period wave tests.

The short period tests *B* and *F* were both positioned close to the longer period test *D*, however each test resulted in a different wave breaker type. When the tests were grouped by their wave period, a more consistent wave breaker pattern emerged. The long period tests (*A*,*C*,*D*) ranged in turn from spilling, to impacting, to pulsating with increasing $d_t / L_m$. In the short period tests (*B*, *E*, *F*), Test *E* produced unbroken pulsating conditions, however the shallow water depth and increased wave steepness caused tests *B* & *F* spill offshore and then either reform at a smaller amplitude or produce a spilling impact at the wall. Though these breaker types were less well defined then the long period tests, the intensity of the wave structure interaction and resulting flows velocities broadly corresponded to the $d_t / L_m$ ratio. In these tests, the most intense flows occurred for Test *F* ($d_t / L_m = 0.1$).

The non-dimensional parameter $d_t / L_m$ provides continuous indicator for predicting the flow intensity for a range of wave conditions, however the variable does not predict wave breaking which is dependent on $H_0 / d_t$. In the prototype situation, the beach profile shape and slope, wind strength and wave spectrum would also affect wave breaking and hence scour. The effect of beach profile was evident in the scour profile tests where an accretion bar had formed offshore of the seawall, it is speculated that these may cause enhanced shoaling or breaking prior to the wall. If the water depth was less then the incident wave height, the accretion bar would act as a wave height filter, protecting the toe from further scour.

### 6.5.3. Analysis of sediment transport

To predict the position and magnitude of sediment transport due to orbital and wave flows, the concept of net drift was devised by summing the velocity vectors for each grid point. The greatest toe scour tended to occur on profiles with strong offshore net drift. Profiles with reduced scour tended to have a lower net drift or the drift rate was directed toward the wall toe.

The flow velocities were established to be significantly greater then the threshold for sediment transport, therefore particles at the bed would be readily transported by the flow and suspended. The effect of longshore and entrained currents were not considered, but could increase the rate of sediment transport, although not necessarily the depth, due to the resulting increase in toe water depth preventing wave downrush reaching the bed and promoting reflective wave conditions.

The limitations of the PIV flow analysis in accurately measuring the fastest velocity vectors associated with the wave downrush and the smoothing associated with the large interrogation cells may have reduced the resolution and accuracy of the net drift rate. Despite these limitations, the net drift provided a conservative estimate of the magnitude and direction of sediment transport at the bed and wall toe under complex flow processes, and hence the likely position and severity of scour.

### 6.5.4. Combining the wave breaking intensity and resulting scour

The results of the wave flow intensity and net drift results were combined to define three key wave structure interaction types and the resulting sediment transport / risk of scour:

**Weak spilling wave breaker – low scour risk**

When the toe water depth was shallow or the waves became overly steep, wave spilling occurred. This caused wave energy to be dissipated away from the seawall. The flow velocities at the wall toe were therefore reduced, but sufficient in the longer period test for a small toe vortex to be generated briefly. Scour in these conditions will be relatively shallow and localised at the wall ($S_t / H_0 < 0.5$) toe due to the turbulence generated by the interaction of the wave and seawall.

**Impacting waves – high scour risk**

When the incident wave, or reformed waves break at the wall, a high velocity vertical uprush is produced, shortly followed by the wave downrush, which generates a clockwise a rotating toe vortex. The turbulence generated by the breaking wave and the high flow velocities associated with the downrush and vortex lead to deep scour at the wall ( $0.5 < S_t / H_0 < 1$), and the potential for removal of rock toe armour constructed for scour protection. Across the beach profile the net sediment transport would remain offshore, extending the width of the scour hole and leading to an accretion bar offshore beyond the influence of the wave impact flows.

As the bed scours, the toe water depth is increased (+82% Test *C*, +58% Test *F* ) which causes the downrush to dissipate in the water column, reducing the peak flow velocities at the bed and the scour depth as equilibrium is reached.

**Pulsating waves – low scour, potential accretion**

Pulsating waves remain unbroken at the wall and generate large uprush flows. However the increased water depth prevents the downrush flow from reaching the bed and forming a scour vortex. Sediment transport will be directed toward the wall and quarter wavelength node offshore, leading to only slight scour or possible accretion at the wall toe ($S_t / H_0 < 0.1$).

## 6.6. Conclusions

### 6.6.1. Study objectives

**Can particle image velocimetry (PIV) be used to make observations and measurements of the scouring wave flows?**

PIV techniques were successfully applied to investigate wave flows in front of a vertical seawall with a fixed seabed. The result provided evidence of the flow velocity and through the concept of net drift, the position of sediment transport hence scour was inferred. However the fastest flows and the detailed flow structure at the point of impact were not successfully measured by the current PIV system, these were however established from the still images and particle streaks.

When investigating a specific design or the point of wave impact, the use of laser illumination and camera with higher frame rate is recommended, though it may only be practical to analyse the wave downrush element the wave impact, due to the complex analysis required.

**What are the flow patterns at the seawall and seabed? What effect do these flows have on sediment transport and toe scour?**

The intensity of flow at the wall toe and hence potential for sediment transport was found to fall into three categories, spilling, impacting or pulsating. Impacting waves, breaking at the seawall were found to generate uprush flows. A clockwise rotating scour vortex and deep toe scour.

Where waves had broken, shallow scour occurred at the wall toe due to the reduction in wave energy, downrush velocity and vortex size. Under pulsating conditions, despite a large uprush, the toe water depth was sufficient to prevent an increase in bed velocities or a toe vortex, and sediment would be moved to the reflected wave nodal points.

In the prototype situation, the wave spectrum is likely to contain different proportions of each type of breaker depending on the wave height, period and toe water depth. The toe scour depth will therefore depend on the relative number of each type that occurs at the wall. Furthermore factors such as wind strength, which can induce spilling waves when directed onshore, may also become important.

**How does the flow structure change on a scoured beach profile?**

In general the scoured beach profiles increased the toe water depth. This reduced the intensity of the breaking waves and the near bed velocities and hence the potential for further toe scour would be reduced. Most of the scoured profiles led to an accretion bar offshore, the effect of this feature on wave breaking was not investigated; however this may induce wave breaking offshore, protecting the seawall from further scour.

The direction of sediment transport and wave flows did not appear to achieve equilibrium with the scour profile shape, perhaps due to the irregular period waves in the moveable bed tests, which would have produced a range of breaker types.

### 6.6.2. Further research requirements

Scour prediction equations made using the parameter $d_t / L_m$ provide an improved understanding the risk of scour through partial representation of the wave breaking intensity at the seawall. However further research is required to develop an improved understanding of wave breaking in front of coastal structures and the effect of wave spectrum, beach slope, wind and clapotis.

To measure the maximum uprush and downrush flow velocities at the wall face for impacting waves, a PIV study utilising a high speed digital camera (200 fps) with high resolution is required This study would need to establish a source of uniform illumination for the fast moving jets, and the problems of air bubble entrainment in these flows, perhaps using bubble PIV?

# 7. Combined analysis and discussion

In the following section, the results from the preceding field, sediment transport and hydraulic experiments are combined and contrasted to develop an improved understanding of the key scour processes. This includes validating the sediment transport and toe scour results against the field data observations and correlating these with the wave flow measurements to develop a scour risk envelope. The scour envelope will then be applied to a series of prototype situations to demonstrate the effect of the key variables and to suggest potential design solutions.

## 7.1. Comparison of field and sediment transport studies

### 7.1.1. Scour depth validation

In the sediment transport flume study, the maximum toe scour depth was 0.16 m ($S_t / H_0 = 0.79$) for the vertical wall with a 1:30 seabed slope, 0.09 m ($S_t / H_0 = 0.45$) for a 1:75 seabed slope and 0.10 m ($S_t / H_0 = 0.52$) for the 1:2 sloping wall. By applying Froude scaling and a prototype significant wave height of 2 m, the maximum toe scour at prototype scale would be in the region of 1.6 m, 1.0 m and 0.8 m respectively. In the Blackpool field experiment the maximum toe sour was 0.88 m, for a wave height of 1.8 m ($S_t / H_0 = 0.48$) with a typical beach slope of 1:80. At Southbourne, with a 1:2 sloping seawall on a 1:28 beach slope, the maximum toe scour was 0.6m for a wave height of 1.5 m ($S_t / H_0 = 0.40$).

In comparing beaches of similar slope in the field and flume experiments, the flume results produced conservative estimates of scour for both vertical and sloping seawalls. As noted in Chapter 5 sediment transport study, the effect of significant wave height was not fully investigated during the flume experiments. However, results from the field study showed no clear relationship between wave height and scour depth, as the wave height was often depth limited. The datasets support the 'rule of thumb' that the scour depth will remain less then the incident wave height.

A simple method for defining the position of wave breaking was defined in Section 2.1.1 by the ratio of the water depth to wave height, with waves expected to break when their height is approximately equal to the water depth. This method was applied to compare the field and flume measurement. A more rigorous method was applied in Section 7.2.3 when

comparing the laboratory datasets. Figure 7-1 compares the ratio wave height to water depth for the field and flume datasets to the non-dimensional toe scour depth.

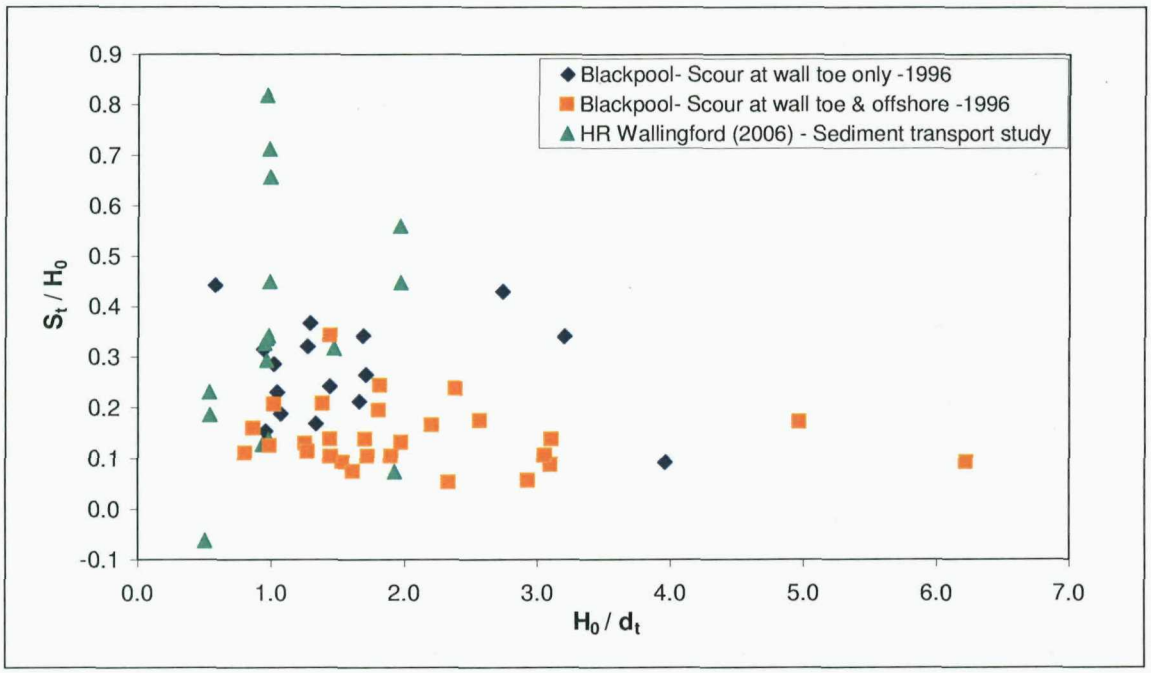


**Figure 7-1: Comparison of medium scale and field toe scour results**

In the field dataset, beach lowering occurs over a wide range of wave height to water depth ratios, but is greatest at $H_0/d_t = 1.4$. Field toe scour is limited to $0.5 < H_0/d_t < 4$, but occurs most frequently in the range $1 < H_0/d_t < 2$. In the flume experiments, the deepest toe scour also occurs in the range $0.5 < H_0/d_t < 2$. Despite significant scatter, a result of the different wave period and beach slopes, the figure suggests a correlation between wave breaking and toe scour. Theoretically waves would be expected to break onto the seawall when $H_0/d_t \approx 1$. Either side of this point, the water depth would either be too shallow or too deep, leading to either shoaling or wave reflection.

Though the sediment transport tests are only representative of waves approaching the seawall from a perpendicular direction, these were assumed to generate the deepest scour. Figure 7-2 compares the toe scour depth collected at Blackpool and the offshore incident wave direction over a ninety degree arc. This shows that scour occurred under both oblique and perpendicular wave directions, and is likely a result of the shallow water depth causing refraction towards a shore normal direction. The use of the 2D wave flume experiments to investigate scour processes and develop improved predictions can therefore be justified.

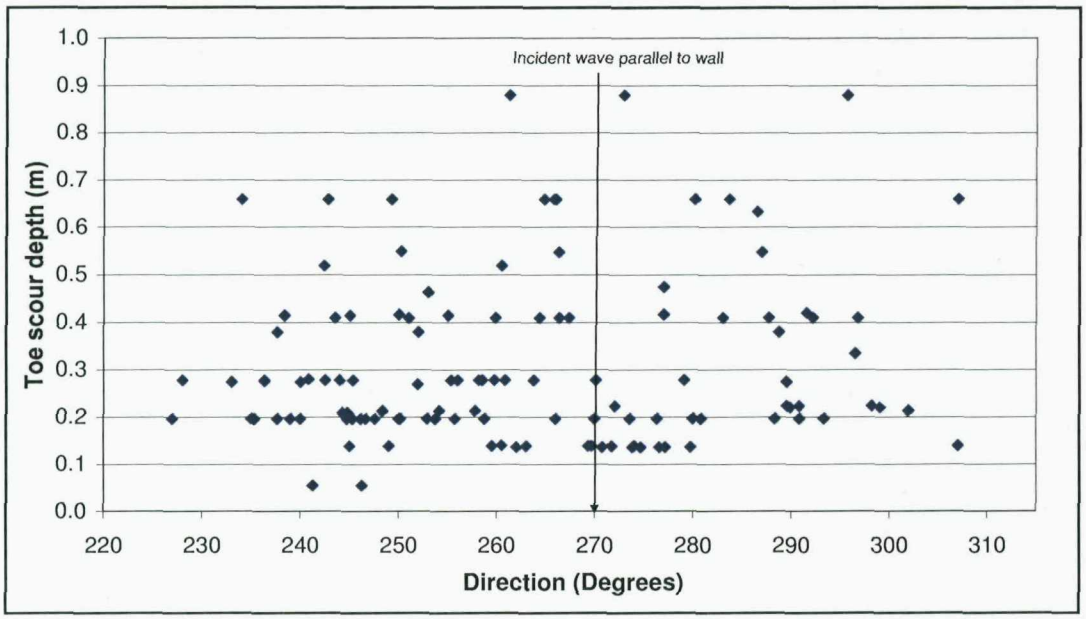


**Figure 7-2: Comparison of scour depth and wave direction**

## 7.2. Scour risk and prediction

### 7.2.1. Validation of scour predictors

The validated flume study results produced a series of toe scour depth measurements which were used to generate toe scour depth predictions using the non-dimensional parameters $d_t / L_m$ and $S_t / H_0$, building upon earlier work by Sumer & Fredsøe (2002). This approach represents a shift in thinking, from empirical predictors based on either breaking waves (Fowler, 1992) or reflected waves (Xie, 1981), towards a more realistic system where both conditions can occur depending on the toe water depth.

The non-dimensional scour predictor equations developed in Section 5.5.3 were validated using the Blackpool field data to confirm that similar patterns occurred in the full scale environment. With the exception of the two outlying points, the field dataset fitted beneath the scour predictor best fit lines (Figure 7-3). The McDougal et al. (1996) equation under predicted the scour depth, though most data points lie beneath this line. In general the maximum toe scour depths observed in the field are considerably smaller then those observed in the sediment transport flume results. This was likely a result of the shallow beach slope at Blackpool, which as discussed in Section 4.6.1 and confirmed in the sediment transport tests (Section 5.6.3), increases the surf zone width and hence offshore energy dissipation.

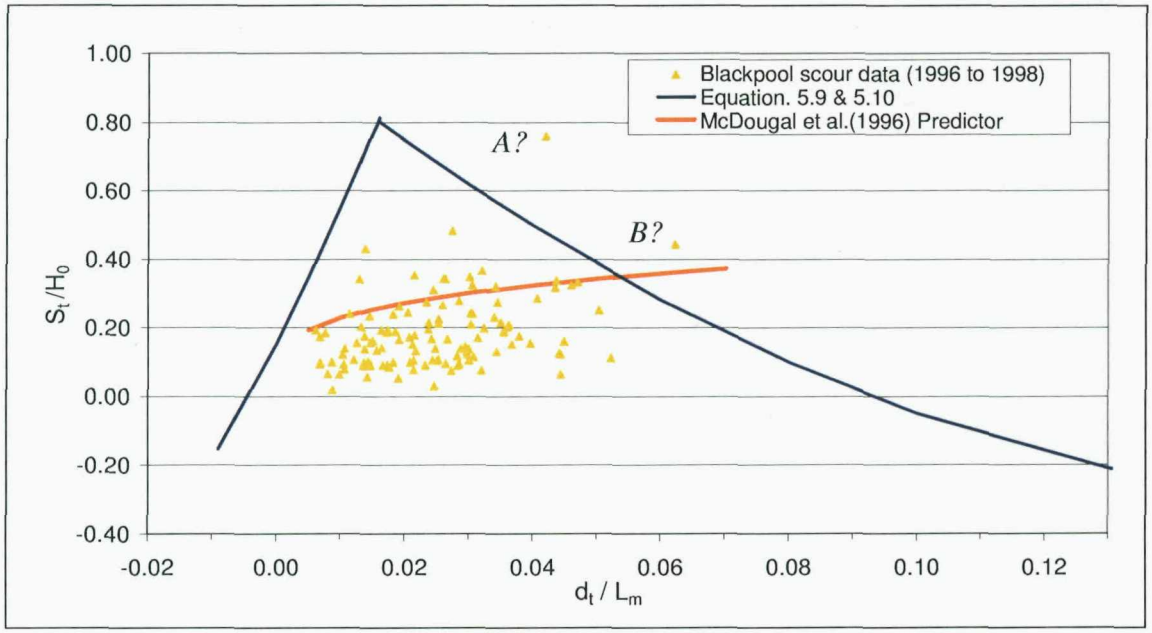


**Figure 7-3: Comparison of scour prediction equations 5.9 & 5.10 to Blackpool field results**

In Figure 7-3 the peak scour values from the Blackpool study only varied slightly with $d_t / L_m$, but were higher in the range $0.01 < d_t / L_m < 0.03$. Closer inspection of the two outlying points showed that point *A*, occurred on the 6th July 1996, with a wave height of only 0.86 m. It is possible that given the popularity of the site in the summer months, the beach sensor may have been interfered with at low tide, producing the erroneous point. In the second outlying point, *B*, the -0.68 m spike in the scour depth occurred 35 minutes before high water, this lasted only for one sampling point (15 minutes), though this point passed all the filter rules, the reliability of this measurement remains in doubt.

Without more detailed field data, it is not possible to conduct a complete validation of the scour predictor equations. As noted in Chapter 4, the limitations of the available wind and tide information prevent further investigation of cause of the scatter in the field data. These difficulties are compounded by the natural variability of the coastal zone, where other factors such as sand bars, wind speed and the wave spectrum may also influence the final scour depth. The field dataset represents the best available and sits within the ranges predicted by the scour prediction equations. Both field and flume datasets suggest a dependency on wave breaking, this is investigated further below.

### 7.2.2. Combining the sediment transport and wave flow results

Following the comparison of scour depth and wave flow structure in Section 6.4.2, a more detailed analysis was conducted to develop a causal relationship between scour and wave breaking.

The scour depth results from the sediment transport study are shown in Figure 7-4 with the corresponding hydraulic study test label. The scour results for the sediment transport test where $d_t = 0$ were included for comparison, but were not modelled hydraulically, as the waves spilled offshore on the exposed beach. Table 7-1 summarises the wave breaker type witnessed in each hydraulic flow test.

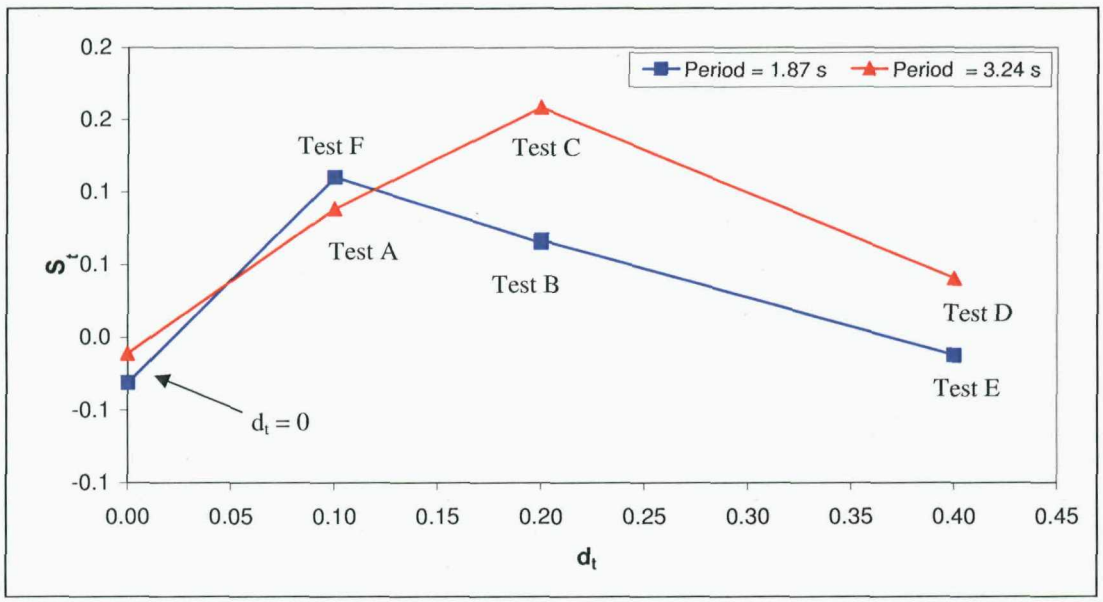


**Figure 7-4: Comparison of wave period, scour depth and toe water depth for the sediment transport tests**

**Table 7-1: Hydraulic test wave breaker type**

| Test | Wave Breaker type | Test | Wave Breaker type |
|---|---|---|---|
| A | Spilling | F | Near impact |
| C | Impact | B | Spilling |
| D | Pulsating | E | Pulsating |

The results for the long wave period (*A*, *C*, *D*) were analysed first. These demonstrated a clear relationship between the wave breaker type and depth of scour, with the greatest scour occurring with impacting waves. Only moderate scour occurred under spilling waves. Flow velocities were significantly reduced under deep water, pulsating conditions, which produced net drift toward the wave antinode at the wall toe, and scouring further offshore.

The relationship between toe water depth, wave breaker type and resulting scour depth for the short period tests (*F*, *B*, *E*) deviated from the longer period results above. In tests *F* & *B*, the increased wave steepness caused the waves to break offshore and reform with a reduced height or continue spilling at the wall. This suggests that dissipation of wave energy is occurring offshore, leading a reduction in wave impacts intensity and associated flow velocity and drift rates near the wall. This appears to correspond to the shallower toe scour observed in these tests. In Test *E*, the flow conditions were pulsating and similar in structure to Test *D*, though the peak velocities were slower.

The two test groups demonstrate the effect of wave breaking on the scour depth, either by depth limited wave shoaling at the structure or shoaling further offshore causing waves to become overly steep and spill. This exposes the limitations of using the non-dimensional variable $d_t / L_m$ to define the type of wave breaking for wide range of wave periods. As a consequence, the scour guidance provided by Sumer & Fredsøe (2002) in Figure 3-9, which suggests that breaking wave scour occurs when $d_t / L_m < 0.025$ and reflected wave scour occurs when $d_t / L_m > 0.07$, is misleading.

Unfortunately there were insufficient data points to extend Figure 7-4 to enable scour predictions for the other wave periods. The figure is also complicated by the use of dimensional units, which would require a scale to be defined before the results could be applied to a prototype situation. To overcome these shortcomings, an investigation was conducted to include the principle scour process, i.e. the type of wave structure interaction, within the scour prediction variables.

### 7.2.3. Defining wave breaking on beaches

In Section 2 the concept of depth limited wave breaking was introduced as defined by the ratio of wave height to water depth. This was extended to include the slope of the beach profile, which defined the wave breaker type. While these provide useful estimates, the following factors also contribute to the wave breaking process on beaches:

- $H_0/L_m$ -wave steepness;
- $d$ -Water depth;
- Wind & current effects;
- Bathymetry, offshore bars and reef;

Of these variables the following were considered to have less significance at seawall structures: Onshore winds can cause premature spilling of the waves, as these effects are relatively short in duration and difficult to predict they were not considered; Offshore bars can induce breaking offshore, however if scoured beach levels are assumed to be low, these features would be of insufficient size to affect the waves; Currents opposing waves increase the wave steepness, which can induce breaking. However close inshore, tidal currents are likely to be small and rip currents would tend to fluctuate in position and be relatively short in duration. With regard wave breaking at the beach, the first two variables were considered the most significant and were taken forward for investigation.

**Nearshore wave characteristics and breaking**

To estimate wave breaking on sloping beaches the Iribarren number (Equation 7.1, Battjes, 1974) is often applied. This parameter represents the balance between the rate of wave shoaling versus the initial wave steepness. When $\xi < 0.4$ spilling breaking waves are dominant. For values $0.4 < \xi < 2.0$, plunging waves occur, and when $\xi > 2.0$, unbroken surging waves occur. For waves of similar steepness, a shallow beach gradient would cause slowly developing spilling waves and a wide surf zone, whereas a steep beach would produce rapidly developing plunging waves.

$$\text{Iribarren number} = \xi = \frac{\cot\alpha}{(H_0/L_m)^{0.5}} \qquad (7.1)$$

However in shallow water ($d/L_m < 0.04$) wave celerity is reduced and hence wave steepness increases. This causes the wave height to increase until the wave becomes unstable and breaks. This is referred to as the depth limited wave height or breaking wave height $H_b$ and can be estimated empirically for sloping beaches with regular waves.

However irregular period waves significantly complicate this process with wave breaking occurring over a wide surf zone (Goda, 2000). However the Iribarren number does not consider water depth, limiting its application to predict wave breaking at seawalls.

### 7.2.4. Wave breaking at structures

At seawalls the wave breaking process is complicated by reflected waves interfering with the near-breaking incident waves. In a physical model study into the onset of wave breaking at structures, Calabrese (1998) derived an empirical equation to predict the maximum $H_b$ for irregular period waves in front of vertical breakwaters (Eqn 7.2).

$$H_b = \frac{1}{k_b}(1.025 + 0.0217C^*)L_0 \tanh(2\pi d_t / L_0) \quad (7.2)$$

$$C^* = \frac{1-k_r}{1+k_r} \quad (7.3)$$

Where $k_b$ represents the ratio of $H_{99\%}$ to $H_s$ and can be approximated to 1.5 for a mean JONSWAP spectrum (Calabrese, 1998). Equation 7.2 includes the parameter C* (Eqn 7.3), which represent the magnitude of reflected waves. Estimating $k_r$ for a seawall depends on the toe water depth, the wave period, the structure shape and factors such as overtopping. Therefore $k_r$ is usually determined from physical model tests (Goda, 2000) and was collected during the HR Wallingford (2006) experiments.

Equation 7.2 and 7.3 were applied to derive the maximum breaking wave height at the toe of the wall. However, these equations do not indicate if the waves are depth limited and would have broken further offshore, therefore the wave breaker depth index was calculated (Eqn 7.4).

$$\text{Breaker depth index} = \frac{H_b}{d_t} = 0.78 \quad (7.4)$$

Following research into solitary waves travelling over a flat seabed, McCowan (1891), defined a threshold value of 0.78 for breaking / non-breaking conditions. Goda (2000), suggest an approximate value of 0.6 should be applied for irregular period waves on a beach. When determining the breaker index at a seawall, the reciprocal of Equation 7.4

was calculated due to the occurrence of toe water depths less then zero. Therefore when the water depth to maximum breaking wave height is approximately equal to 1.7, the highest one third of waves would be expected to start breaking at the seawall. As the depth increases a higher percentage of larger waves ($H > H_s$) would break at the wall.

**Scour risk envelope**

Equations 7.2, 7.3 and 7.4 were applied to the sediment transport results to compare the offshore wave steepness ($H_0 / L_0$) to the nearshore breaker index ($d_t / H_b$). These were plotted with the toe scour to offshore significant wave height ratio ($S_t / H_0$) for the 1:30 beach slope tests to generate a scour risk envelope (Figure 7-5). For each test the type of wave breaking was objectively assigned from the video images broadly following the criteria in Figure 2-3. In the tests reproduced in the hydraulic flow study, the wave breaking was confirmed with greater confidence; these tests were also identified.

Figure 7-5 combines nearshore variables similar to those used by Powell & Whitehouse (1998) in their isometric scour diagram of COSMOS-2D numerical model results (Figure 3-8). Though the variation in scour depth appears broadly consistent, the depth of scour was significantly greater in their simulations and they did not indicate the type of wave breaking expected in each region of the figure, a drawback of numerical modelling.

By combining the sediment transport results, the estimated nearshore wave characteristics and the hydraulic flow results, Figure 7-5 can be applied to describe the wave breaker type and toe scour risk for a vertical seawall with a 1:30 sand beach. Deep scour requires low steepness waves combined with optimal wave breaking conditions at the wall.

The scour risk regions to be broadly categorised as follows:

Broken waves occur when the toe water depth is shallow ($d_t / H_b \leq 2$) (e.g. Test A). In the sediment transport tests these led to beach accretion at the toe however, these are not shown in Figure 7-5 as the equations produce complex numbers. Spilling waves also occur when waves became overly steep ($H_0 / L_p$) > 0.03, where the wave shoal, break offshore and reform at the wall (e.g. Test *F*). Breaking waves dissipate energy over the beach profile, and generate less significant scour.

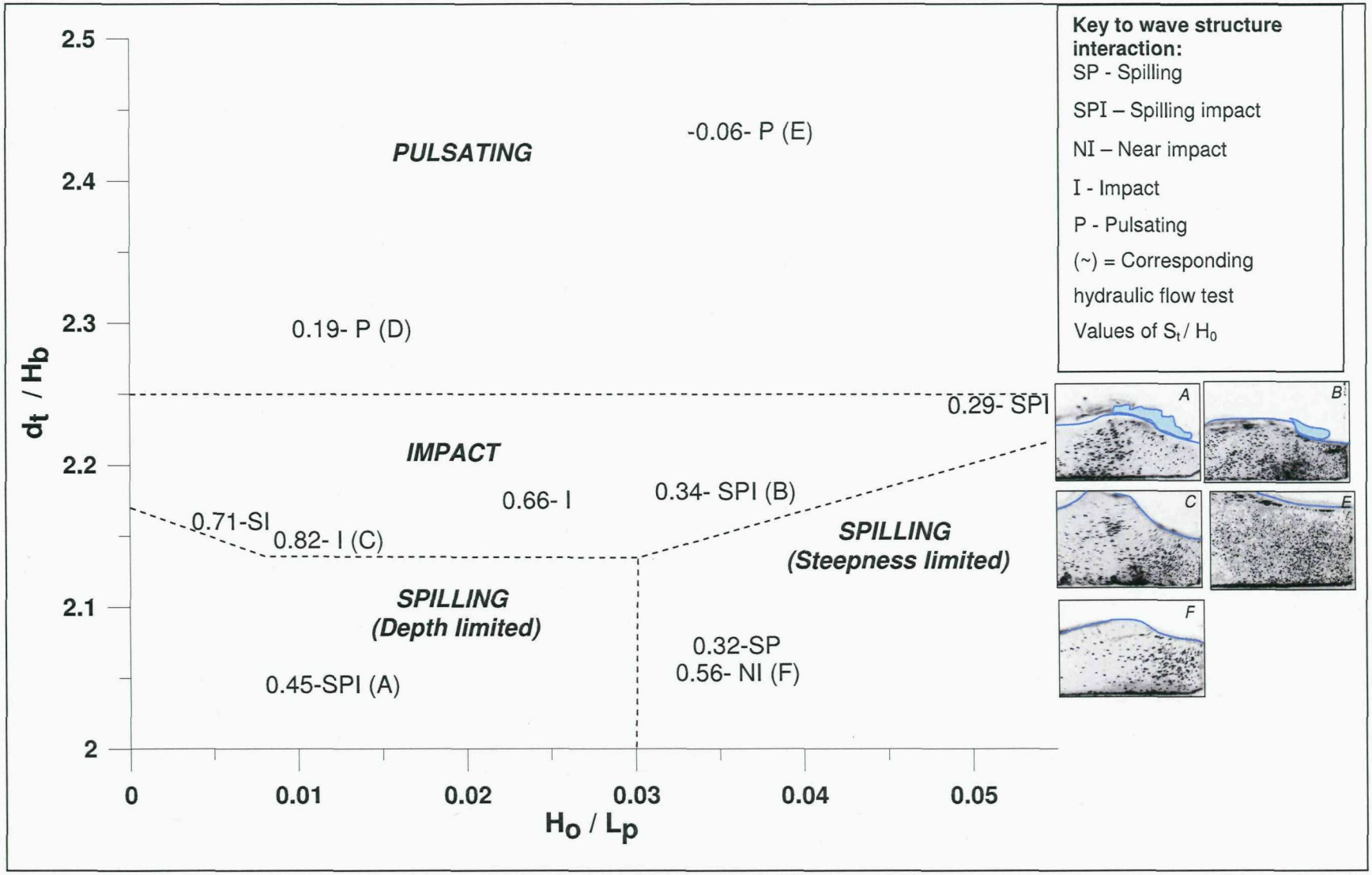


**Figure 7-5: Toe scour risk envelope and images of wave structure interaction-shallow water**

Figure 7-5 suggests the threshold wave steepness for wave impacts is close to 0.02 $(H_0/L_0)$. The threshold breaker index $(d_t/H_b)$ appears closer to 2.1, this is slightly higher then the value suggested in Equation 7.5 for solitary waves and the value of 0.6, suggested by Goda (2000).

Where $d_t/H_b \approx 2.15 - 2.25$, wave impacts occur at the structure, producing high velocity wave downrush, toe vortices and deep toe scour. The toe scour depth is greatest for waves of lower steepness, which as discussed earlier contain a greater mass of water and shoal more slowly, producing violent wave impacts (e.g. Test *C*). Test *B* appears close to the wave impacts region, but has a high wave steepness. During this test the waves tended to break offshore.

Beyond $d_t/H_b > 2.25$ the water depth is sufficient to reduce wave breaking to a minimum and produce pulsating conditions (e.g. Tests *D* & *E*). In turn the toe scour depth is significantly reduced, and the potential for toe accretion under reflective wave transport increased. Waves in this range would also be limited by their wave offshore steepness, though no tests were available to confirm this.

**Summary**

Figure 7-5 represents a first step towards processes based scour prediction for seawalls. To develop the scour risk envelope further, field or flume experiments using video analysis of the surf zone and resulting wave impacts are required to confirm the nearshore wave steepness at the structure and how wave reflections affect this process. These would enable the boundaries between each wave breaker type to be defined more precisely and clarify the breaker conditions for a wider range of wave and beach types. Figure 7-5 can be applied to demonstrate the key toe scour processes and estimate the risk of scour for a range of conditions.

## 7.3. Application to prototype examples

### 7.3.1. Effect of tidal range on maximum scour

The depth of toe scour was investigated for a hypothetical seawall scour problem at Blackpool. Characteristic spring and neap tides, wave period and the maximum wave height from the field deployment dataset were used ($H_0$ = 3.5 m, $T_m$ = 6 s, Figure 7-6). In the examples, the difference in tidal range and duration was found to significantly affect the water depth at the toe of the seawall and hence the maximum toe scour depth.

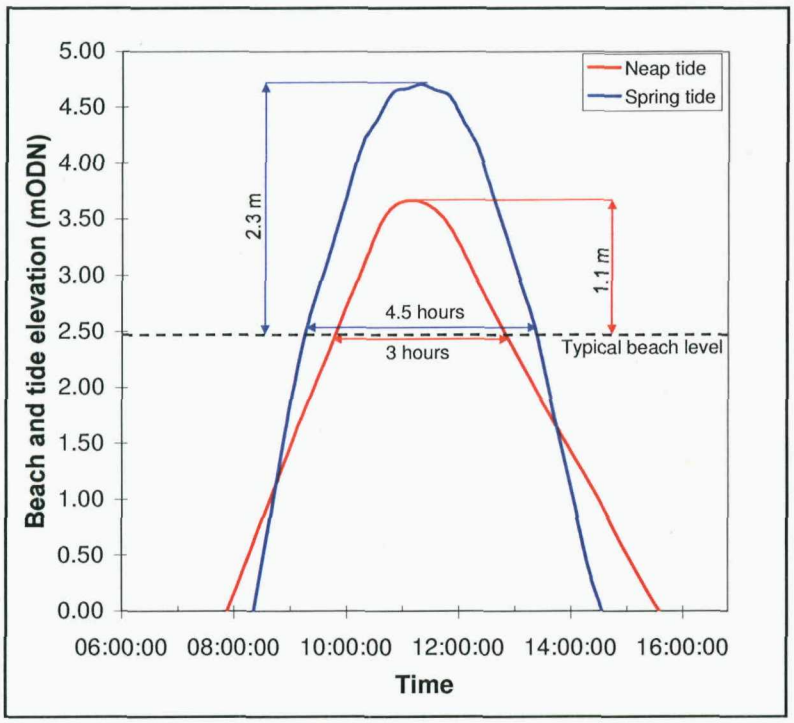


**Figure 7-6: Effect of tidal range on seawall toe water depth**

In the spring tide example, at the peak tidal height the waves are depth limited to a maximum height of 1.8 m at the wall and $d_t / L_m = 0.04$. However during the rise and fall of the tide the toe water depth is reduced to $0.01 < d_t / L_m < 0.035$, leading to a greater risk of scour. Fortunately these conditions only occur for an hour or approximately 600 waves either side of high water, far short of the 3000 waves used to in the flume to determine the maximum scour depth. Based on Equations 5.4 & 5.5, and the depth limited wave height, the maximum toe scour would be limited to 0.86 m ($S_t / H_0$ =0.48) at the high tide. Due to the limited duration of high tide and the rapid transition through the region of highest scour risk, scour is unlikely to achieve this

depth. Furthermore the increased water depth at high tide may induce slight infilling of the scour hole.

In the neap tide example, despite the tidal range being significantly reduced, the wall remains in the range $0.01 < d_t / L_m < 0.035$ throughout the tide for a single period of 2 hours. Based on equations 5.4 & 5.5 and the depth limited wave height at high tide (0.86 m), a scour depth of 0.96 m ($S_t / H_0 = 1.1$) is predicted. Though a similar scour depth to the spring tide example, in this case the wall is continuous exposed to approximately 1200 impacting waves, increasing the risk of maximum toe scour occurring, with no potential for infilling at high tide. The calculations show that under these design conditions, toe protection should be provided to a depth of at least 0.9 m, though an appropriate factor of safety would also need to be included.

The example demonstrates that seawalls exposed to wave impacts under neap tide conditions, or locations with very small tidal ranges (e.g. the Mediterranean Sea) would be at greater risk of scour erosion and failure then regions of large tidal range. This would be most severe where the water depth in front of the structure was equal to the typical storm wave height. The 'exposure risk' concept is explored in Section 7.3.3.

### 7.3.2. Detailed analysis of wave breaking and scour for specific events

To illustrate the type of wave breaking and resulting scour risk for a 1:30 sand beach, Figure 7-5 was applied to a series of prototype conditions (Table 7-2). In the examples, four toe water depths were tested, with an offshore wave height of either 3 or 5 m for a fixed mean wave period of 8 s.

**Table 7-2: Comparison of scour depth and breaker types**

| | $H_0$ | $d_t$ | $L_o$ | $H_b$ (max) | $d_t / H_b$ | $H_0/L_0$ | $S_t/H_b$ | Breaker |
|---|---|---|---|---|---|---|---|---|
| *A* | 3 | 1.5 | 100.0 | 0.7 | 2.05 | 0.03 | 0.36 | Spilling |
| *B* | 3 | 3 | 100.0 | 1.4 | 2.17 | 0.03 | 0.64 | Impact |
| *C* | 3 | 6 | 100.0 | 2.5 | 2.40 | 0.03 | 0.00 | Pulsating |
| *D* | 5 | 5 | 100.0 | 2.3 | 2.22 | 0.05 | 0.34 | Spilling impact |

In example *A*, the waves are limited by the toe water depth and the toe scour risk is moderate ($S_t = 1.1$ m). The increased water depth in example *B* leads to severe wave impacts, which when combined with the low wave steepness, significantly increases the risk of toe scour ($S_t = 2.0$ m)

For example *C*, the water depth was increased further, producing a pulsating wave / structure interaction, this significantly reduces the risk of scour ($S_t$ = 0 m). In the final example, *D*, the wave height and toe water depth were increased to maintain the same $H_0 / d_t$ ratio offshore. However in the nearshore these conditions are less affected by wave shoaling, leading to an increase in wavelength but only a comparatively small increase in wave height. As a results the wave steepness increases, leading to a spilling impact and slightly reduced toe scour depth ($S_t$ = 1.7 m). Despite producing less intense wave breaking which would suggest a decrease in scour, the correlation of scour depth to incident wave height, causes the scour depth to be greater then might otherwise be expected.

### 7.3.3. Link to wave impact, pressure and overtopping research

In placing the scour risk envelope and the wave breaking results into to context with the other seawall failure mechanisms, similarity was found with recent research into wave impact and downfall pressures and wave overtopping. These also produce a 'peak envelope' at mid water depths, not at the maximum as previously expected.

The results of Allsop *et al.*(2005), show that wave overtopping volumes peak when waves wash over the structure and when plunging waves break directly onto the structure, but are reduced under spilling and pulsating conditions. This concurs with large scale flume experiment at the GWK, Germany, where wave downfall pressures were found to be highest when near impacting wave conditions occurred at a vertical wall structure (Walters *et al.* 2005). Furthermore, in a parameter map developed as part of the MAST *PROVERBS* project, using physical model tests by Oumeraci and Kortenhaus (1999), the highest wave impact loads were mapped to occur when $0.35 < H_0 / d_t$, and large plunging waves could hit the structure.

These similarities were pulled together and contrasted in the authors joint paper with Müller *et al.* (2007), and suggest a significant step change is required in the examination of risk to coastal structures, which tends to assume a combination of the maximum wave height and maximum tide or surge, cause the most extreme conditions. The paper suggests that the duration of exposure to these conditions is more relevant then those where the highest wave heights and water depths occur.

The 'scour envelope' concept represents a first step toward developing an Iribarren type equation for the prediction of wave breaker type in front of shallow water coastal structures. Further model testing and field validation is required to incorporate a wider range of wave conditions, beach slopes and structure types to develop this concept and produce more detailed predictions. The concept should be extended to determine its validity in predicting the wave breaker type for peak overtopping volumes and wave impact pressures.

## 7.4. Application to seawall design

Today seawalls are typically constructed with a smooth vertical face, with either a straight or recurved crest at the top of the wall, as shown in Figure 7-7. By applying the seawall toe scour envelope, the risk of scour can be reduced by optimising the design of new seawalls and protection measures for existing structures. A range of novel scour protection and mitigation measures are presented in Figure 7-8 and discussed below.

**Figure 7-7: Seawall with small recurve, Newton's Cove Coastal protection scheme, Weymouth, completed 2004 (NCE, 2004)**

### 7.4.1. Protecting existing structures

The simplest method of reducing scour risk would be to provide a wide beach to dissipate wave energy. This would require the seawall to either be moved inland or the existing beach to be artificially nourished. Where this is not feasible the construction of a rock berm further offshore on the beach profile may be sufficient to induce wave breaking. However defining the correct berm elevation is difficult in tidal regions.

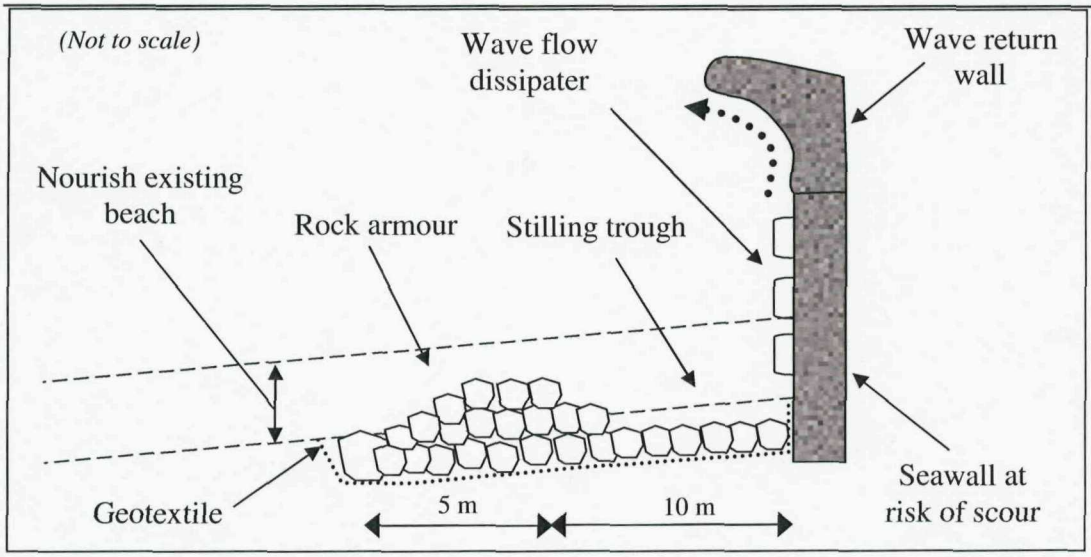


**Figure 7-8: Seawall scour risk mitigation and protection methods**

### 7.4.2. Structural options

At the structure an irregular wall facing or compound wall shape could be provided to aid wave flow dissipation and break up high velocity jets. These would reduce the wave downrush and scour risk, but would require robust construction and a significant void ratio to have any effect on scour.

In the past wave return walls have been constructed at the crest of seawalls to reduce the volume of overtopping (Thomas & Hall, 1992). The principle could be developed using a parabolic shape to eject the wave uprush flow seaward, reducing wave down rush flows and scour. This would require careful investigation to prevent increased overtopping and potential flooding when the wind is directed onshore. Furthermore to install a wave return wall post construction would be quite difficult, as the structure would require substantial reinforcement and ties to resist the large forces associated with the high velocity wave flows.

#### Rock aprons

When an existing seawall requires immediate protection, a rock apron is often placed at toe of the wall (Whitehouse, 1998). Based on the experimental results in this study and the limited rock armour tests reported in Sutherland *et al.* (2006), it would be expected that rock toe armour would aid in the dissipation of wave downrush flows, reducing the risk of sediment transport and scour. However if the apron was too short, the flow may be directed towards the apron toe, creating a new scour problem. The rock must also be

of a suitable weight to resist movement under the highest velocity wave downrush flows. Based on the hydraulic flow study, and Froude scaling, this could be in the region of 4 $m.s^{-1}$ or greater at the wall toe.

An alternative remedial solution, using a smaller quantity of rock, would be to construct a scour apron in a similar profile to scour Test *C*. This would include a stilling trough at the seawall toe to absorb the wave downrush and a berm offshore to induce earlier breaking. This configuration would also provide additional support and protection to prevent rotational failure. However this configuration would come at a high cost to the amenity use of the beach, unless there was sufficient beach material for the summer beach profile to accrete and cover the revetment.

### 7.4.3. Novel approach to future sea level rises

Looking ahead to the next century, if accelerated sea level rise occurs as predicted, seawalls protecting critical infrastructure, which cannot be relocated, will come under increasing risk of toe scour as beach levels fall. A more radical solution to avoid breaking wave impacts would be to move seawalls offshore into deeper water. This would promote reflective wave conditions which are less likely to scour, and would be more prudent then constructing larger seawalls with toe armour further inshore. Determining the optimal position for these structures would require a balance between the risk of large unbroken waves, the increased expense of building structures in deep water and the cost of providing increasingly deep toe protection measures. This would only be an option for the most critical infrastructure, in regions of limited fetch length.

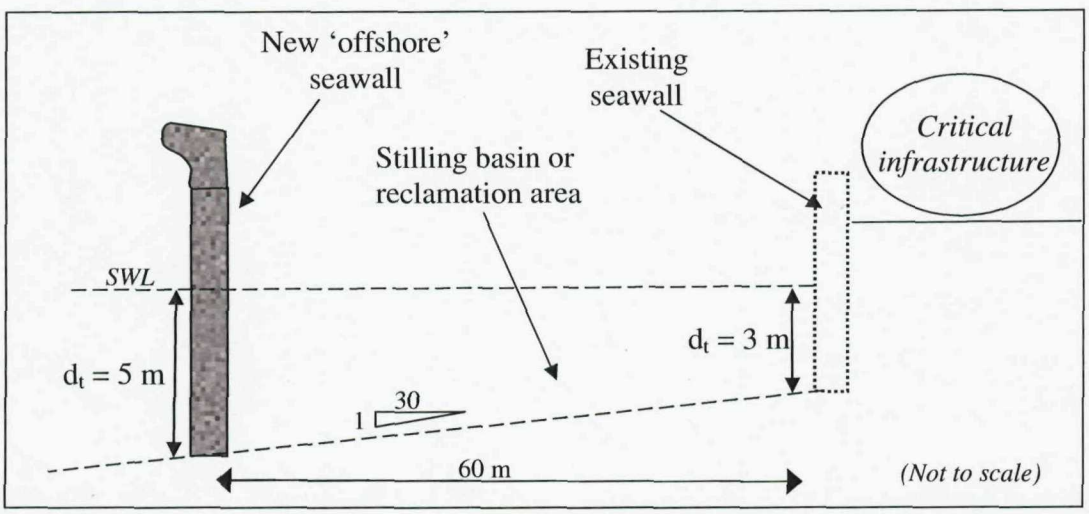


**Figure 7-9: Radical approach to protecting critical infrastructure**

# 8. Conclusions

## 8.1. Hypothesis response

*"Through a unique combination of sediment and hydraulic flow experiments, an improved understanding of wave flows at seawalls and the resulting scour was achieved. By combining knowledge of the near wall wave breaker type, flow pattern and sediment response, improved methods to predict scour risk and magnitude were demonstrated and potential mitigation measures suggested."*

## 8.2. Existing knowledgebase

- The literature review determined that existing studies into seawall scour have relied predominantly on small scale sediment transport tests which are prone to scale effects;
- The scour process has been speculated to result from flows generated by breaking waves, causing sediment suspension. This process had not been visualised or measured in detail at vertical seawall structures;
- Field evidence of seawall toe scour was found to limited to mostly anecdotal reports and opportunist photographs;
- More recent medium scale tests have overcome the key scaling issues, but scour depth guidance remains limited to empirical equations fitted to these datasets. These do not cover the full range of conditions expected;
- A process based scour prediction model does not exist for seawalls structures.

## 8.3. New evidence

- Through a series of field experiments, continuous measurements of beach level and toe scour were obtained at a vertical and 1:2 sloping seawall for the first time. These confirmed the magnitude of scour and the transient nature of the scour process, which often leads to infilling with the falling tide or wave height;
- By conducting both sediment transport tests and analysing a sub set of these experiments in a hydraulic flow study using PIV, this research is the first to demonstrate a causal relationship between wave breaking and the risk of toe scour at seawalls;

- By defining the concept of 'net drift' in the PIV experiments, the resultant direction of sediment transport as a result of incident and reflected waves, and flows associated with wave breaking, was successfully measured;
- Breaking waves which impact onto a seawall were found to produce the deepest scour. These generated high velocity downrush flows and intense vortices at the wall toe following impact, which persisted following wave reflection;
- The flows velocities were reduced under spilling and pulsating wave conditions and when the water depth was increased. This reduced the toe scour depth;
- In a 1:40 scale model, a peak downrush velocity of 60 $cm.s^{-1}$ was measured close to the seawall toe and followed a breaking wave impact. Near the water surface, downrush flows velocities were greater (c. 80 $cm.s^{-1}$). However these could only be inferred from particle streak lengths. These high flow velocities have the potential to remove blockwork facings or undersized toe rock armour;
- By analysing a fixed scoured beach profile, the increased water depth associated with scour was found to absorb the energy of wave downrush flows and reduce the velocity of near bed flows. It would be expected that the toe scour would continue until equilibrium is restored at the wall toe. This could not be confirmed in the hydraulic tests, due to the beach profile representing the average effect of the irregular waves modelled in the sediment transport tests.

## 8.4. Scour prediction

- Statistical equations were fitted to the sediment transport results, and validated using a unique series of field experiments. The equations are the first to unify the approaches of Xie (1981) and Fowler (1992), enabling probabilistic and deterministic prediction for a range of incident deep water wave conditions, including the range $0.03 < d_t / L_p < 0.06$;
- The predicted toe scour depth (deterministic) peaked at $0.016\ d_t / L_p$ ($S_t / H_0 = 0.80$) with an upper predicted limit of $S_t / H_0 = 0.96$;
- In both the field and sediment transport experiments, the scour depth remained less then the incident significant wave height;
- Equations 5.4 & 5.5 are recommended for the probabilistic prediction on mean toe scour at a vertical seawall. Equations 5.11 & 5.12 are recommended for determining the upper limit for toe scour at a vertical seawall and tentatively suggested for 1:2 sloping seawalls. The equations are limited to sand beaches with a gradient between 1:15 and 1:75 and conditions where $-0.015 < d_t / L_m < 0.12$.

## 8.5. Scour risk guidance and wave breaker prediction

- To provide informed toe scour guidance, the hydraulic flow and sediment transport results were unified to develop a 'scour envelope' diagram, where the wave breaker type and resulting scour risk can be conceptualised;
- The development of a scour risk envelope takes forward the current approach, where waves are only considered to be depth limited, and includes the nearshore wave steepness and breaking wave height. This provides a first step in developing a processes based scour predictor and significantly improves our ability to understand the conditions leading to enhanced scour risk;
- The parameters $H_0/L_p$ and $d_t/H_b$ were found to correlate to the magnitude of wave breaking and scour depth. Unbroken incident low steepness waves reaching a depth limited condition at the seawall ($d_t/H_b = 0.215$ & $H_0/L_p < 0.025$) were found to generate the most intense impacts and deepest scour.
- Spilling waves were associated with shallow toe water depths and steep waves, which reduced the toe scour depth;
- When $d_t/H_b$ is > 2.25, reflected wave processes become dominant and the risk of toe scour is significantly reduced;
- The scour envelope and predictions equations significantly extend the ability of coastal engineers and managers to make informed decisions regarding toe scour risk.

## 8.6. Application to practice and improved design

- Through key examples the risk of scour was demonstrated for a range of conditions and demonstrated identified that the highest risk of scour was not necessarily associated with the highest waves and water levels, but with the duration of exposure to the most critical conditions. This has spawned new research into the 'exposure' of coastal structures to wave processes;
- Novel scour mitigation methods were developed, which suggest a 'stilling' region at the wall could be used to absorb wave downrush flows, or that a re-curve seawall may deflect uprush wave flows offshore, reducing the risk of scour;
- Alternatively where critical infrastructure is at risk of long term sea level rise, a more radical approach would be to reposition seawalls further offshore, increasing the toe water depth and reducing the scour risk through wave reflection.

## 8.7. Future research requirements

- Though field evidence of toe scour has been successfully collected, further experiments, with a wide range of beach types, tidal ranges and structures is required. Ideally real-time beach level and velocity measurement should be collected across the beach profile and supported by local tide and wave measurements;
- Field measurements of wave steepness, breaking waves character and waves impacts are required to validate the scour risk envelope concept and confirm the results of the physical model studies;
- Additional sediment transport tests are required at full and medium scale to explore the effect of wave height on the scour processes. These tests should include a plainer beach slope to enable repeatable measurement, and comparison to this study. Full scale model test would enable concerns regarding scale effects to be explored;
- Further hydraulic modelling of the interaction of breaking waves and seawalls is required. This should utilise PIV measurements with a frame rate of at least 200 fps and examine the use of bubble PIV techniques to obtain measurement at the point of wave impact and during the high velocity downrush;
- By combining the field and physical model experiments, the scour processes can be investigated in greater detail to improve the definition of the scour risk envelope concept. Once the key scour processes are understood, numerical modelling techniques can be developed to provide validated scour predictions.

# 9. References


Adrian, R.J. (1991). Particle-imaging techniques for experimental fluid mechanics. *Annual Review Fluid Mechanics*, 23, p261-304.

Allsop, N.W.H., Bruce, T, Pearson, J. and Besley, P. (2005). Wave overtopping at vertical and steep seawalls, *Proc. ICE Maritime Eng.*, 2005, 158, September Issue, 103-114.

ASCE. (2003). Surf zone hydrodynamics. In *Coastal Engineering Manual*, Chapter II-4-3, Engineering manual: 1110-2-1100 (Part II), July 2003. Headquarters, US Army Corps of Engineers, Washington, USA.

ASCE. (2006). Scour and Scour Protection. In *Coastal Engineering Manual*, Chapter VI-5-6, Engineering manual: 1110-2-1100 (Part VI), June 2006. Headquarters, US Army Corps of Engineers, Washington, USA.

Barnett, M.R. (1987). *Laboratory study of the effects of a vertical seawall on beach profile response. Report 87/005*, Coastal and Oceanographic Engineering Department, University of Florida, Gainsville, FL.

Barnett, M. & Wang, Hsiang. (1998). Effects of vertical seawall on profile response. *Proceedings of the 21st Coastal Engineering Conference*, ASCE, p1493-1507.

Battjes, J.A. (1974). Surf similarity. *Proceedings of the 14th Coastal engineering conference*. June 24-28 1974. Copenhagen, Denmark. ASCE. p266-479.

Bettess, R. (1990). Survey of lightweight sediment for use in mobile bed physical models. Chapter in: *Movable bed physical models*. Kluwer Academic Publishers, Netherlands, p115-123.

Bruun, P. (1962). Sea level rise as a cause of shore erosion. *Journal of Waterways Harbours Division,* 88, p117-130.

Calabrese, M. (1998) Onset of breaking in front of vertical and composite breakwaters. Proceedings of the 8th International Offshore and Polar Engineering Conference, Montreal Canada. May 24-29 1998. Vol III, p590-595.

Chesnutt, C.B & Schiller, R.E (1971). *Scour of simulated Gulf Coast sand beaches due to wave action in front of sea walls and dune barriers.* COE Report No.139, TAMU-SG-71-207. Texas A&M University, College Station, TX.

CIRIA. (1986). *Seawalls: Survey of performance and design practice*. Tech Note 125, ISBN 086017 266X, CIRIA, UK.

Clark, R.R. (2005). Impact of the 2004 North Atlantic Hurricane Season on the Coast of Florida. *Shore and beach*, 73, No 2 & 3. p2-9.

Cooker, M.J. & Peregrine, D.H. (1990). Violent water motion at breaking-wave impact. *Proceedings of the twenty second Coastal Engineering conference*, Delft, Netherlands. Ed B.L Edge. Vol 1, p165-176.

Dean, R.G. (1977). *Equilibrium beach profiles: U.S. Atlantic and Gulf Coasts.* Department of Civil Engineering, Ocean Engineering Report No. 12, University of Delaware, Newark.

Dean, R.G. (1985).Physical modelling of littoral processes. In:*Physical Modelling in Coastal Engineering*. ed: R.A. Dalrymple. Taylor & Francis New York, USA. 276pp.

Dean, R.G. (1986). Coastal Armouring: Effects, principles and mitigation. *Proceedings 20th Coastal Engineering Conference, American Society of Civil Engineers*, p1843-1857.

Defra (2001).*Shoreline management plan – a guide for coastal protection authorities.* Defra Publications, London. Ref: PB5519.

Fowler, J.E. (1992). *Scour problems and methods of prediction of maximum scour at vertical seawalls.* Report CERC-93-8. U.S Army Corps of Engineers, Waterways Experiment Station, 3909 Halls Ferry Road, Vicksburg, MS.

French, P.W. (2001). Coastal defences- processes, problems, and solutions - Chapter 3 in *Seawalls & Revetments*. Routledge Publications, UK, London. pp362

Gao, X. & Inouchi, K. (1998). The characteristics of scouring and deposition in front of vertical breakwaters by broken waves. *Coastal Engineering Journal.* Vol 40, No1, p99-113.

Goda, Y (2000). Random sea and design of maritime structures. World Scientific, Singapore 443pp.

Griggs, G.B, Tait, J.F & Corona, W. (1994). The interaction of seawalls and beaches: Seven years of monitoring, Monterey Bay, California. *Shore and beach* 62(3) p21-28.

Hanson, H. & Kraus, N.C. (1989). *GENESIS: Generalised model for simulating shoreline change. Report 1:Technical Reference.* Tech Report: CERC-89-19. US Army Engineer Waterways Experiment Station, Coastal Engineering Research Centre, Vicksbury Miss.

Herbich, J.B & Ko, S.C. (1968). Scour of sand beaches in front of seawalls. *Proceedings of 11th Coastal Engineers conference*, London, UK, Vol1, p 622-633.

Holman,R.A & Sallenger, A.H. (1985). Set-Up and Swash on a Natural Beach. *Journal of Geophysical Research* 90 (C1) p945-953.

Hotta S, Marui, N (1976). Local scour and current around a porous breakwater. *Proceedings 15th International Conference*, Honolulu, Hawaii, ASCE Vol 2. p1590-1604.

HR Wallingford. (2001). *COAST3D Final Volume- Paper B4.1, COSMOS modelling and the development of model performance statistics.* Report TR121, HR Wallingford, UK.

HR Wallingford. (2005). *Understanding the Lowering of Beaches in front of coastal defence structures, Scour monitor deployment at Blackpool.* HR Wallingford Technical Note CBS0726/04.

HR Wallingford (2006). *Understanding the Lowering of Beaches in front of coastal defence structures- Phase 2.* Medium scale 2D physical modelling tests of scour at a sea wall. HR Wallingford Technical Note CBS0726/06.

HR Wallingford (2006a). *Understanding the Lowering of Beaches in front of coastal defence structures- Phase 2.* Improved predictors for wave-induced scour at seawalls. HR Wallingford Technical Note CBS0726/09.

HR Wallingford. (2007). *2D bed profiling system for physical models.* Internet: from: http://www.hrwallingford.co.uk/index.aspx?facets=equipment (page accessed 01/07/07).

Hsu, J.R.C & Silvester,R (1989). Model test results of scour along breakwater. J.*Waterway, Port, Coastal Ocean Engineering*, American Society Civil Engineers, 115, 1, p66-85.

Hughes, S.A. & Fowler, J.E. (1991). Wave-induced scour prediction at vertical walls. *Proceedings Coastal Sediments 1991*, ed. Kraus N.C. Vol 2 , p1886-1900.

Hughes, S.A. (1993). *Physical model and laboratory techniques in coastal engineering*, World Scientific Publishing, London.

Ichikawa, T. (1967). Scouring damages to vertical breakwaters of Tagonoura Port. *Coastal Engineering in Japan*, Vol 10 p95-108.

Institution of Civil Engineers-(ICE). (1985). *Coastal Engineering Research.* Thomas Telford, London. p21.

Irie, I. & Nadaoka,K. (1984). Laboratory reproduction of seabed scour in front of breakwaters. *Proceedings of 19th Coastal Engineers conference*, 1984, Houston, Texas, edited by B.L Edge, ASCE, Vol II, p1715.

Kamphuis, J.W. Rakha,K.A. Jui, J. (1992). Hydraulic model experiments on seawalls. *Proceedings of the twenty-third international conference on Coastal Engineering*, (ed.B.L.Edge), New York: American Society of Civil Engineers. 3516pp.

Karambas, TH.V., Koutandos, E., Kampanis, N. (2007). ALS - A coastal engineering model for wave propagation, wave structure interaction and bed morphology evolution. *Proceedings of 32nd Congress of IAHR* 1-6th July 2007, Venice, Italy. ed Silvio,G & Lanzoni, S, Corila [CD-ROM]. Paper 887.

Keane, R.D. & Adrian, R.J. (1990). Optimization of particle image velocimeters – Part 1: Double pulsed systems. *Measurement science technology*, 1. p1202-1215.

Komar, P.D (1998). *Beach processes and sedimentation.* Prentice-Hall International (UK), London.

Komar, P.D. & Gaughan, M.K. (1972).Airy wave theory and the breaker height prediction. Proceedings of the 13th International coastal engineering conference, Vancouver, Canada, July 1972. ASCE. p405-418.

Kraus, N.C. (1988). The effect of seawalls on the beach: An extended literature review, *Journal of coastal research*, SI4, p1-28.

Kraus, N.C,. Pilkey, O.H ed's (1988). The effects of seawalls on the beach. *Journal of Coastal Research*, Special edition, Issue 4. The Coastal Education and Research Foundation (CERF),Charlottesville, USA.

Kraus, N.C. Smith, J.M. & Sollitt, C.K. (1992). SUPERTANK laboratory data collection project. *Proceedings of the 23rd Coastal Engineering Conference*, ASCE, p2191-2204.

Kraus, N.C. and Smith, J.M- editors. (1994). *SUPERTANK Laboratory data collection project. volume 1: Main text.* Technical report CERC-94-3, US Army Corps of Engineers Waterways Experiment Station, Coastal Engineering Research Center, Vicksburg. Mississippi, USA.

Kraus, N.C,. McDougal, W.G. (1996). The effects of seawalls on the beach. Part I, An updated literature review. *Journal of Coastal Research*, Vol 12, 3, pp691-701.

Larson, M., & Kraus, N. C. (1989). *SBEACH: Numerical model for simulating storm-induced beach change.* Report 1: Empirical foundation and model

development, " Technical Report CERC-89-9, U.S. Army Engineer Waterways, Experiment Station, Coastal Engineering Research Center, Vicksburg, MS.

Lee, G-H, Nicholls, R.J, Birkemeier, W.A. (1998). Storm-driven variability of the beach-nearshore profile at Duck, North Carolina, USA, 1981-1991. *Marine Geology* 148, p163-177.

Loveless, JH (1994). Modelling Toe Scour at Coastal Structures. *Proceedings, 2nd International Conference on Hydraulic Modelling.* p479-492, London Mechanical Engineering Publications.

Loveless, J.H and Grant, G.T (1995). Physical modelling of scour at coastal structures, *Proceedings XXVIth Congress of IAHR,* 11-15 Sept 1995, HYDRA 2000, London, Vol.3, p293-298.

Loveless, J.H., Grant, G.T, Karlsson, R.I (1996). The effect of groundwater on scour near structures. *Proceedings of 25th Coastal Engineers conference,* Orlando, Florida. Edited by B.L Edge, ASCE, Vol. 2, p2152-2165.

McCowan, J. (1891). On the Solitary Wave. *Philosophical Magazine,* 5th Series, Vol 36, pp 430-437.

McDougal, W.G., Kraus, N.C,.& Ajiwibowo, H. (1996). The effects of seawalls on the beach. Part II, numerical modelling of SUPERTANK seawall tests. *Journal of Coastal Research,* Vol 12, No 3, pp702-713.

McInnes, R.G. (2003). *Coastal Defence -A non technical guide-* Standing Conference on Problems associated with the coastline (SCOPAC), Ventnor. Cross Publishing, Chale UK.

Miles, J.R. Russell, P.E and Huntley, D.A. (2001). Field measurements of sediment dynamics in front of a seawall. *Journal of coastal research* 17 (1) p195-206

Miller, R.L. (1972) The role of surface tension in breaking waves. *Proceedings of the 13th International coastal engineering conference.* Vancouver, Canada, July 1972. ASCE. p433-449.

Müller,G., Allsop,W., Bruce,T., Kortenhaus, A., Pearce,AMC., Sutherland, J., (2007). The occurrence and effects of wave impacts. *Proc ICE Maritime Engineering.* (Submitted and accepted July 2007).

Nairn, R.B. & Southgate, H.N. (1993). Deterministic profile modelling of nearshore processes: Part 2. Sediment transport and beach profile development, *Coastal Engineering* 19, p57-96.

NCE. (2006). Winner: Netwons cove coastal protection scheme, Weymouth. *New Civil Engineer magazine.* 15/10/04, p25.

O'Donoghue, T & Goldsworthy, C.J. (1995). Nearbed velocities in front of seawalls. *Proceedings XXVIth Congress of IAHR,* 11-15 Sept 1995, HYDRA 2000, London, Vol.3, p311-316.

Oumeraci, H., Klammer, P., Partenscky, H.W. (1993) Classification of breaking wave loads on vertical structures. *Journal of waterway, port, coastal and ocean engineering. Vol 119, No.4.* p381-397.

Oumeraci, H., & Kortenhaus, A. (eds) (1999). *Final report: probabilistic design tools for vertical breakwaters.* MAST III, PROVERBS-Project: Probabilistic Design Tools for Vertical Breakwaters, Vol. I, Braunschweig, Germany.

Pearce, A.M.C., Sutherland, J., Obhrai, C., Müller, G. and Whitehouse, R., (2006). Scour at a seawall – field measurements and physical modelling. *Proceedings, 30th Int' Conf, Coastal Engineering*, 2006, San Diego, USA. Vol 3, p2378-2390.

Peregrine, D.H., Bredmose, H., McCabe, A., Bullock, G., Obhrai, C., Müller, G. & Wolters, G. (2004). Water wave impact on walls and the role of air. *Proceedings 24th Coastal Engineering conference*, National Civil Engineering Laboratory, Lisbon, Portugal, 19 – 24 September 2004. Ed J.M Smith. ASCE. Vol 4, p4005-4017.

Powell, K. & Whitehouse, R.J.S. (1998). The occurrence and prediction of scour at coastal and estuarine structures. *33rd MAFF Conference of River and Coastal Engineers*, 1-2 July 1998. Keele University, UK. p 3.3.1-3.3.13.

Powell, K.A & Lowe, J.P. (1994). The scouring of sediments at the toe of seawalls. In *Proceedings of the Hornafjordur International Symposium*, Iceland -June 20-24. Edited by Gisli Viggosson, pp749-755.

Rakha, K.A. & Kamphuis, J.W. (1993). Wave setup near a seawall: experiments and a numerical model. *Proceedings Ocean wave measurement and analysis*, 2nd Intl Symposium, 25-28 July 1993, New Orleans. Ed O.T. Magoon and J.M Hemsley, ASCE New York. p835-848.

Rakha, K.A. & Kamphuis, J.W.(1997). Wave-induced currents in the vicinity of a seawall. *Coastal Engineering* 30, (1-2), p23-52.

Russell, P.E. (1993). Mechanisms for beach erosion during storms. *Continental shelf research*, Vol 13, No11, p1243 – 1265.

Russell, R.C.H. & Inglis, C. (1953). The influence of a Vertical Wall on a Beach in Front of it *Proceedings of the Minnesota International, Hydraulics Convention*, American Society of Civil Engineers, pp. 221-226.

Ryu, Y., Chang, K-A., Lim H-J. (2005). Use of bubble image velocimetry for measurement of plunging wave impinging on structure and associated greenwater. *Meas. Sci. Technol.* 16. p1945–1953.

Sato,S., Tanaka, N., Irie,I. (1968). Study on scouring at the foot of coastal structures. *Proceedings of 11th International Coastal Engineers conference*, London, UK, Vol1, p579.

Seaman C.R & O'Donoghue, T. (1996). Beach response in front of wave-reflecting structures. *Proceedings of the Twenty-fifth International Conference* held in Orlando, Florida, September 2-6, 1996. Ed B.L Edge. Chapter 177, p2284-2297.

Silvester, R. & Hsu, J.R.C.(1997). *Coastal Stabilization*. World Scientific, 578pp ISBN 98 1023 1547.

Silvester, R. (1986). The influence of oblique reflection on breakwaters. *Proceedings of 20th Coastal Engineers conference*, 9-14th November, Taipei, Tawain. Edited by B.L Edge, ASCE, Vol III, p2253.

Song, W.O & Schiller, R.E. (1977). *Experimental studies on beach scour due to wave action.* Texas A&M University, CoE Report No:166. TAMU-SG-73-211.

Soulsby, R. (1997). *Dynamics of marine sands*. Thomas Telford, London, England. 272pp.

Sumer, B M,. Fredsøe, J. (2000). Experimental study of 2D scour and its protection at a rubble-mound breakwater. *Coastal Engineering*, Vol 40, Issue 1, p5-87, Elsevier Science, UK.

Sumer B.M., Fredsøe, J. (2002). *The Mechanics of Scour in the Marine Environment* (Advanced Series on Ocean Engineering:17). World Scientific Publishing, London, 550pp.

Sutherland, J., Brampton, H., Motyka, G., Blanco, B. and Whitehouse, R.(2003). *Beach lowering in front of coastal structures, research scoping study.* Defra R&D Technical Report FD1916/TR1. ISBN 0-85521-163-6. Available from http://sciencesearch.defra.gov.uk (page accessed 27/06/2007).

Sutherland, J., Obhrai, C., Whitehouse, R.J.S. and Pearce, A.M.C. (2006). Laboratory tests of scour at a seawall. *Proceedings, 3rd Int Conf Scour and Erosion*, Amsterdam. A,A, Balkema, CD-ROM.

Thomas, R.S. & Hall, B. (1992). *Seawall Design.* CIRIA Publications. Butterworth-Heinemann, Oxford, UK. 359pp.

Toue, T. & Wang. H. (1990). Three dimensional effects of seawall on adjacent beach. *22nd Coastal Engineering Conference.* The Netherlands, ASCE Vol 3, Chapter 211, pp2782-2795.

Tsai, C.P, Wang, J.S, Lin,C. (1998). Downrush flows from waves on sloping seawalls. *Ocean Engineering*, Vol 25, No4-5, p295-308, Elsevier Science, UK.

Whitehouse RJS (1998). *Scour at marine structures. A manual for practical applications.* Thomas Telford, 216pp. ISBN 07 277 26552

Wolters, G., Müller, G., Bruce, T. and Obhrai, C. (2005). Large scale experiments on wave downfall pressures, *Proc. ICE Maritime Eng.*, 2005, **158**, Issue MA4, 137-145.

Wright, L.D. & Short, A.D. (1984). Morphodynamic variability of surf zones and Beaches: A synthesis. *Marine Geology*, 56 p93-118.

Xie, S-L. (1981). *Scouring patterns in front of vertical breakwaters and their influence on the stability of the foundations of breakwaters.* Thesis report, Department of Civil Engineering, Delft University of Technology, The Netherlands, September, 1987.

# 10. Bibliography

ASCE. (2000). *Hydraulic Modeling: Concepts and Practice.* Manuals and Reports on Engineering Practice No. 97. American Society of Civil Engineers, USA. 408pp.

Beach, R.A & Sternberg, R.W (1992). Suspended sediment transport in the surf zone: response to incident wave and longshore current interaction. *Marine Geology,* 108 p275-294.

CIRIA (1996). *Beach Management Manual.* Ciria Report 153, edited by JD Simm, AH Brampton, NW Beech, J.D Brooke, CIRIA, London, UK.

Dalrymple, R.A (ed's) (1985). *Physical Modelling in Coastal Engineering.* Taylor & Francis New York, USA. 276pp.

Gonzalez, R.C., Woods,R.E., Eddins.S.L (2004). *Digital image processing using MATLAB.* Pearson/Prentice Hall, Upper Saddle River, NJ, USA. 609pp.

Grant.I. (1997). Particle image velocimetry: a review. *Proceedings Institute of Mechanical Engineers,* Vol 211, Pt C, p55-76.

Graw, K., and Lengricht, J. (2002). Particle image velocimetry (PIV) in coastal engineering. *1st German-Chinese join Symposium on Coastal and Ocean Engineering.* April 10-12, Rostock Germany.

Gray, C., Greated, C.A., Easson, W.J., Fancey, N.E. (1987) The application of PIV to measurements under water waves. *2nd International Conference on Laser Anemometry - Advances and Applications.* 21-23rd Sept 1987. Strathclyde, UK. Paper 15, p281-287.

Griggs, G.B., Moore, L.J., Tait, J.F., Scott,K., Pembrook, D. (1996). The effects of the Storm waves of 1995 on beaches adjacent to a long-term seawall monitoring site in Northern Monterey bay, California. *Shore and beach,* 64, p339-341.

Hughes, S.A. (1992). Estimating wave-induced bottom velocities at vertical wall. *Journal of waterway, port, coastal and ocean engineering.* Vol 118, No.2. March/ April 1992.

Lengricht, J., Kaldenhoff, H., Graw, K-U. (1994). Measuring wave-induced turbulence near structures. *Proceedings of the international symposium: waves - physical and numerical modelling,* Volume 1, (ed.M.Isaacson & M.Quick). Vancouver: University of British Columbia, Department of Civil Engineering. pp.80-89.

Melville, W.K. Veron, F. White, C.J (2002). The velocity field under breaking waves: coherent structures and turbulence. *Journal of Fluid Mechanics,* 454 p203-233.

Müller, G & Whittaker T.J.T (1994) The influence of seabed slope on wave impact pressures. *Underwater technology,* Vol 20, No 3 p 14-22.

Oumeraci, H (1994). Review and analysis of vertical breakwater failures- lessons learned. *Coastal Engineering,* 22, 1-2, p3-29.

Pearce, A.M.C. (2005). *The effect of initial beach profile and water level on small scale physical models.* Laboratory Report, University of Southampton, Civil & Environmental Engineering Department, Southampton, UK.

Plant, G.N., & Griggs, G.B. (1992). Interactions between nearshore processes and beach morphology near a seawall. *Journal of Coastal Research,* Vol 8,1, p183-200.

Raffel, M. Willert, C.E. Kompenhaus, J (1998). Particle Image velocimetry- A Practical Guide Springer - Verlag, Berlin. 253pp.

Rendel, Palmer & Tritton (1996). *History of coastal engineering in Great Britain,* In: *History & Heritage of coast engineering*, Ed Kraus. N.C, ASCE New York. p214-274.

Sumer B,M., & Fredsøe, J. (1997). Scour at the head of a vertical breakwater. *Coastal Engineering*, 29, 201- 230.

Sumer, B.M, Whitehouse,. & R.J.S, Tørum, A. (2001). Scour around coastal structures - a review of recent research. *Coastal Engineering*, 44, p153-190.

Sutherland, J.S. Brampton, A. Whitehouse, R.J.S. (2006). Toe scour at seawalls: Monitoring, Prediction and Mitigation. *Proceedings 41st Defra Flood and Coastal Management Conference*, 5-6 July 2006. University of York, UK.

Tsai, C.P. (1995). Wave-induced liquefaction potential in a porous seabed in front of a breakwater. *Ocean Engineering*, Vol 22, No1, p1 -18, Elsevier Science, UK.

USACE (1995) *EM110-2-1614: Design of coastal revetments, seawalls and bulkheads.* USACE, Department of the Army, U.S. Army Corps of Engineers, Washington, DC 20314-1000, (EM 1110-2-1614).

Van Rijn, L.C. (1998). *Principles of coastal morphology.* Aqua Publications, PO Box 9896, 1006 AN. Amsterdam.

Westerweel, J. (1997). Fundamentals of digital particle image velocimetry. *Measurement, Science Technology*, Vol 8. p1379-1392.

# 11. Appendices

**Appendix A:** Pearce et al. (2006) *Scour at a seawall- field measurements and laboratory modelling*. Paper presented at the International Coastal Engineering Conference, San Diego, 3-8 September 2006. ASCE, New York. Vol 4, p2379-2390.

The paper in appendix A has been removed due to copyright, an online version may be accessed here.

https://doi.org/10.1142/9789812709554_0201

# Appendix B: Blackpool field study – data filter criteria.

**Filter rule criteria for extraction of Tell-Tail data from Blackpool dataset**

A minimum sensor vibration rate of three pulses per minute was chosen to eliminate data points triggered by wave impacts shaking the instrument shaft and causing vibrations in sensors buried below the beach level. This filter was the only rule to be applied to the Southbourne dataset, which was not affected by the other issues.

At Blackpool, the significant tidal range led to the lowest active sensor remaining several metres below the zone of turbulent wave breaking, this sometimes led to insufficient flow velocities at the wall toe to trigger a beach level measurement. Instead, sensors high up in the water column were activated; these produced misleading beach level results which appeared to show the beach level fluctuating rapidly by a couple of metres at high tide. Fortunately the deepest scour depth generally occurred before high water; and did not affect data extraction.

A plot of beach and tide height indicated that during low wave activity the water surface disturbance would tend to activate successive sensors as the tide rose and fell, producing false readings. To ensure adequate turbulence a minimum offshore wave height of 0.75 m was chosen. A minimum sensor immersion depth of 0.1 m was also selected following photographic evidence which suggested pools of water, approximately 0.1 m deep were sometimes present in front of the seawall at low tide. During a flood tide the surface water in the pool would be disturbed by swash and activate sensors raised above the bed, inferring a slightly higher beach level. Setting a conservative threshold of 0.1 m sensor immersion, ensured that sufficient water depth and turbulence were present to activate the sensor closest to the bed. This filter also eliminated false signals generated by the wind or by persons moving a sensor.

In some cases the scour features in front of the wall appeared to persist over several tidal cycles, these features are were excluded from the analysis as their scour rate appeared excessive (greater then 2 $cm.^{s-1}$), only new scour events were considered, from a flat beach profile. In the final filter criteria, the offshore incident wave angle was limited to between 225° and 315° to exclude strongly oblique wave angles. This also excluded false signals associated with waves in an offshore direction.

## Appendix C: Blackpool field study- comparison of scour depth to incident wave height

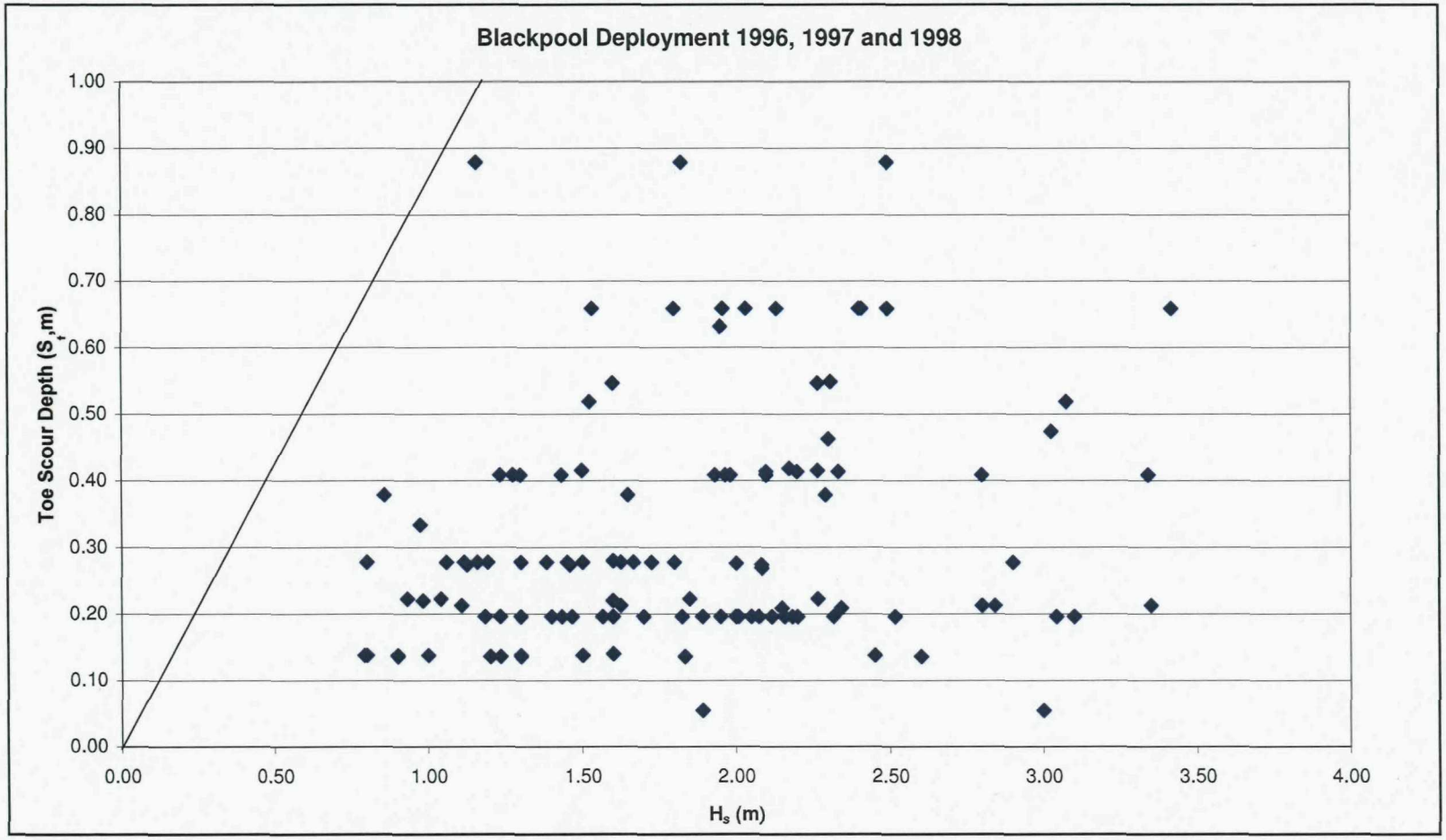

## Appendix D: Plots toe scour depth versus wave height, wavelength, water depth and Iribarren number

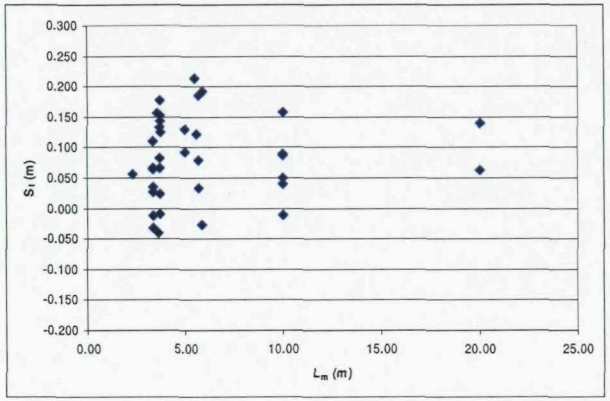


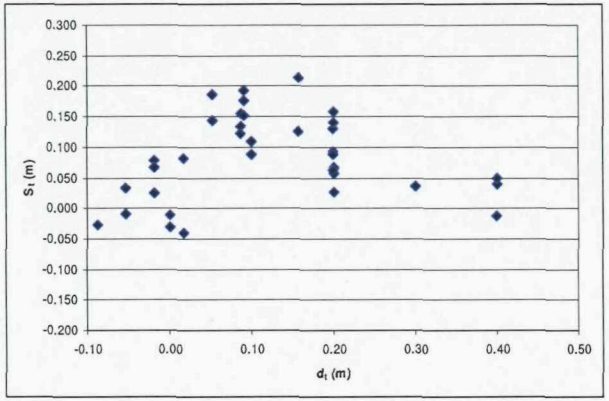


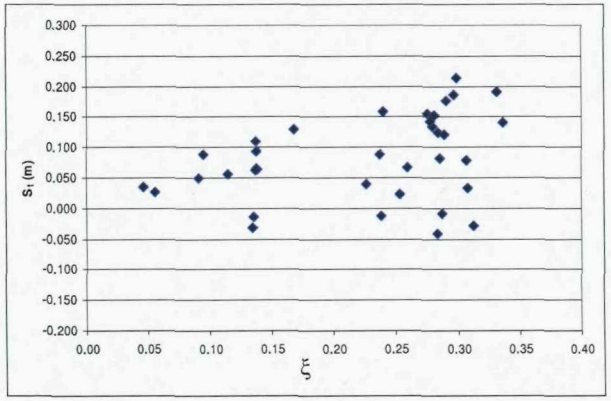


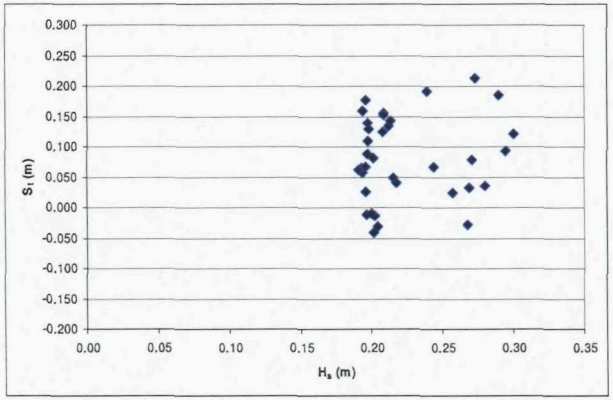

## Appendix E: Comparison of residuals from Equations 5.4 and 5.5 to wave height, wavelength, water depth to wavelength ratio and Iribarren number parameters

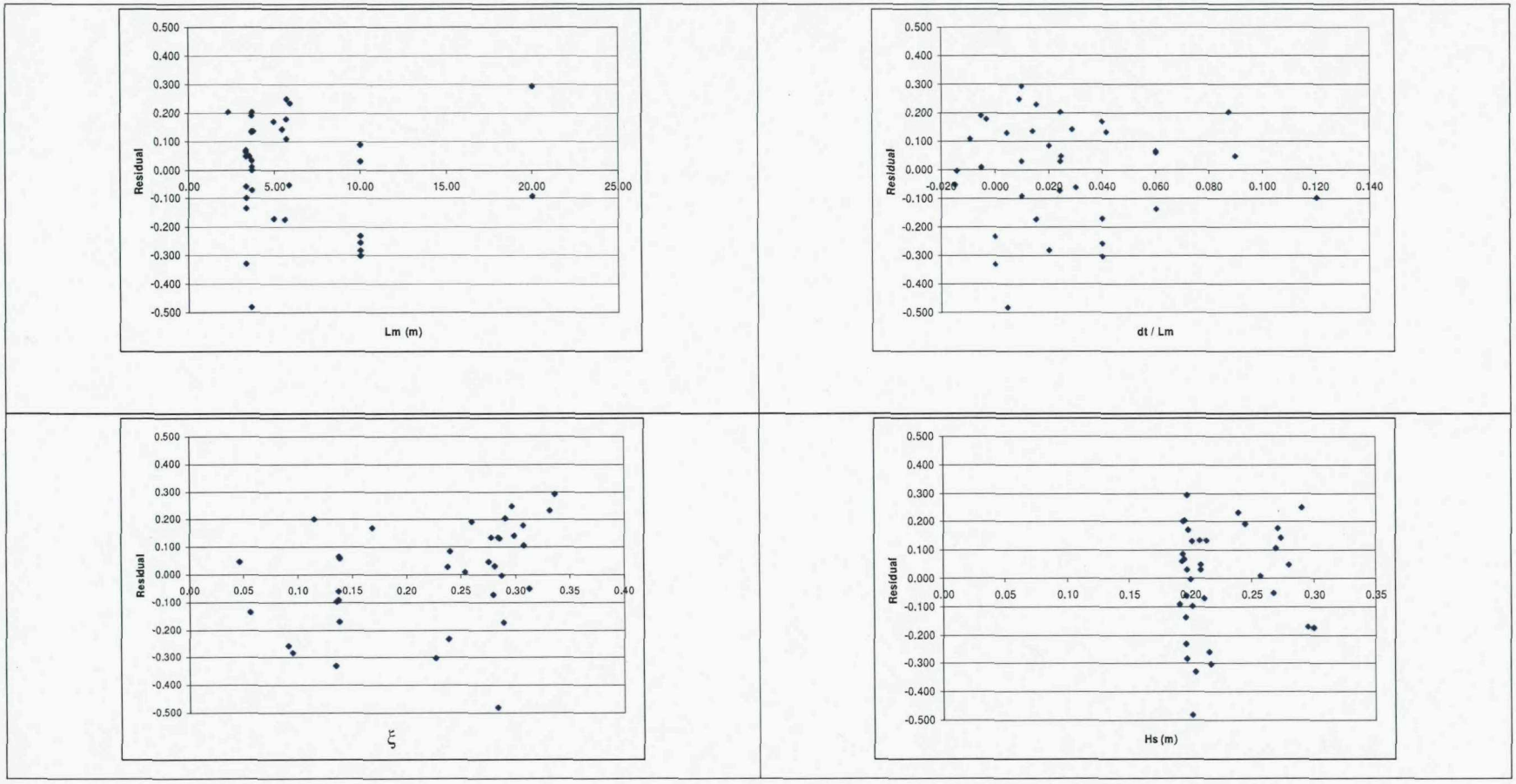

## Appendix F: Plots showing the goodness of fit for Equation 5.9 and 5.10